Electronic Supplementary Material (ESI) for Physical Chemistry Chemical Physics.

Supporting Information for

Photoswitchable Luminescent Lanthanide Complexes Controlled and Interrogated by Four Orthogonal Wavelengths of Light

Charlie H. Simms[a], Villads R. M. Nielsen[b], Thomas Just Sørensen[b], Stephen Faulkner[a], Matthew J. Langton[a]

[a]Chemistry Research Laboratory, University of Oxford, Mansfield Road, Oxford, OX1 3TA, UK

[b] Nano-Science Center & Department of Chemistry, University of Copenhagen, Universitetsparken 5, 2100 København Ø, Denmark.

General Methods and Reagents:

Unless stated otherwise, experiments were performed at 25 °C using reagents and solvents purchased commercially and used without further purification. Anhydrous solvents were acquired by passing them through an MBraun MPSP-800 column followed by degassing with nitrogen. Triethylamine was distilled from and stored over potassium hydroxide. Deionised, microfiltered water was obtained from a Milli-Q™ Millipore machine. Merck silica gel 60 under nitrogen pressure was used for silica gel flash column chromatography. Thin layer chromatography was performed on silica-coated (60G F254) aluminium plates from Merck and aluminum oxide coated with 254 nm fluorescent indicator aluminium plates from Merck. Samples were visualized by UV-light (254 and 365 nm) and/or using permanganate stain. Solvent systems containing a mixture of solvents are reported as a ratio by volume of each solvent.

Float-A-Lyzer® G2 dialysis tubes (500, 1000 MWCO) equipped with regenerated cellulose were purchased from Spectrum and used to purify the lanthanide complexes. The dialysis tube was activated by 10 % ethanol or isopropanol solution followed by MilliQ type 1 deionised water before being used. The corresponding complexes were dissolved in water and transferred into dialysis tube. The dialysis tube was placed in a 2.5 L-beaker filled with MilliQ type 1 deionised water. The dialysis lasts for at least two days under stirring and the deionised water was replaced with fresh deionised water more than three times during dialysis.

Characterisation Information:

Mass spectra were carried out on a Waters BioAccord LC-MS system; flow injection analysis was performed on an ACQUITY I-Class PLUS UPLC System (Waters, Millford, MA, USA) coupled to an AQUITY RDa mass spectrometer (Waters, Milford, MA, USA) equipped with an ESI probe, in positive ion mode. The flow rate was set to 0.300 mLmin-1 using 50 % methanol (aq) + 0.1 % formic acid eluent. Scan parameters were set as follows: analyser mode, full scan; scan range 50-2000 m/z; scan rate, 2 Hz; cone voltage, 40 V; capillary voltage, 0.8 kV; desolvation temperature, 550 °C; and intelligent data capture, on.

NMR spectra were obtained using a Bruker Avance III HD nanobay NMR equipped with a 9.4 T magnet (^{1}H 400.2 MHz , ^{19}F 376.5 MHz, ^{13}C 100.6 MHz) Bruker Avance NMR equipped with a 11.75 T magnet and a ^{13}C detect cryoprobe (^{1}H 500.3 MHz, ^{13}C 125.8 MHz) and Bruker NEO 600 with broadband helium cryoprobe (^{1}H 600.4 MHz, ^{13}C 151.0 MHz). Chemical shifts were referenced to residual solvent peaks and are given as follows: chemical shift (δ, ppm), multiplicity (s, singlet; br, broad; d, doublet, t, triplet; q, quartet; m, multiplet), coupling constant (*J*, Hz), integration. All NMR spectra were recorded at 298K, unless stated otherwise.

Abbreviations:

NMP: N-methyl-2-pyrrolidone, **µW**: microwave radiation, **THF**: tetrahydrofuran, **DCM**: dichloromethane, **NCS:** N-chlorosuccinimide, **DBU:** 1,8-diazabicyclo[5.4.0]undec-7-ene, ***p*-TsCl:** 4-toluenesulfonyl chloride, **MeCN:** acetonitrile, **TFA:** trifluoroacetic acid, **EtOH:** ethanol, **MeOH:** methanol, **rt:** room temperature, **HR-ESI-MS:** high resolution electro-spray ionisation mass spectrometry, **HPLC:** high performance liquid chromatography, **PSS:** photostationary state, **λ_{ex}:** excitation wavelength, **λ_{em}:** emission wavelength.

Synthesis and Characterisation of complexes:

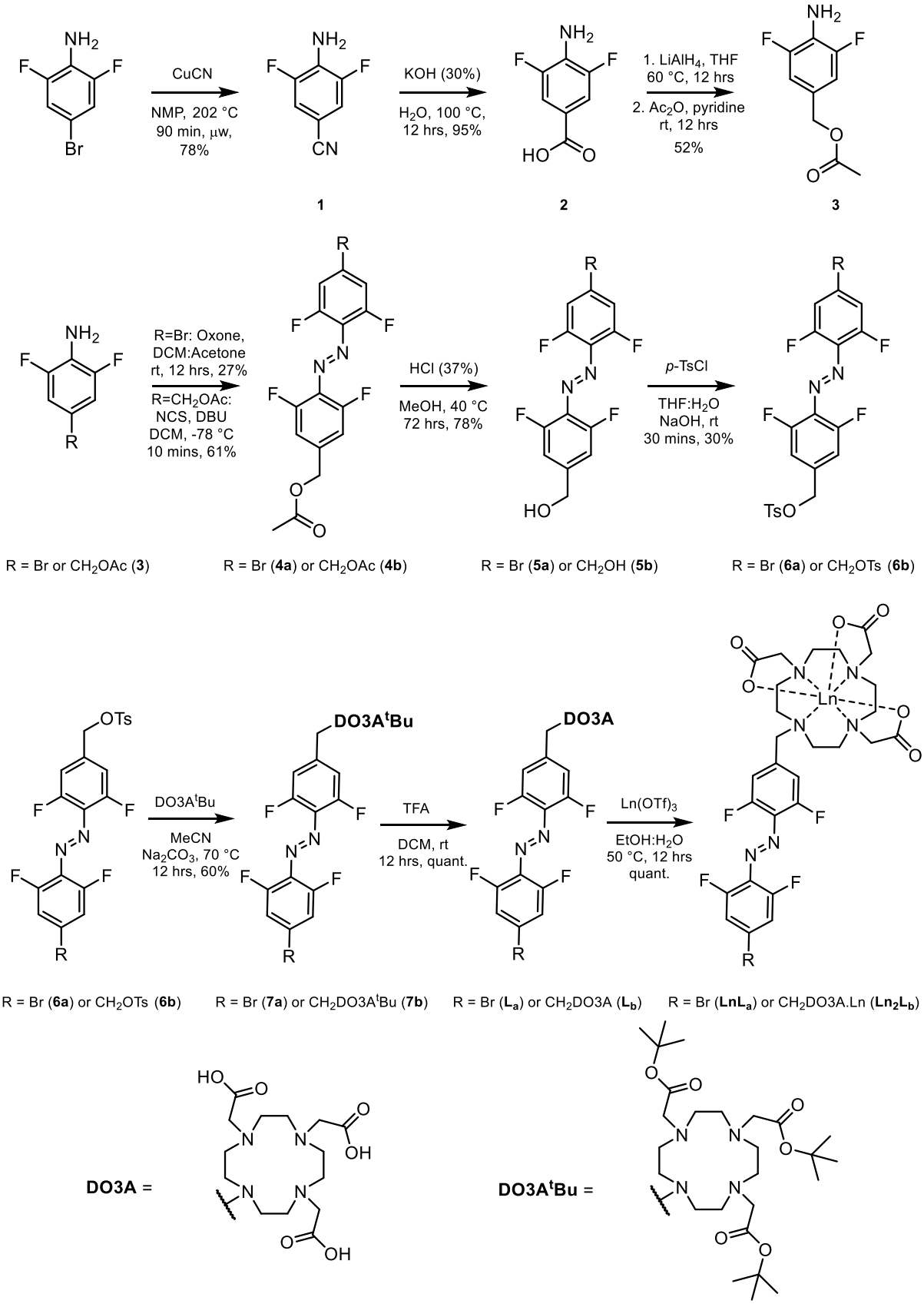

Scheme S1: Synthesis of photo-switchable lanthanide complexes ***LnL$_a$*** and ***Ln$_2$L$_b$***.

Compounds **1**,[1] **2**,[2] **3**[2], **4b**[2] and **5b**[2] and **DO3A^{t}Bu**[3] were all synthesised according to previously reported literature procedures.

Synthesis of **4a**:

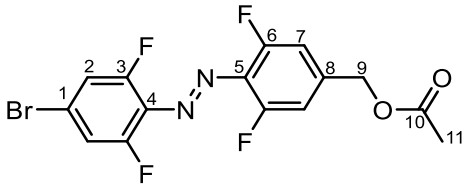

4-bromo-2,6-difluoroaniline (1.56 g, 12.0 mmol, 1.2 eq.) was dissolved in 48 mL DCM: Acetone (5:1). Oxone (20 g, 65 mmol, 5.5 eq.) was dissolved in water (48 mL) and added to the 2,6-difluoroanaline containing solution. The resulting biphasic solution was stirred overnight at room temperature. The organic layer was separated and reduced under vacuum. The resulting solid was re-dissolved in 50 mL of acetic acid: toluene: TFA (6: 6: 1) solution, to which **3** (2.03 g, 10 mmol, 1.0 eq.) was added. The reaction was stirred for 3 days at room temperature. The solution was concentrated under reduced pressure and purified by silica gel flash column chromatography with DCM to yield an orange crystalline product (0.903 g, 2.77 mmol, 27 %).

HR-ESI-MS obsd 404.9855, calcd 404.9856 [$(M + H)^+$, M = $C_{15}H_{10}BrF_4N_2O_2$].

^{1}H NMR (400 MHz, DMSO-d_6) δ: 7.82 – 7.74 (m, 1H, H_2), 7.39 (d, J = 10.6 Hz, 1H, H_7), 5.17 (s, 1H, H_9), 2.14 (s, 1H, H_{11}).

^{13}C NMR (151 MHz, DMSO-d_6) δ: 170.1 (C_{10}), 155.5 (t, *J* = 5.0 Hz, C_3), 153.8 (d, *J* = 4.9 Hz, C_6), 143.1 (t, *J* = 10.2 Hz, C_8), 129.9 (t, *J* = 9.7 Hz, C_4), 129.7 (d, *J* = 9.8 Hz, C_5), 124.5 (t, *J* = 12.4 Hz, C_1), 117.1 (dd, *J* = 23.3, 3.8 Hz, C_2), 111.8 (dd, *J* = 20.9, 3.3 Hz, C_7), 63.7 (C_9), 20.6 (C_{11}).

^{19}F NMR (377 MHz, DMSO-d_6) δ: -119.68 (F_2), -120.64 (F_7)

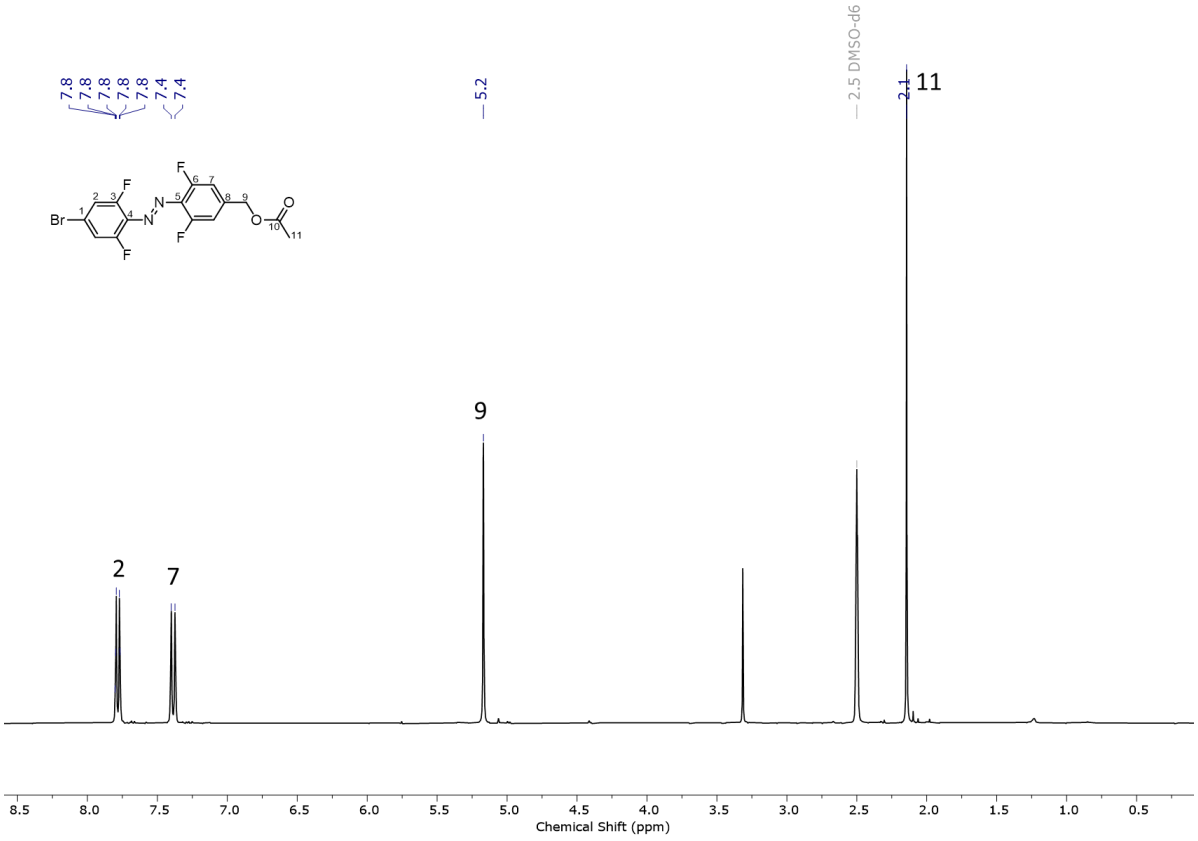

*Figure S1: [1]H NMR spectrum of compound **4a** (DMSO-d_6, 400 MHz, 298 K).*

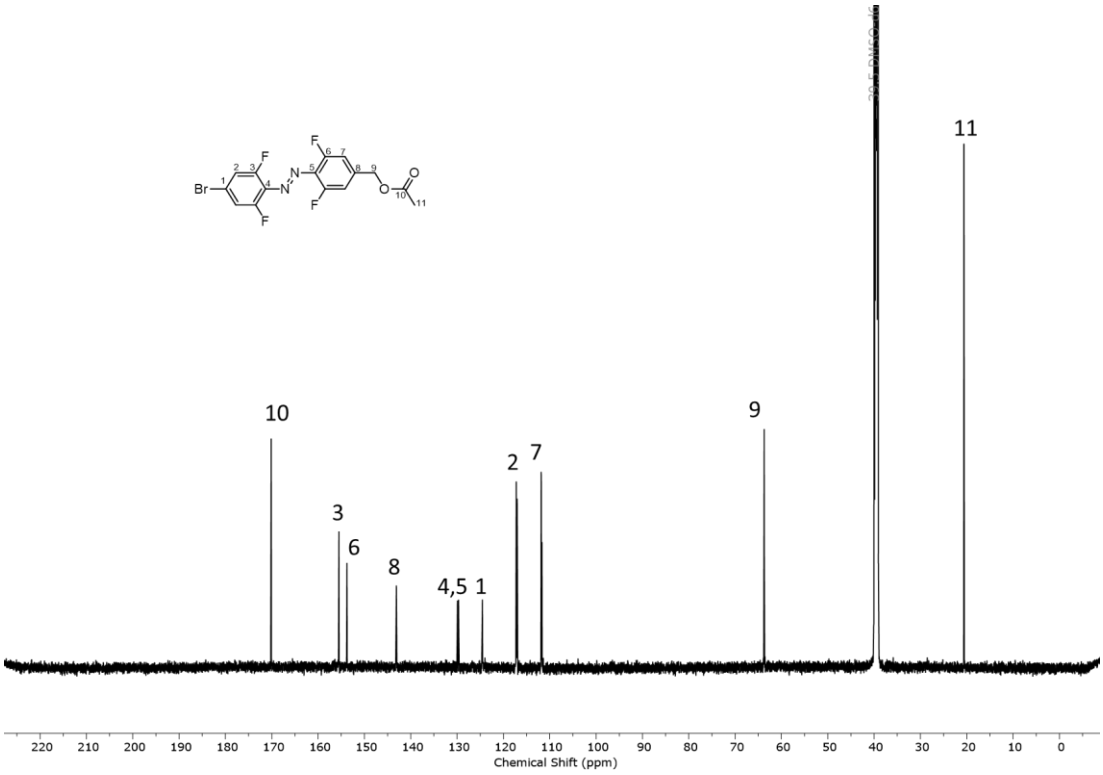

*Figure S2: [13]C NMR spectrum of compound **4a** (DMSO-d_6, 151 MHz, 298 K)*

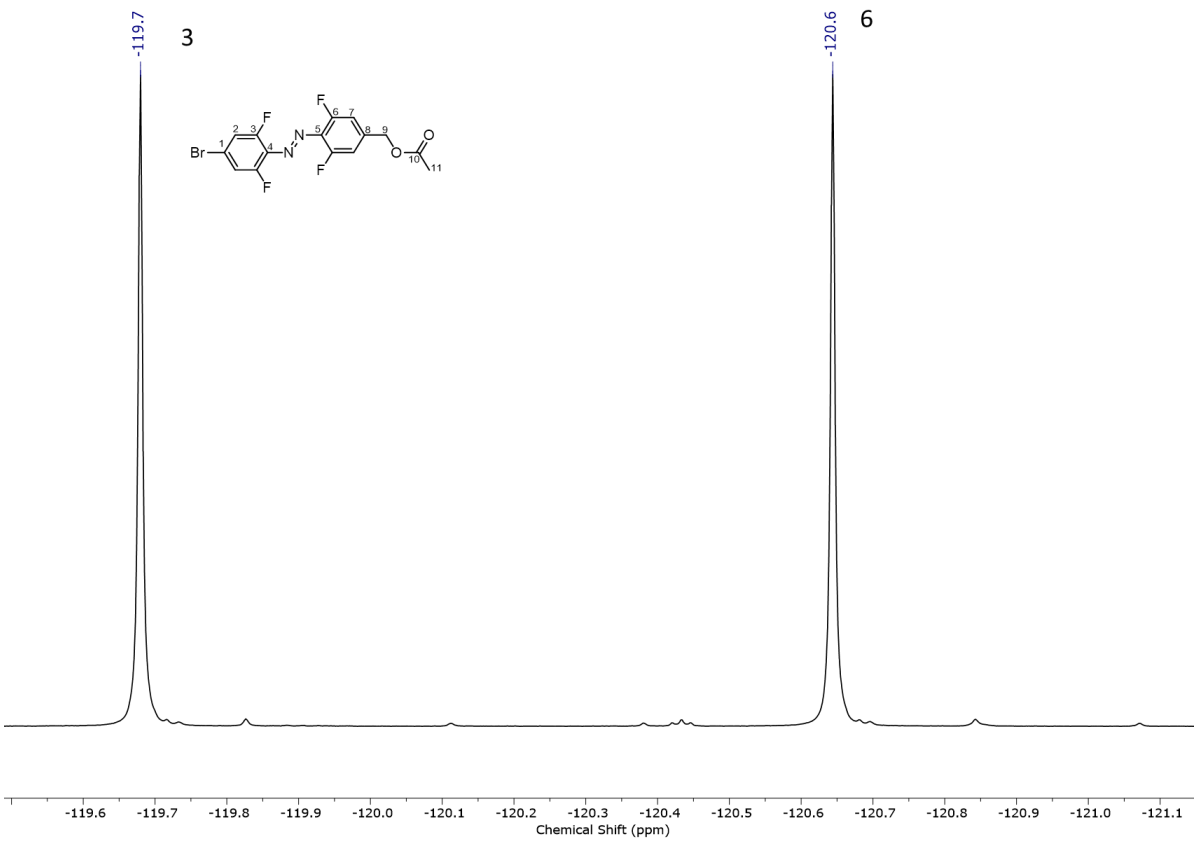

*Figure S3: ^{19}F NMR spectrum of compound **4a** (DMSO-d_6, 377 MHz, 298 K),*

Synthesis of **5a**:

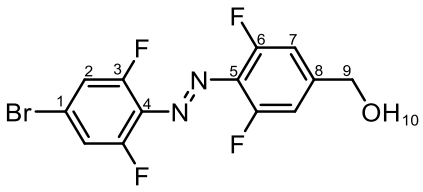

4a (900 mg, 2.22 mmol) was dissolved in 250 mL of a solution of 37 % HCl : MeOH (1: 100) and left to stir at 40 °C for 72 hrs. The reaction was diluted with toluene (100 mL) and the solution concentrated under reduced pressure. The crude product was purified by silica gel flash column chromatography eluted with ethyl acetate: DCM (1:5) to yield an orange crystalline solid (630 mg, 2.76 mmol, 77 %).

^{1}H NMR (400 MHz, DMSO-d_6) δ 7.80 – 7.72 (m, 2H, H_2), 7.27 (d, *J* = 10.8 Hz, 2H, H_7), 5.63 (t, *J* = 5.8 Hz, 1H, H_{10}), 4.60 (d, *J* = 5.8 Hz, 2H, H_9) ppm.

^{13}C NMR (151 MHz, DMSO-d_6) δ 156.1 (dd, *J* = 27.4, 4.7 Hz, C_3), 154.3(dd, *J* = 29.7, 4.7 Hz, C_6), 150.9 (t, *J* = 9.2 Hz, C_8), 130.5 (t, *J* = 9.8 Hz, C_4), 129.4 (t, *J* = 9.7 Hz, C_5), 124.6 (t, *J* = 12.4 Hz, C_1), 117.6 (d, *J* = 3.9 Hz, C_2), 110.7 (d, *J* = 3.0 Hz, C_7), 62.0 (d, *J* = 35.3 Hz, C_9) ppm.

^{19}F NMR (565 MHz, DMSO-d_6) δ -119.93 (d, *J* = 9.9 Hz, F_3), -120.67 (d, *J* = 11.4 Hz, F_6) ppm.

HR-ESI-MS obsd 362.9750, calcd 362.9751 [$(M + H)^+$, M = $C_{13}H_7BrF_4N_2O$].

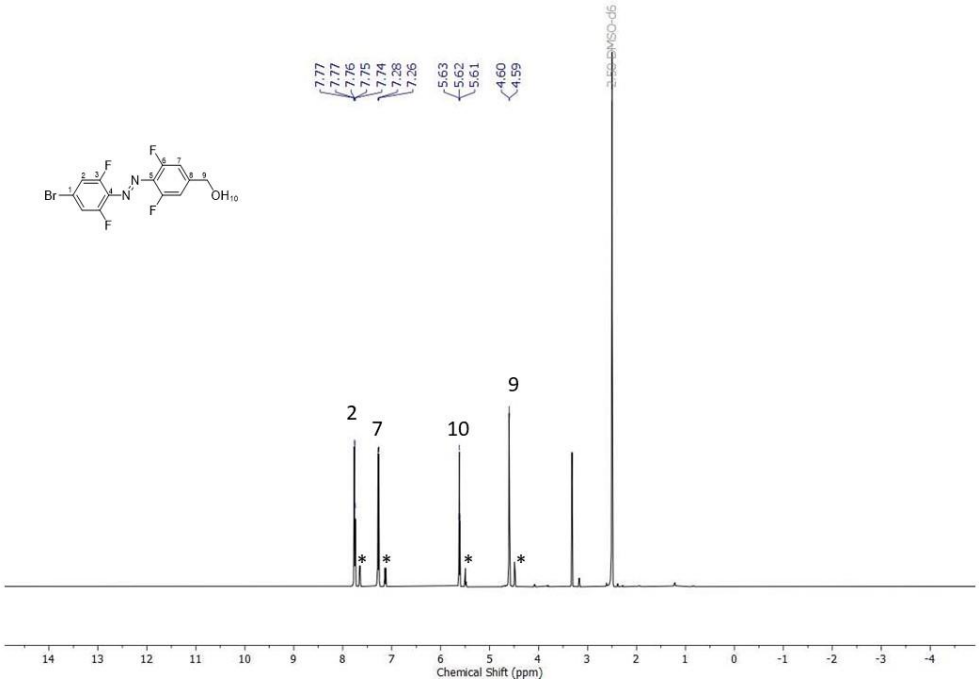

*Figure S4: ^{1}H NMR spectrum of compound **5a** (DMSO-d_6, 400 MHz, 298 K), * represent the signals from the corresponding Z-isomer.*

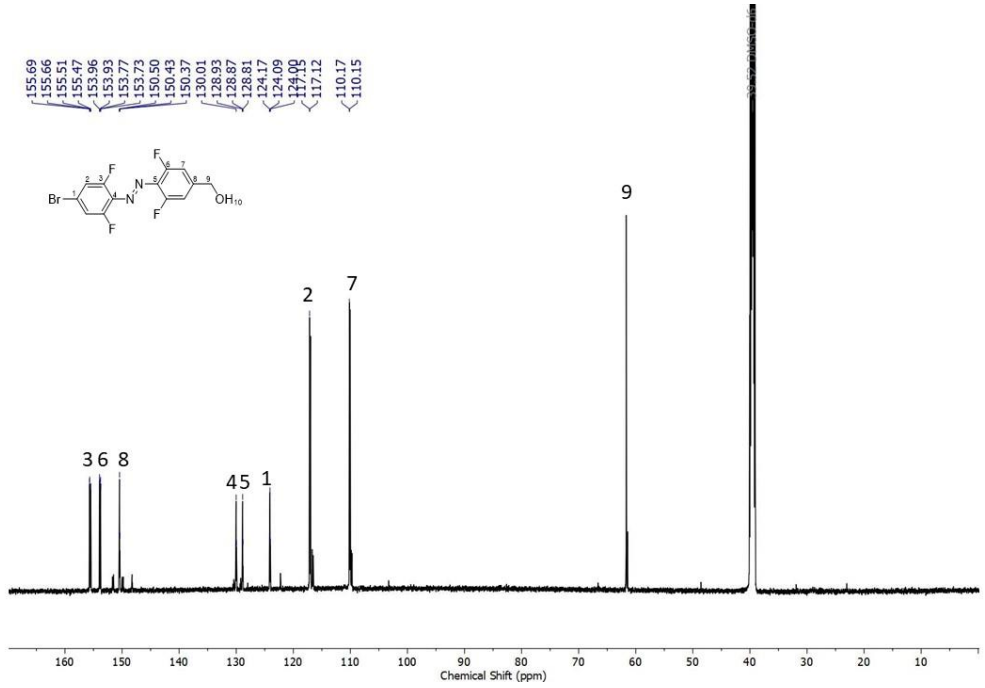

*Figure S5: [13]C NMR spectrum of compound **5a** (DMSO-d_6, 151 MHz, 298 K)*

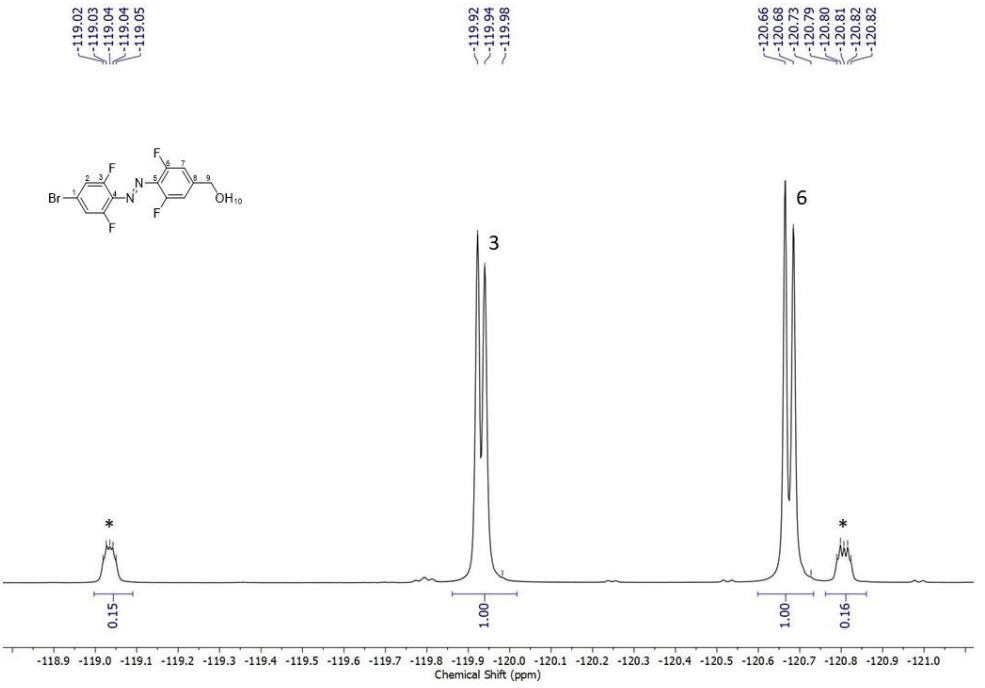

*Figure S6: [19]F NMR spectrum of compound **5a** (DMSO-d_6, 565 MHz, 298 K), * represent the signals from the corresponding Z-isomer.*

Synthesis of **6a**:

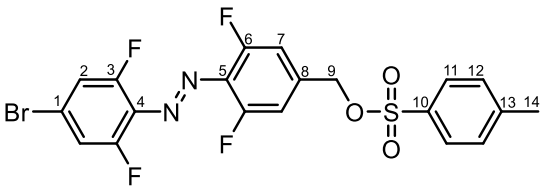

5a (250 mg, 0.88 mmol) and 4-toluenesulfonyl chloride (252 mg, 1.32 mmol, 3 eq.) were suspended in 40 mL of THF: H_2O (1:3). To this NaOH (53 mg, 1.32 mmol, 3 eq.) was added and the solution was left to stir rapidly at room temperature for 30 mins. The resulting solution was diluted with DCM and washed with water (3 × 50 mL). The organic layer was then concentrated under reduced pressure and purified by silica gel flash column chromatography eluted with DCM to yield a pale orange crystalline solid (150 mg, 0.34 mmol, 39%).

^{1}H NMR (400 MHz, DMSO-d_6) (**6**-*E*) δ 7.83 (d, *J* = 8.2 Hz, 2H,H_{11}), 7.78 (d, *J* = 9.2 Hz, 2H, H_2), 7.47 (d, *J* = 8.0 Hz, 2H, H_{12}), 7.27 (d, *J* = 10.4 Hz, 2H, H_7), 5.24 (s, 2H, H_9), 2.40 (s, 3H, H_{14}) ppm.

^{13}C NMR (151 MHz, DMSO-d_6) (**6**-*E*) δ 155.7 – 155.0 (m, C_6), 154.0 – 153.2 (m, C_3), 145.3 (C_{13}), 139.9 (t, *J* = 10.3 Hz, C_8), 132.3 (C_{10}), 130.6 (t, *J* = 9.9 Hz, C_5), 130.2 (C_{12}), 129.9 – 129.8 (m, C_4), 127.8 (C_{11}), 125.47(C_1), 117.2 (ddd, *J* = 23.3, 6.7, 3.5 Hz, C_2), 112.5 (dd, *J* = 21.2, 3.3 Hz, C_7), 69.7 (C_9), 21.0 (C_{14}) ppm.

^{19}F NMR (377 MHz, DMSO-d_6) δ -119.56 (F_3), -120.62 (F_6) ppm.

HR-ESI-MS obsd 518.9817, calcd 518.9819 [$(M + H)^+$, M = $C_{20}H_{13}BrF_4N_2O_3S$].

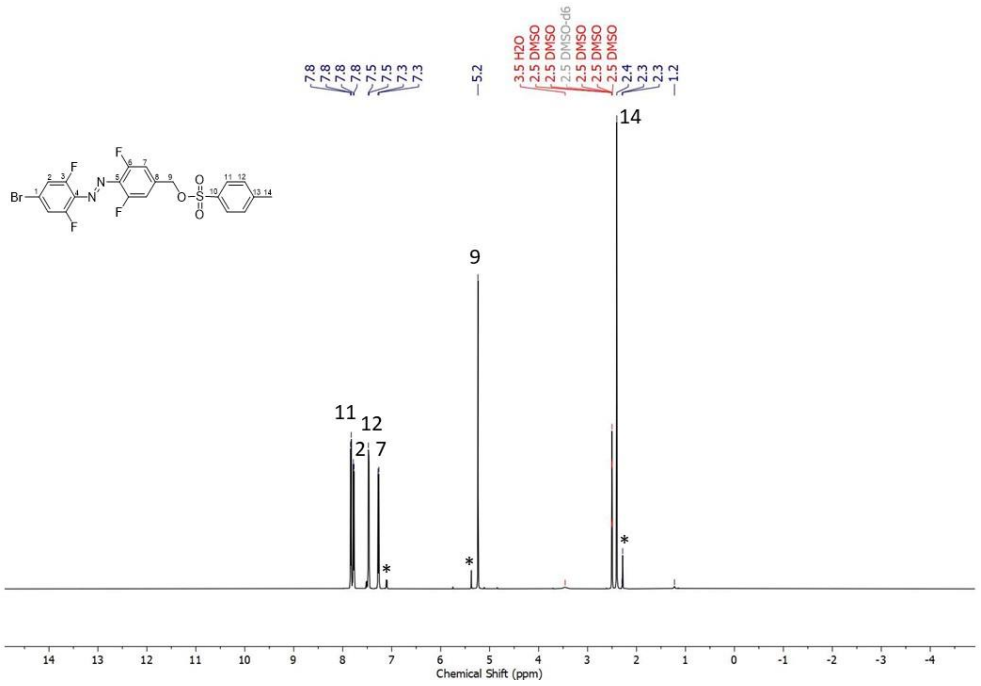

*Figure S7: ^{1}H NMR spectrum of compound **6a** (DMSO-d_6, 400 MHz, 298 K), * represent the signals from the corresponding Z-isomer.*

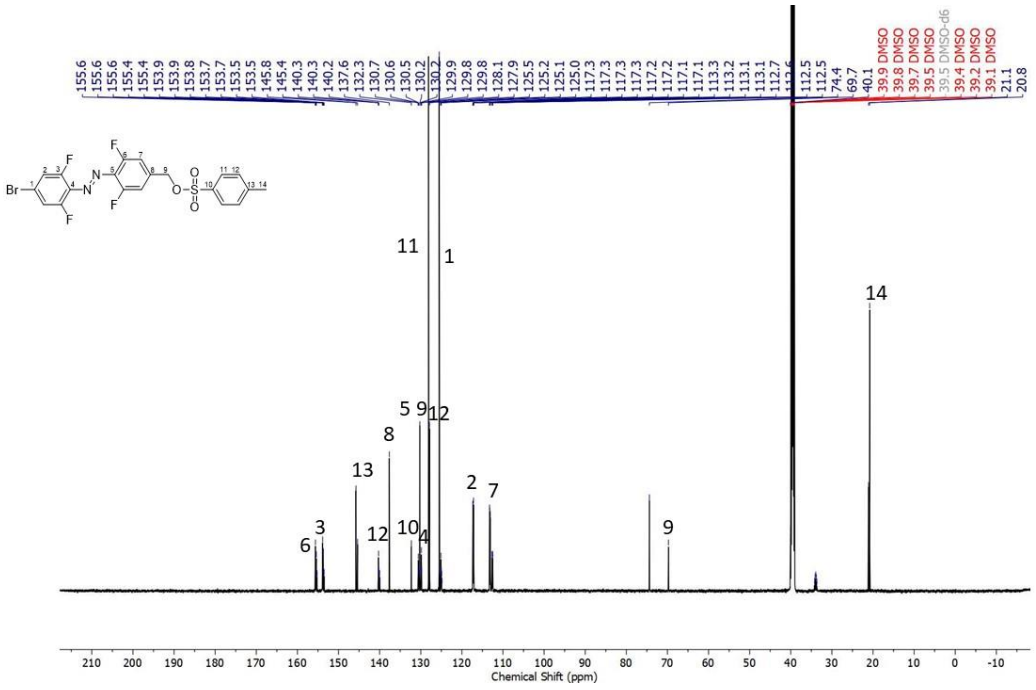

*Figure S8: ^{13}C NMR spectrum of compound **6a** (DMSO-d_6, 151 MHz, 298 K).*

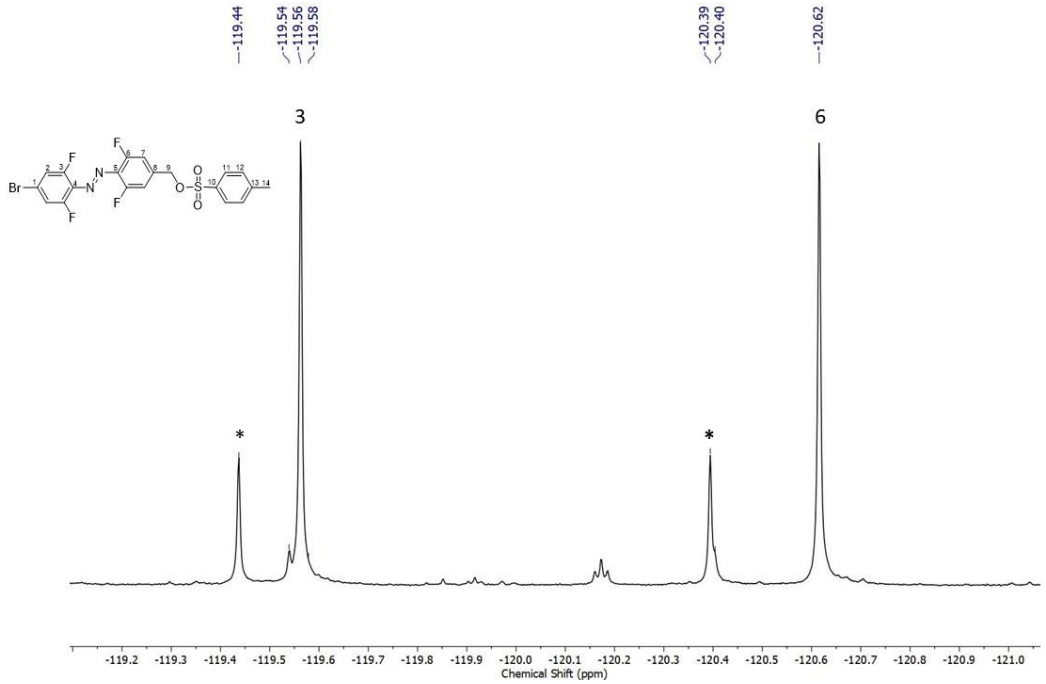

*Figure S9: ^{19}F NMR spectrum of compound **6a** (DMSO-d_6, 565 MHz, 298 K), * represent the signals from the corresponding Z-isomer.*

Synthesis of **6b**:

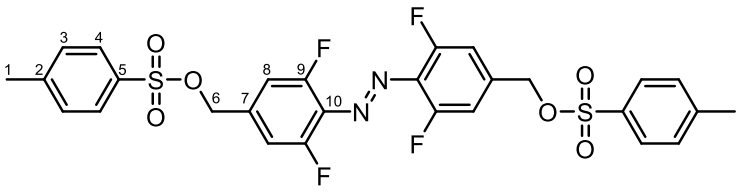

5b (680 mg, 2.16 mmol) and 4-toluenesulfonyl chloride (1.24 g, 6.49 mmol, 3 eq.) were suspended in 100 mL of THF: H_2O (10:3). To this NaOH (260 mg, 6.49 mmol, 3 eq.) were added and the solution was left to stir rapidly at room temperature for 30 mins. The resulting solution was diluted with DCM and washed with water (3 × 50 mL). The organic layer was then concentrated under reduced pressure and purified by silica gel column chromatography with DCM to yield a pale orange crystalline solid (578 mg, 0.93 mmol, 43%).

^{1}H NMR (600 MHz, DMSO-d_6) δ 7.83 (d, *J* = 8.2 Hz, 4H, **H_4**), 7.49 – 7.45 (m, 4H, **H_3**), 7.26 (d, *J* = 10.5 Hz, 4H, **H_8**), 5.24 (s, 4H, **H_6**), 2.40 (s, 6H, **H_1**) ppm.

^{13}C NMR (151 MHz, DMSO-d_6) δ 156.2 – 152.6 (m, **C_9**), 145.3 (**C_2**), 140.0 (dt, *J* = 36.3, 10.3 Hz, **C_7**), 132.3 (**C_5**), 130.6 (t, *J* = 10.0 Hz, **C_{10}**), 130.2 (**C_3**), 128.0 (**C_4**), 113.1 (dd, *J* = 21.1, 3.5 Hz, **C_8**), 69.7 (**C_6**), 21.0 (**C_1**) ppm.

^{19}F NMR (565 MHz, DMSO) δ -119.88 (dd, *J* = 555.7, 10.0 Hz, **F_9**) ppm.

HR-ESI-MS obsd 623.0925 , calcd 623.0928 $[(M + H)^+$, M = $C_{28}H_{22}F_4N_2O_6S_2]$.

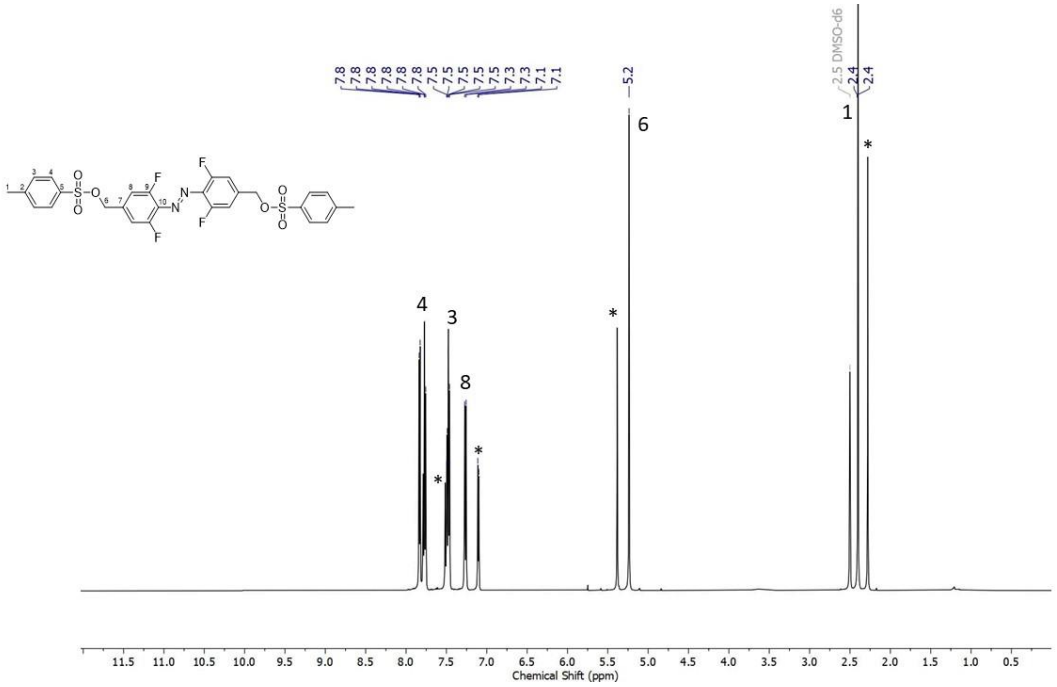

*Figure S10: ^{1}H NMR spectrum of compound **6b** (DMSO-d_6, 400 MHz, 298 K), * represent the signals from the corresponding Z-isomer.*

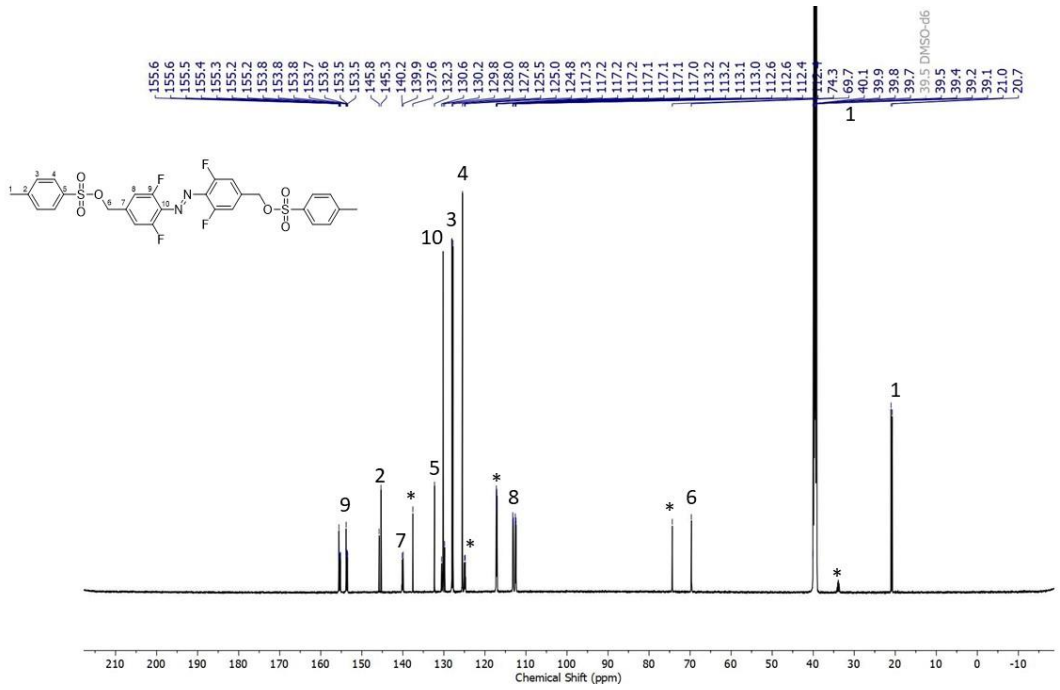

*Figure S11: ^{13}C NMR spectrum of compound **6b** (DMSO-d_6, 151 MHz, 298 K), * represent the signals from the corresponding Z-isomer.*

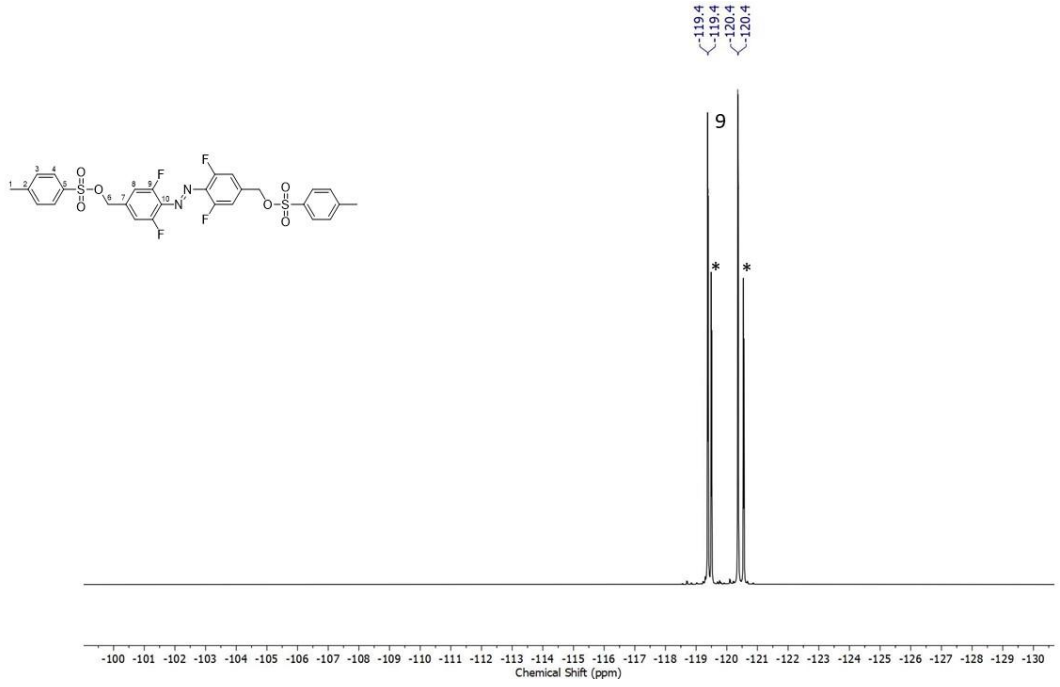

*Figure S12 : ^{19}F NMR spectrum of compound **6b** (DMSO-d_6, 565 MHz, 298 K), * represent the signals from the corresponding Z-isomer.*

Synthesis of 7a:

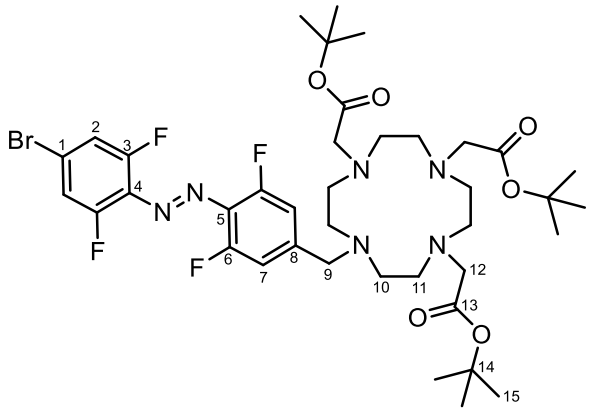

DO3A^{t}Bu (370 mgs, 0.66 mmol) and Na_2CO_3 (148 mgs, 1.4 mmol, 2.2 eq.) were dissolved in MeCN (10 mL). To this **6a** (340 mgs, 0.78 mmol, 1.2 eq.) was added and the resulting orange suspension was left to stir at 70 °C overnight. The remaining solid was then removed by filtration and the filtrate reduced under pressure to yield a dark red oil. This was then purified by silica gel flash chromatography eluting with DCM (5 % MeOH), yielding a red crystalline solid (530 mgs, 0.62 mmol, 94 %)

^{1}H NMR (600 MHz, DMSO) δ: 7.79 – 7.75 (m, 2H, **H_2**), 7.49 (d, J = 11.0 Hz, 2H, **H_7**).3.61 (m, b, 2H), 3.08 (m, b, 13H), 2.25 (m, b, 7H) (cyclen methylene protons), 1.43 (d, J = 6.2 Hz, 32H, **H_{15}**) ppm.

^{13}C NMR (151 MHz, DMSO) δ: 173.1 (s, **C_{13}**), 172.6, 155.4 (dd, *J* = 20.6, 4.8 Hz, **C_3**) , 153.6 (dd, *J* = 18.5, 4.8 Hz, **C_6**), 143.5 (d, *J* = 9.3 Hz, **C_8**), 130.0 (t, *J* = 9.8 Hz, **C_4**), 129.5 (t, *J* = 9.6 Hz, **C_5**), 124.4 (t, *J* = 12.3 Hz, **C_1**), 117.2 (s, **C_2**), 115.0 (s, **C_7**), 81.9 (s, **C_{14}**), 57.2 (cyclen methylene carbons), 55.7 (s, **C_{12}**), 55.4 (s, **C_9**), 27.6 (s, **C_{15}**) ppm.

^{19}F NMR (565 MHz, DMSO) δ -119.01, -120.05, -120.89, -121.10 ppm.

HR-ESI-MS obsd 691.1497 , calcd 691.1491 [$(M + H)^+$, M = $C_{39}H_{55}BrF_4N_6O_6$].

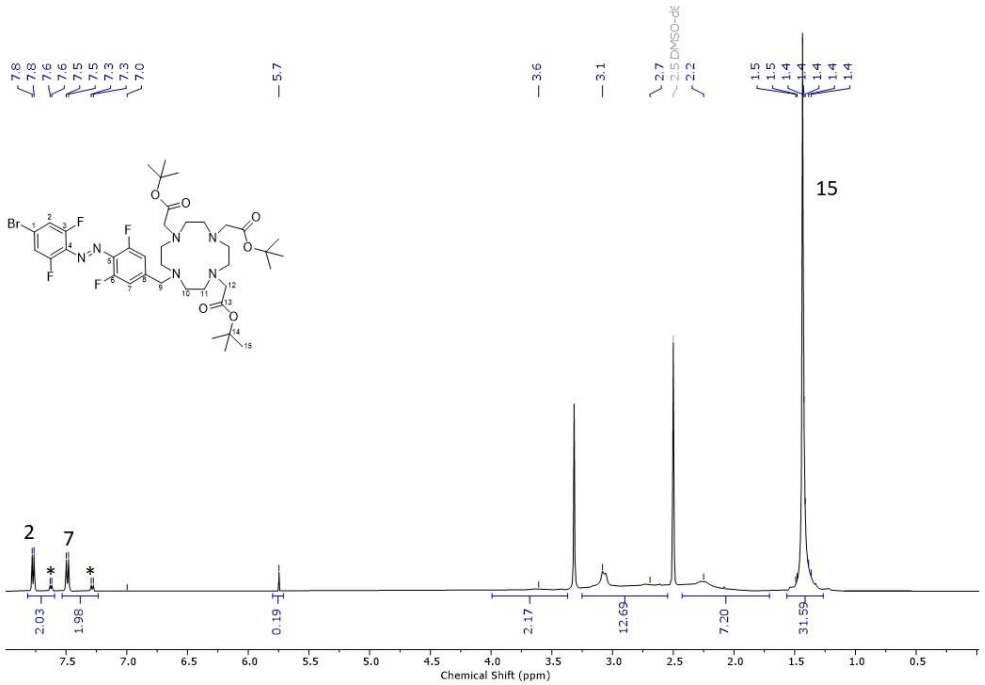

*Figure S13: [1]H NMR spectrum of compound **7a** (DMSO-d_6, 400 MHz, 298 K), * represent the signals from the corresponding Z-isomer.*

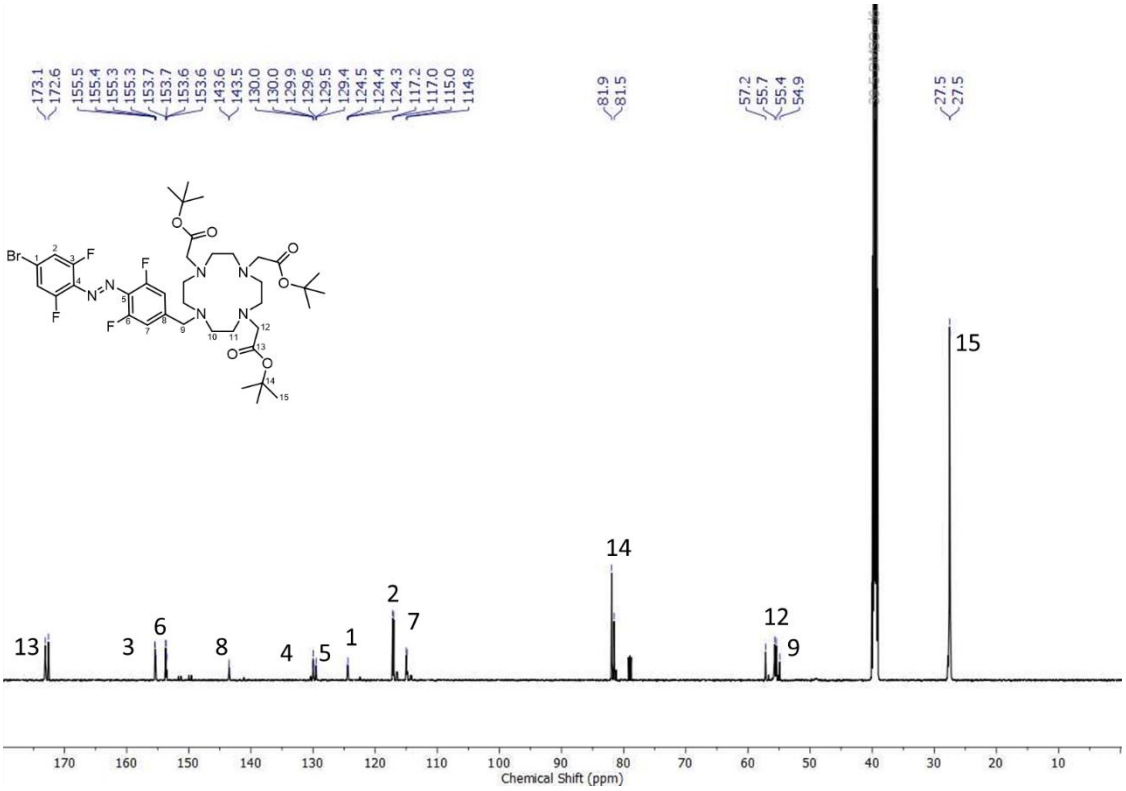

*Figure S14: [13]C NMR spectrum of compound **7a** (DMSO-d_6, 151 MHz, 298 K)*

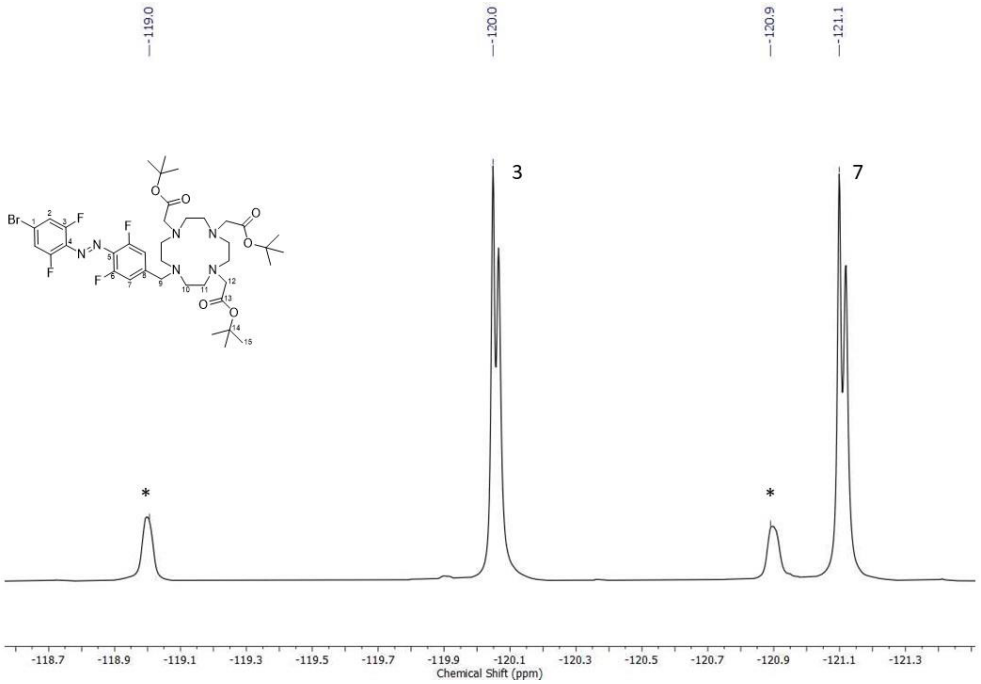

*Figure S15: ^{19}F NMR spectrum of compound **7a** (DMSO-d_6, 565 MHz, 298 K), * represent the signals from the corresponding Z-isomer.*

Synthesis of **7b**:

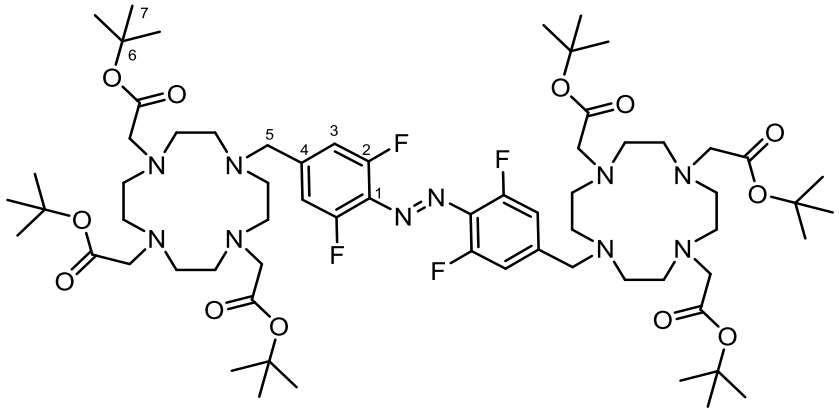

DO3A^{t}Bu (501 mgs, 0.84 mmol, 1.75 eq.) and Na_2CO_3 (300 mgs, 1.4 mmol, 2.7 eq.) were dissolved in MeCN (15 mL). To this **6b** (300 mgs, 0.48 mmol) was added and the resulting orange suspension was left to stir at 70 °C for 24 hrs. The remaining solid was then removed by filtration and the filtrate dried under reduced pressure to yield a dark red oil. This was then purified by silica gel flash column chromatography eluting with DCM (5% MeOH) to yield a red crystalline solid (371 mgs, 0.28 mmol, 60%)

^{1}H NMR (600 MHz, DMSO) δ 7.50 (d, *J* = 11.0 Hz, 4H, **H_3**), 3.61 (s, 5H,), 3.20 – 2.63 (m, 24H), 2.41 – 1.71 (m, 15H), 1.44 (s, 56H, H_a) ppm.

^{13}C NMR (151 MHz, DMSO) δ 172.9 (d, *J* = 74.4 Hz), 157.1 – 153.0 (m, **C_2**), 143.0 (**C_1**), 129.6 (d, *J* = 9.8 Hz, **C_4**), 114.9 (d, *J* = 20.0 Hz, **C_3**), 81.9, 81.5 (**C_6**), 57.1 (**C_5**), 55.4, 48.6, 33.5, 27.5 (d, *J* = 13.6 Hz, **C_7**), 21.7, 13.9 ppm.

^{19}F NMR (565 MHz, DMSO) δ -121.95 (d, *J* = 11.4 Hz, **F_2**) ppm.

HR-ESI-MS obsd 1307.7977, calcd 1307.8001 [$(M + H)^+$, M = $C_{66}H_{106}F_4N_{10}O_{12}$].

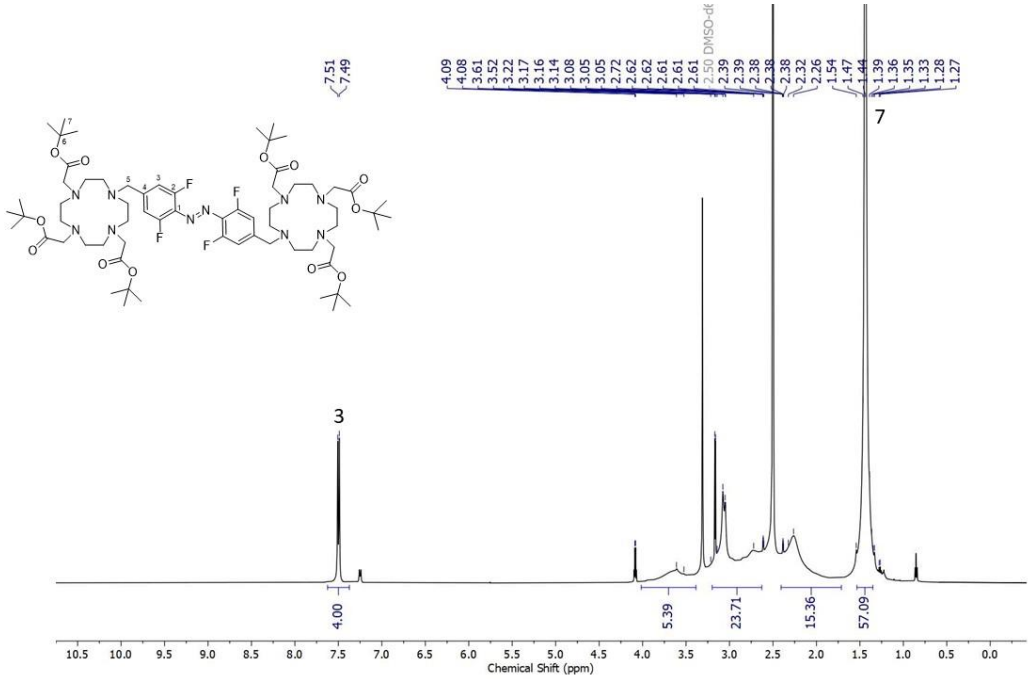

*Figure S16: ^{1}H NMR spectrum of compound **7b** (DMSO-d_6, 400 MHz, 298 K).*

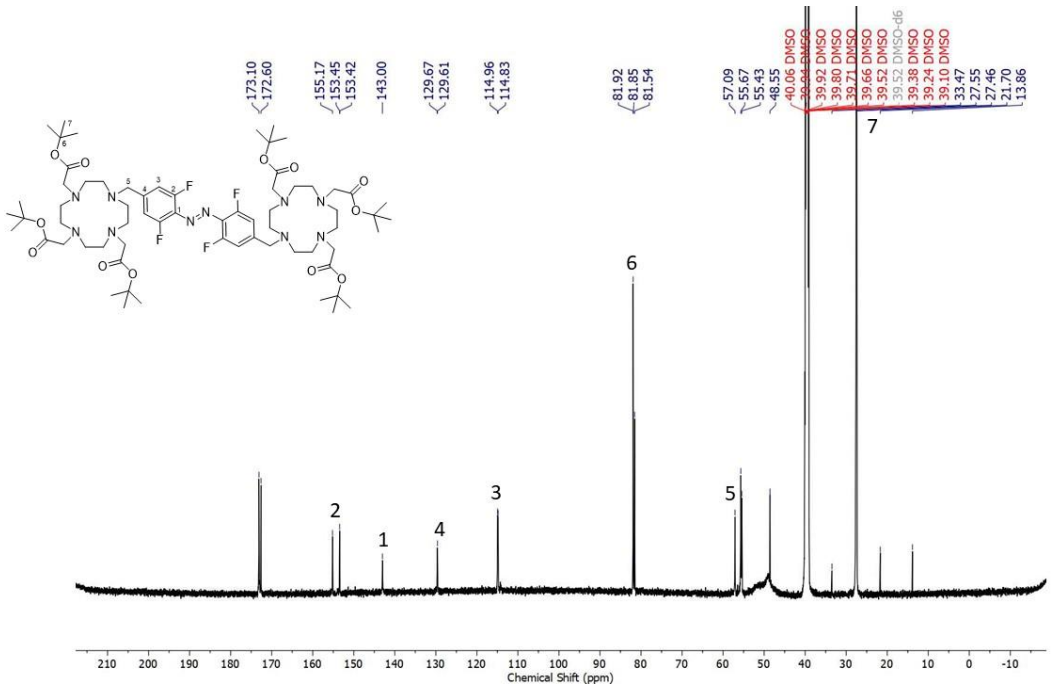

*Figure S17: ^{13}C NMR spectrum of compound **7b** (DMSO-d_6, 151 MHz, 298 K).*

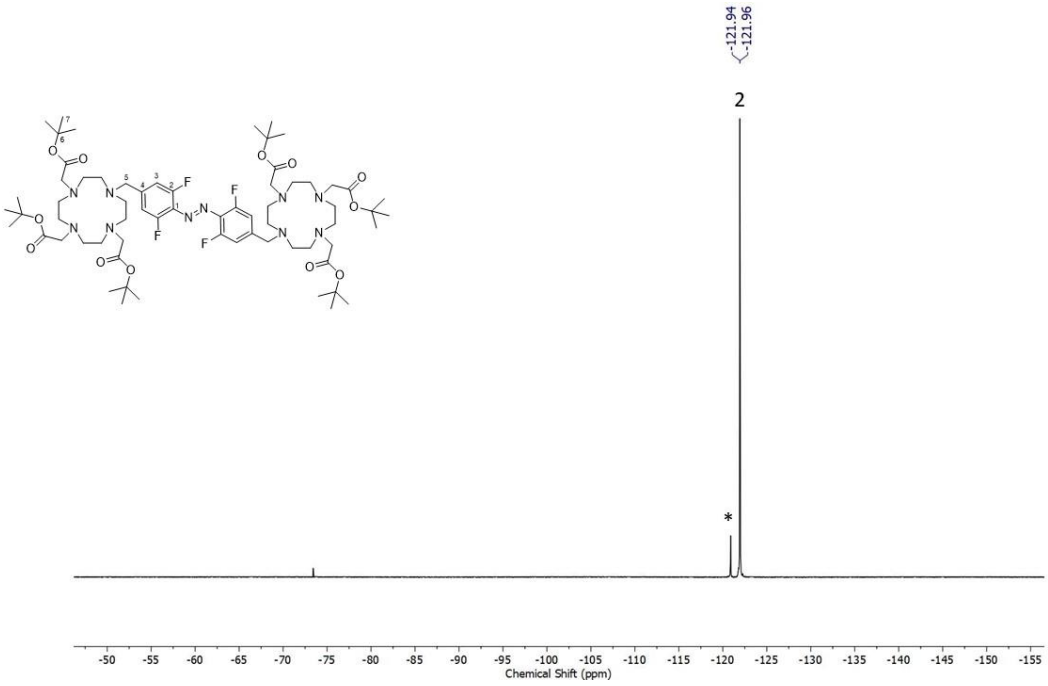

*Figure S18: ^{19}F NMR spectrum of compound **7b** (DMSO-d_6, 565 MHz, 298 K), * represent the signals from the corresponding Z-isomer.*

Synthesis of $\mathbf{L_a}$:

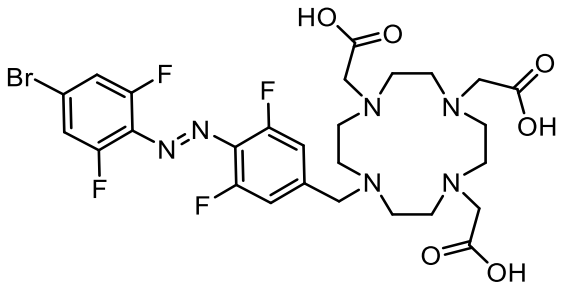

7a (350 mgs, 0.41 mmol) was dissolved in a DCM:TFA solution (1:1, 4.2 mL) and left to stir at room temperature overnight. The solvent was then removed under pressure and the resulting solid dissolved in the minimum amount of MeOH. This was then added dropwise to ether, crashing out the product. The product was then centrifuged and the supernatant discarded. This precipitation was repeated twice, the orange solid was then dried under vacuum to yield the $\mathbf{L_a}$ in a quantitative yield.

^{1}H NMR (600 MHz, D_2O) δ 7.31-7.15 (m, 4H, **Aromatic Protons**), 4.82 – 2.3.9 (m, 25 H, **cyclen protons**) ppm.

^{13}C NMR (151 MHz, D_2O) δ 173.8, 169.2, 155.9, 154.2, 152.0, 150.3,130.2, 129.9, 124.3, 122.7, 116.7, 116.4,116.2, 115.0, 114.5, 62.5, 56.3, 55.6, 53.8, 51.6, 50.3, 49.0, 48.5, 48.0, 47.8, 42.3, 30.1 ppm.

^{19}F NMR (565 MHz, D_2O) δ -118.23 ppm.

HR-ESI-MS obsd 693.1472 , calcd 693.1480 [$(M + H)^+$, M = $C_{27}H_{31}BrF_4N_6O_6$].

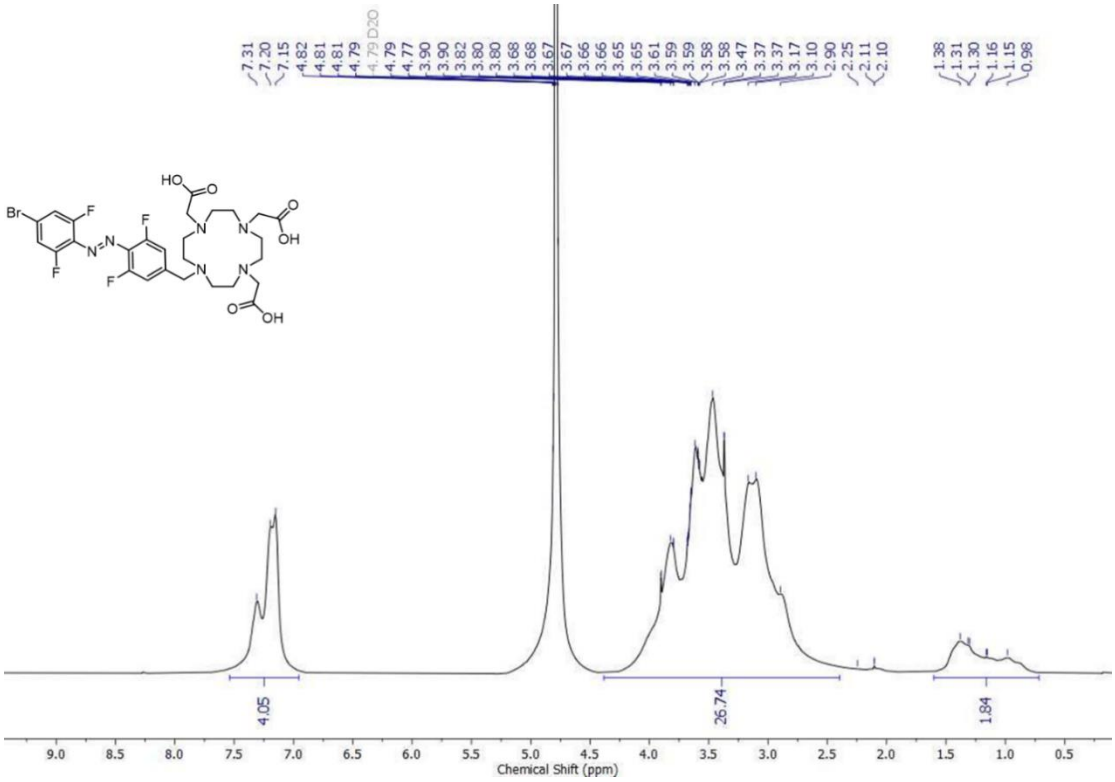

*Figure S19: [1]H NMR spectrum of compound **L_a** (D_2O, 400 MHz, 298 K)*

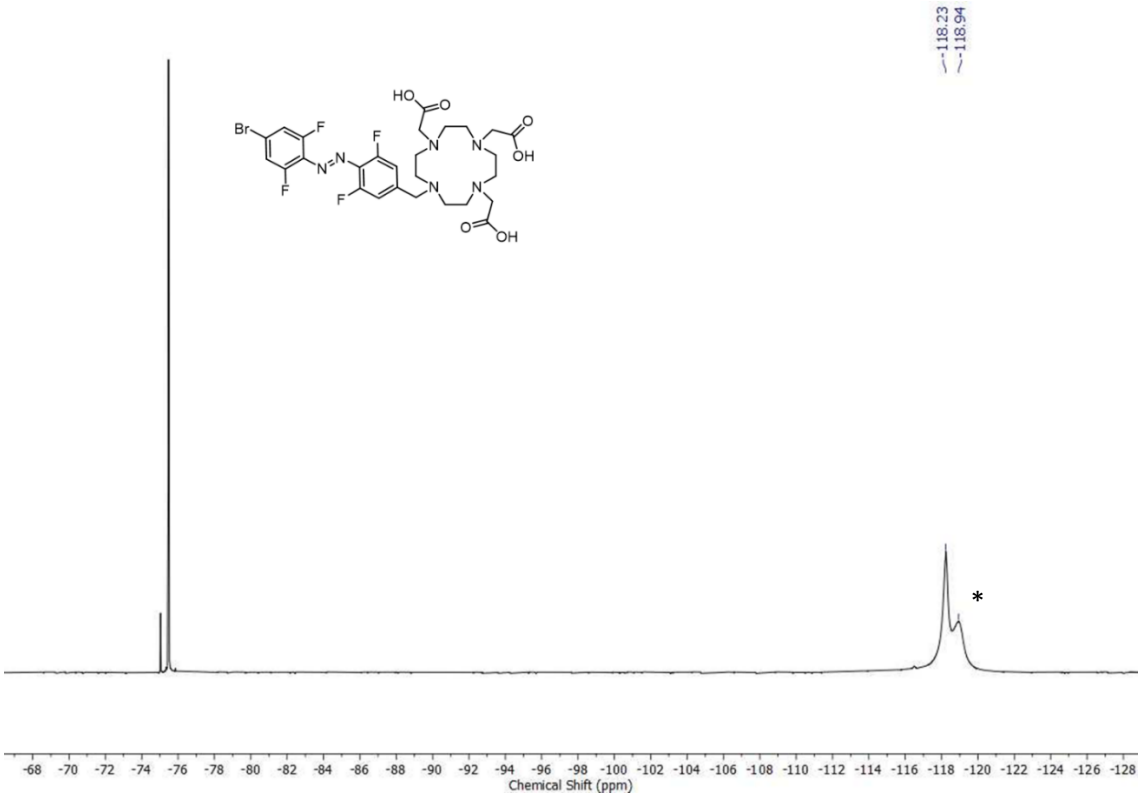

*Figure S20: [19]F NMR spectrum of compound **L_a** (D_2O, 565 MHz, 298 K), * represent the signals from the corresponding Z-isomer.*

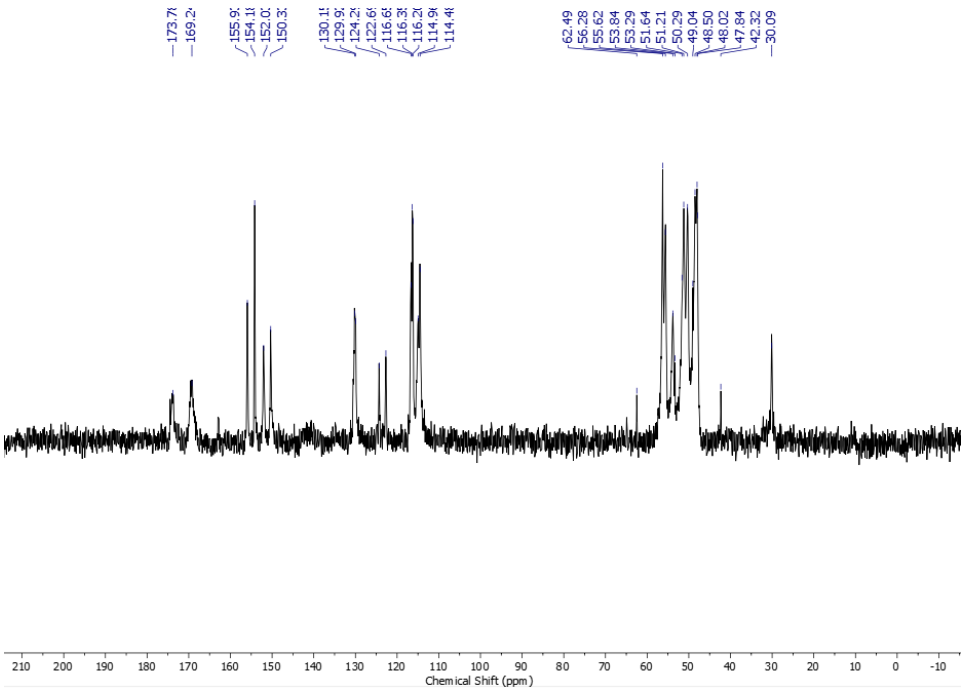

*Figure S21: ^{13}C NMR spectrum of compound **L_a** (D_2O, 151 MHz, 298 K).*

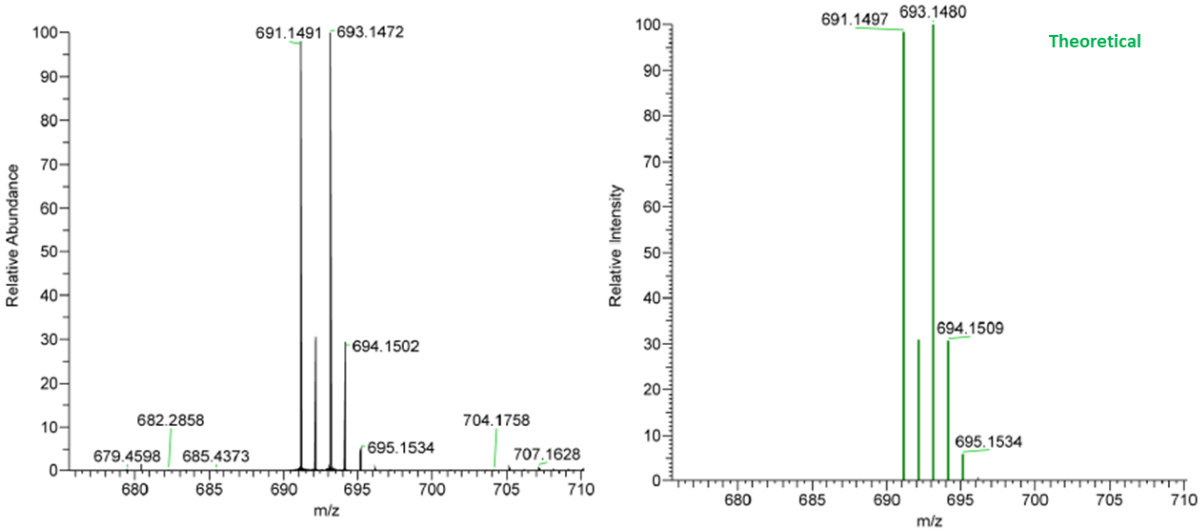

*Figure S22: **HR-ESI-MS** spectrum of compound **L_a**, obsd 691.1497 , calcd 691.1491 [$(M + H)^+$, M = $C_{27}H_{31}BrF_4N_6O_6$]*

Synthesis of $\mathbf{L_b}$:

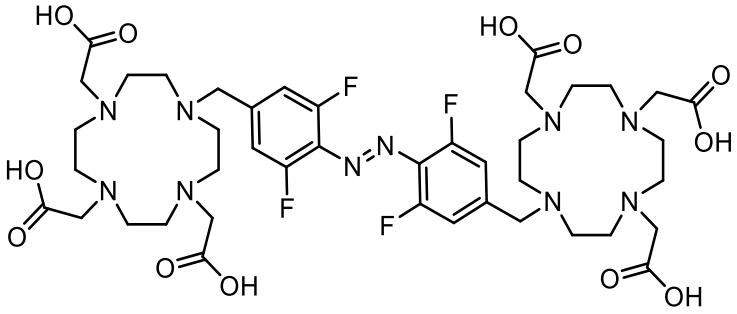

7b (320 mgs, 0.24 mmol) was dissolved in a 1:1 DCM:TFA mixture (4.2 mL) and left to stir at room temperature for 24 hrs. The solvent was then removed under pressure and the resulting orange solid dissolved in the minimum amount of MeOH. This was then added dropwise to ether, crashing out the product. The product was then centrifuged and the supernatant discarded. This precipitation was repeated twice, the orange solid was then died under vacuum to yield the $\mathbf{L_b}$ in a quantitative yield.

^{1}H NMR (600 MHz, D_2O) δ 7.43 (d, *J* = 10.6 Hz, 4H, Aromatic Protons), 4.00 – 2.85 (m, 54H, cyclen protons) ppm.

^{13}C NMR (151 MHz, D_2O) δ 174.5, 169.3, 163.2, 163.0, 156.0, 154.3, 153.5 151.9, 130.3, 117.5, 115.5, 115.2, 115.1, 114.5, 113.8, 56.5, 56.3, 55.5, 53.7, 51.5, 50.7, 49.0, 48.3, 47.9, 27.6, 27.4, 25.3 ppm.

^{19}F NMR (565 MHz, D_2O) δ -119.92 ppm.

HR-ESI-MS obsd 971.4246, calcd 971.4245 [$(M + H)^+$, M = $C_{42}H_{58}F_4N_{10}O_{12}$]

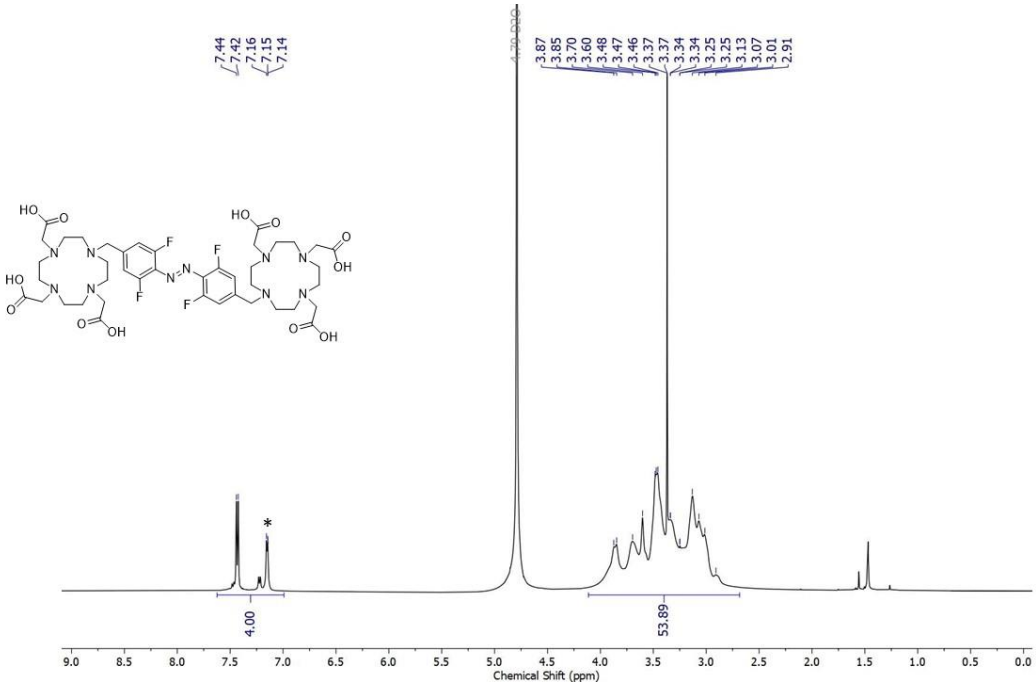

*Figure S23: ^{1}H NMR spectrum of compound $\mathbf{L_b}$ (D_2O, 400 MHz, 298 K), * represent the signals from the corresponding Z-isomer.*

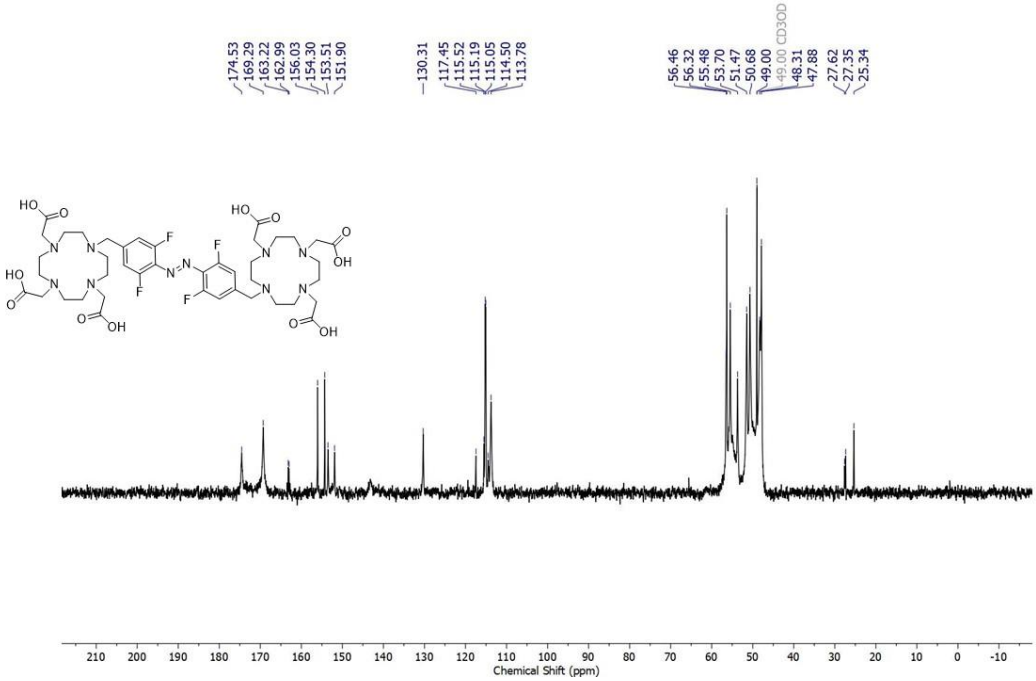

*Figure S24: ^{13}C NMR spectrum of compound **L_b** (D_2O, 151 MHz, 298 K).*

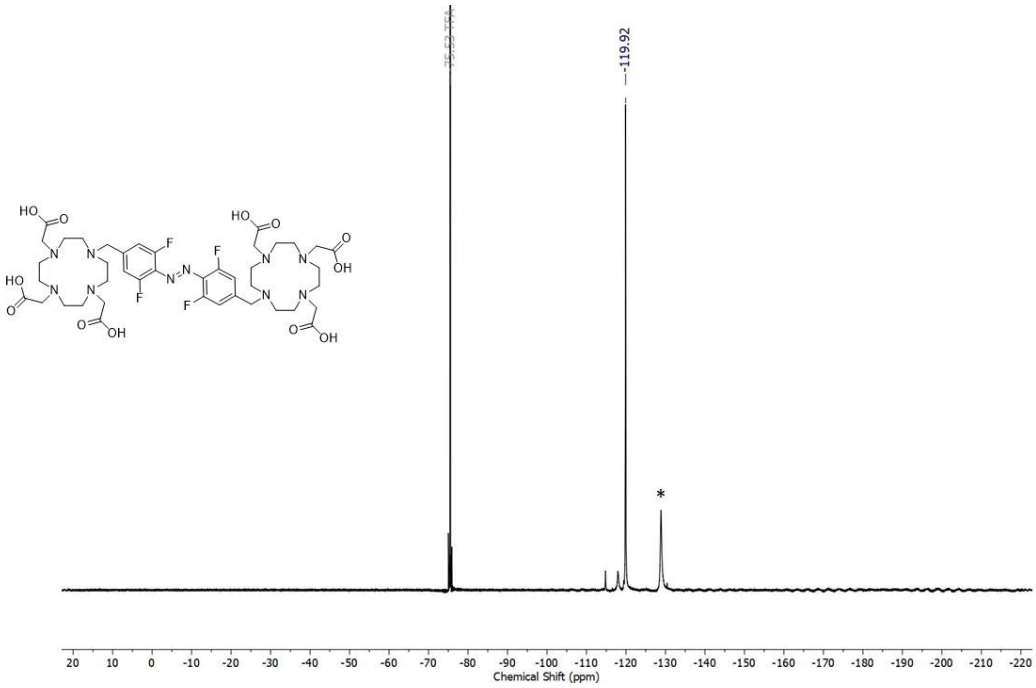

*Figure S25: ^{19}F NMR spectrum of compound **L_b** (D_2O, 565 MHz, 298 K), * represent the signals from the corresponding Z-isomer.*

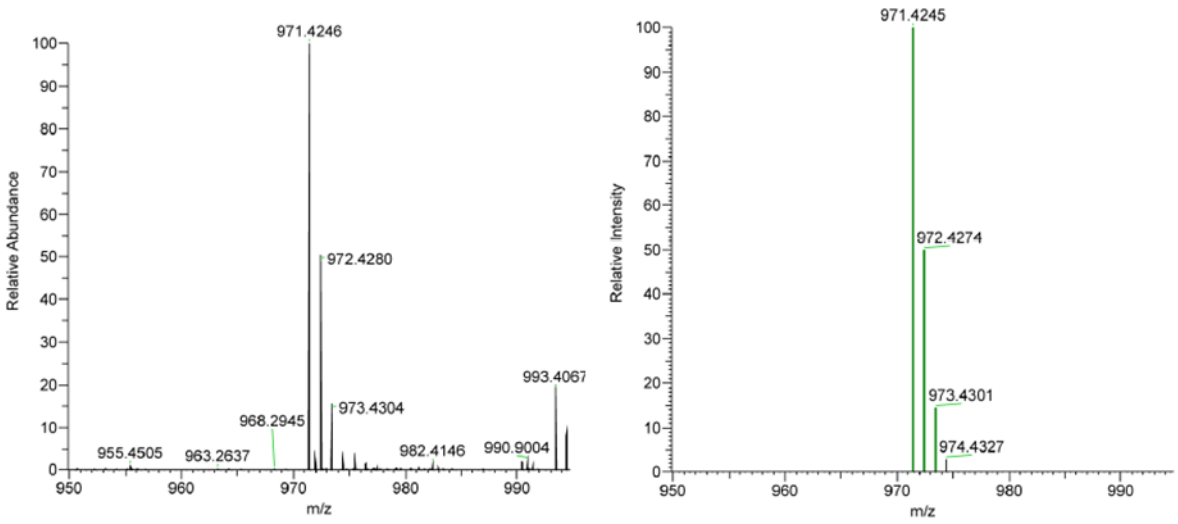

Figure S26: ***HR-ESI-MS*** *spectrum of compound* $\mathbf{L_b}$*, obsd 971.4246 , calcd 971.4245* $[(M + H)^+$*,* $M = C_{42}H_{58}F_4N_{10}O_{12}]$

Synthesis of LnL_a:

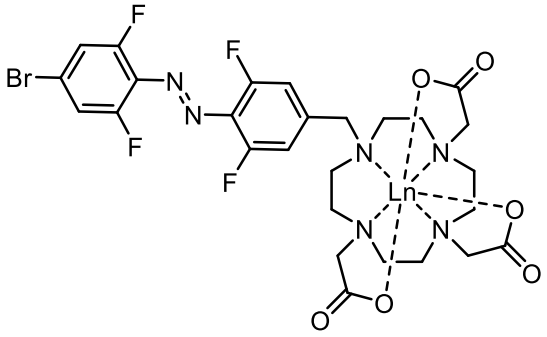

L_a (50 mgs, 72 mmol) and $Ln(OTf)_3$ (1.25 eq.) were added to a HPLC vial and dissolved in 1.44 mL of a EtOH:Water (1:1) solution. The vial was sealed, heated to 50 °C and left to stir overnight. To this NaOH (10 mg, 252 mmol, 3.5 eq.) was added portion wise (1.5 eq, 1.5 eq, 0.5 eq) over the next three hours. The vial was then sealed again and left for 2 days. The precipitate was collected, purified by dialysis and dried to yield an orange solid (quant.) in an orange precipitate forming.

EuL_a HR-ESI-MS obsd 841.0453 , calcd 841.0475 [$(M + H)^+$, M = $C_{27}H_{29}BrF_4N_6O_6Eu$]

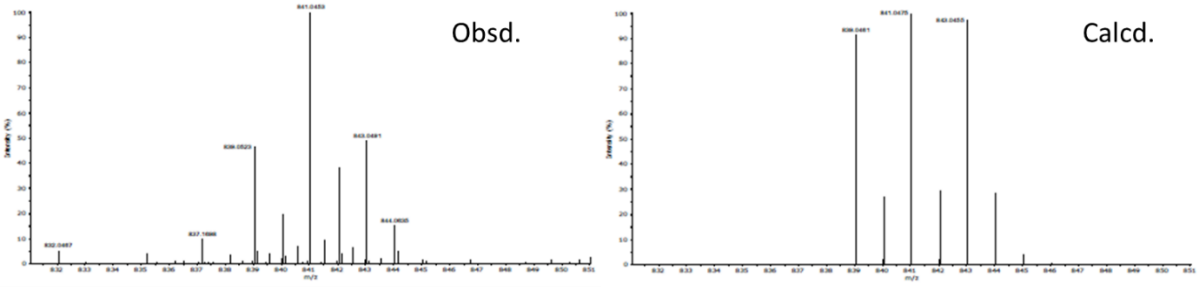

*Figure S27: **HR-ESI-MS** spectrum of **EuL_a**, obsd 841.0453 , calcd 841.0475 [$(M + H)^+$, M = $C_{27}H_{29}BrF_4N_6O_6Eu$]*

NdL_a HR-ESI-MS obsd 831.0378 , calcd 831.0418 [$(M + H)^+$, M = $C_{27}H_{29}BrF_4N_6O_6Nd$]

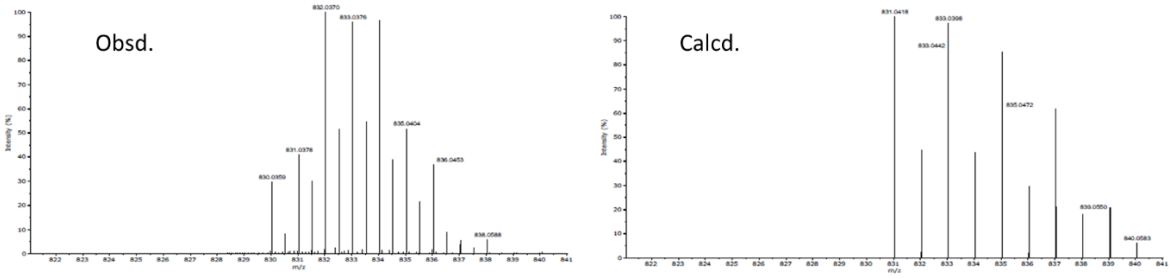

*Figure S28: **HR-ESI-MS** spectrum of **NdL_a**, obsd 831.0378 , calcd 831.0418 [$(M + H)^+$, M = $C_{27}H_{29}BrF_4N_6O_6Nd$]*

Synthesis of Ln_2L_b:

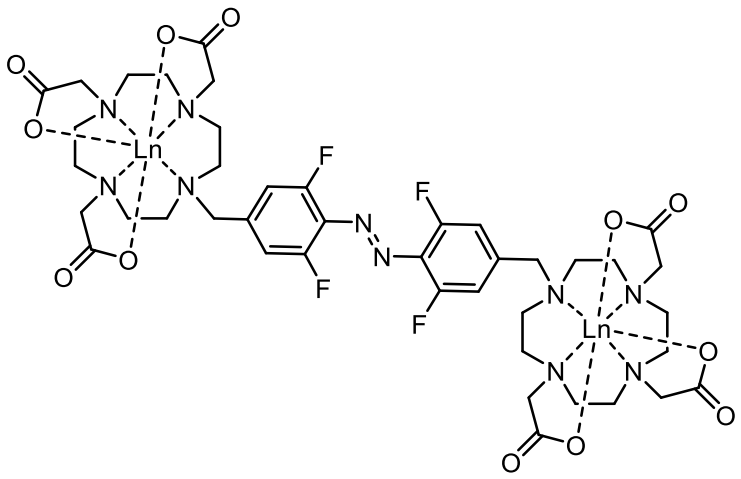

L_b (50 mgs, 52 mmol) and $Ln(OTf)_3$ (2.5 eq.) were added to a HPLC vial and dissolved in 1.00 mL of a EtOH:Water (1:1) solution. The vial was sealed, heated to 50 °C and left to stir for 24 hrs. To this, NaOH (14 mg, 360 mmol, 7 eq.) was added portion wise (3 eq., 3 eq., 1 eq.) over the next three hours. The vial was then sealed again and left for 2 days. The precipitate was collected, purified by dialysis and dried to yield an orange solid (quant.).

Eu_2L_b HR-ESI-MS obsd 1271.2263 , calcd 1271.2200 [$(M + H)^+$, M = $C_{42}H_{53}F_4N_{10}O_{12}Eu_2$]

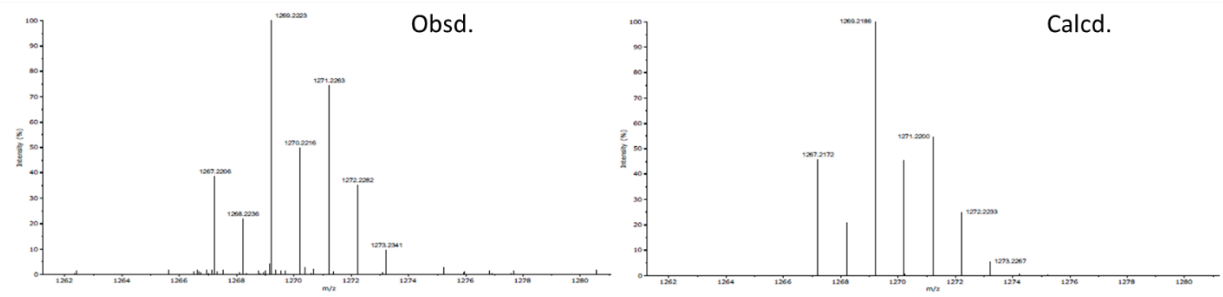

*Figure S29: **HR-ESI-MS** spectrum of **Eu_2L_b**, obsd 841.0453 , calcd 841.0475 [$(M + H)^+$, M = $C_{42}H_{53}F_4N_{10}O_{12}Eu_2$]*

Nd_2L_b HR-ESI-MS obsd 1249.1957 , calcd 1249.1930 [$(M + H)^+$, M = $C_{42}H_{53}F_4N_{10}O_{12}Nd_2$]

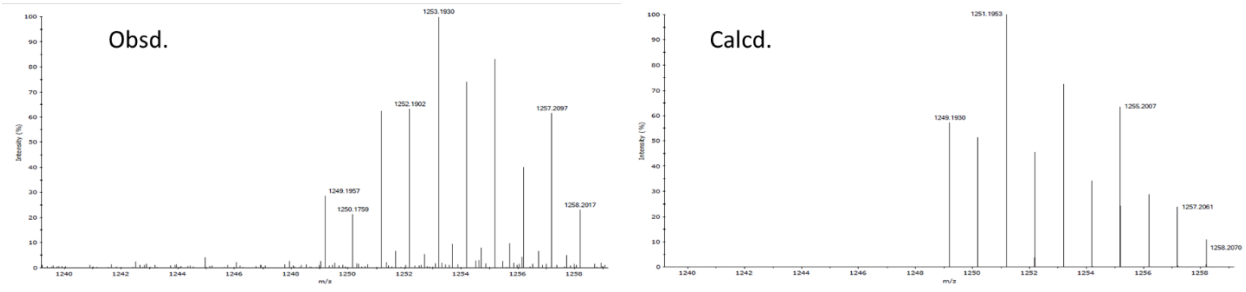

*Figure S30: **HR-ESI-MS** spectrum of **Nd_2L_b**, obsd 1249.1957 , calcd 1249.1930 [$(M + H)^+$, M = $C_{42}H_{53}F_4N_{10}O_{12}Nd_2$]*

^{1}H and ^{19}F NMR:

EuL_a

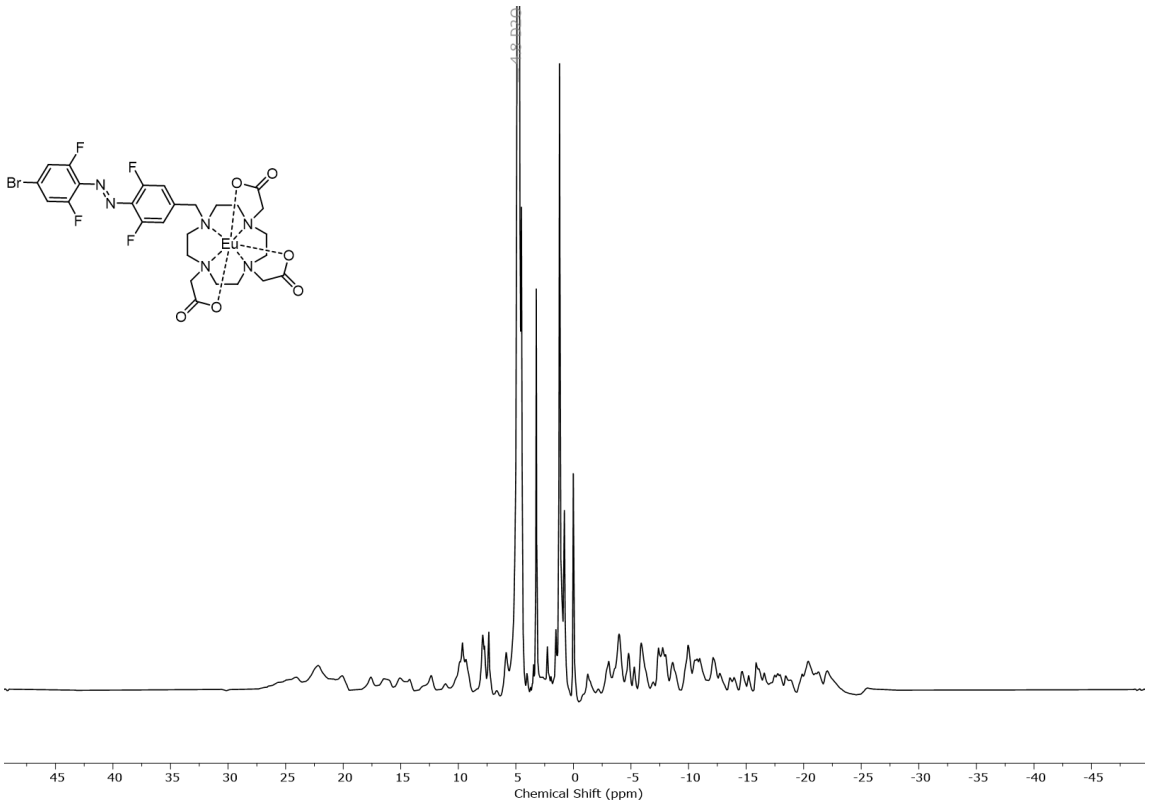

*Figure S31: ^{1}H NMR spectrum of compound **EuL_a** (D_2O, 400 MHz, 298 K)*

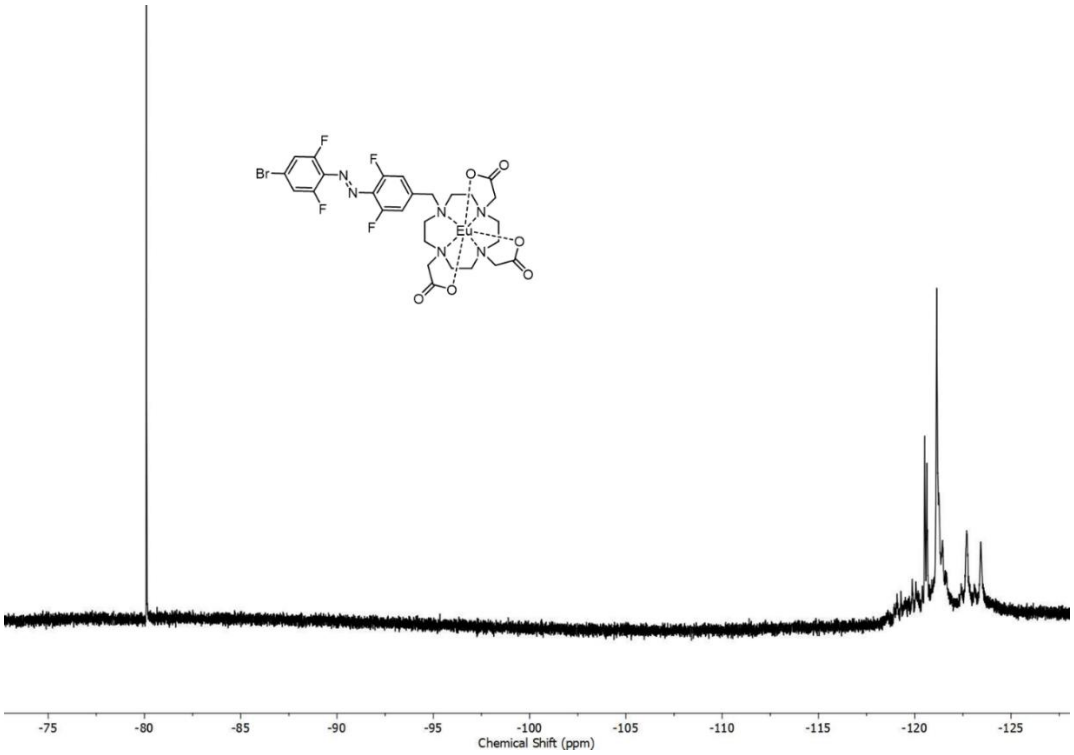

*Figure S32: ^{19}F NMR spectrum of compound **EuL_a** (D_2O, 565 MHz, 298 K)*

Eu_2L_b

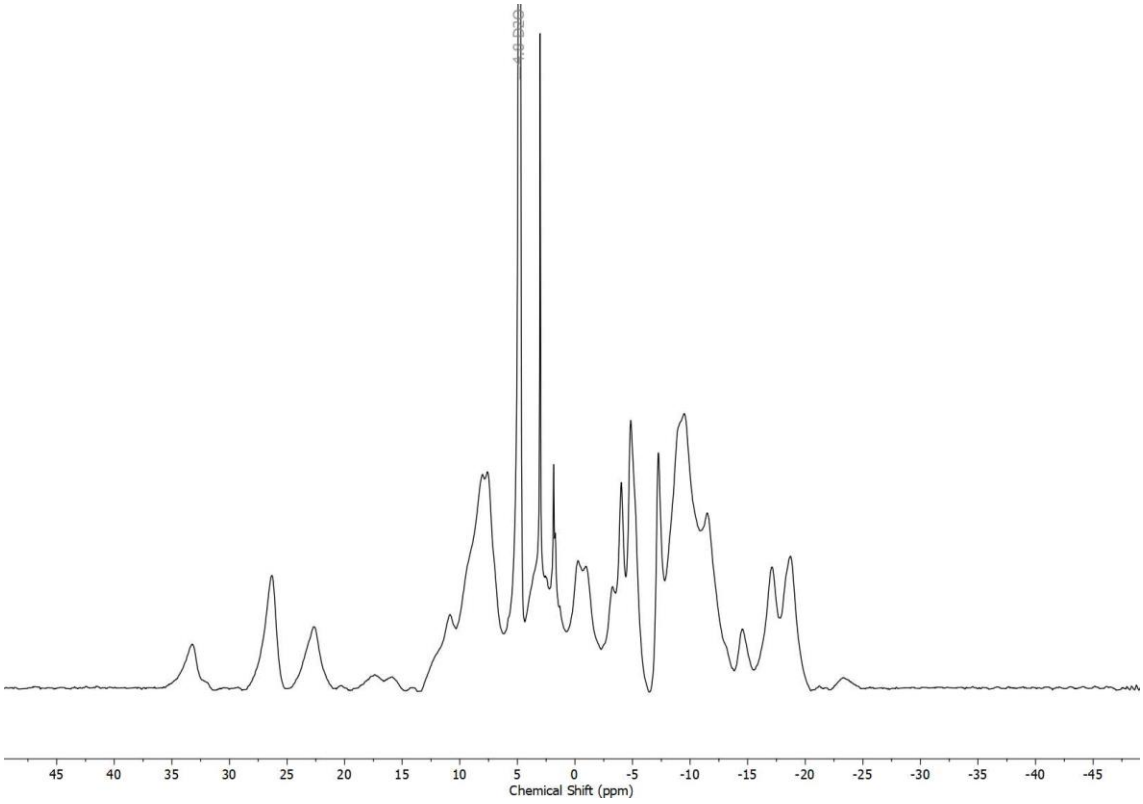

*Figure S33: [1]H NMR spectrum of compound **Eu_2L_b** (D_2O, 400 MHz, 298 K)*

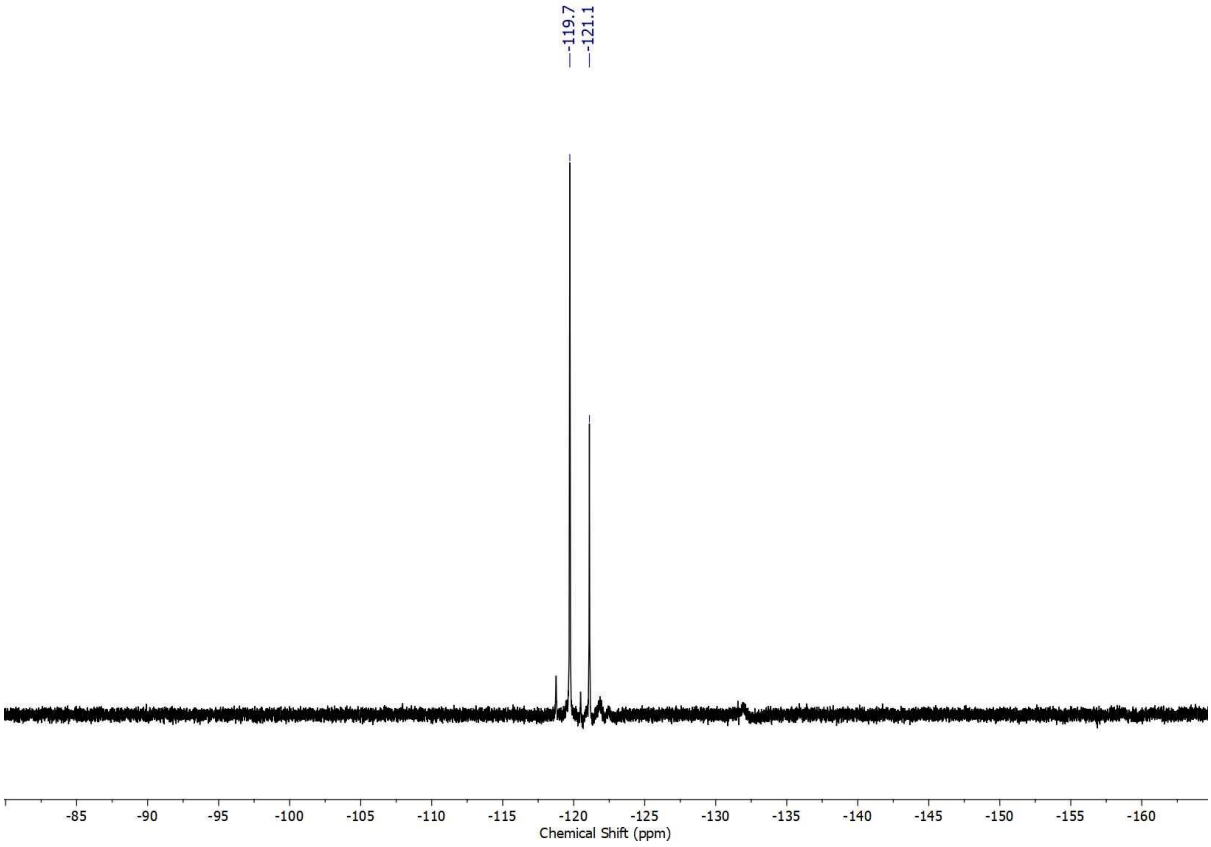

*Figure S34: Figure 1: [19]F NMR spectrum of compound **Eu_2L_b** (D_2O, 565 MHz, 298 K)*

HPLC:

All HPLC analysis were carried out on a Thermo Scientific Vanquish Core HPLC on an analytical Discovery® Cyano 25 cm × 4.6 mm, 5µm column fitted with a Discovery® Cyano 2 cm × 4.0 mm, 5µm guard column. All samples were filtered using a fisherbrand PTFE filter with 0.2um pore size. Unless otherwise stated HPLC traces were monitored at 272 nm. Methods are detailed below.

Flow rate: 1 mL/min

Method 1:

Time (min)	MeCN (0.1% Formic Acid) (%)	H_2O (0.1% Formic Acid) (%)
0.0	5.0	95.0
14.9	50.0	50.0
15.0	95.0	5.0
19.9	95.0	5.0
20.0	5.0	95.0

Method 2:

Time (min)	MeCN (0.1% Formic Acid) (%)	H_2O (0.1% Formic Acid) (%)
0.0	2.0	98.0
5.0	2.0	98.0
25.0	100.0	0.0
27.0	100.0	0.0
29.0	2.0	98.0
35.0	2.0	98.0

EuL_a

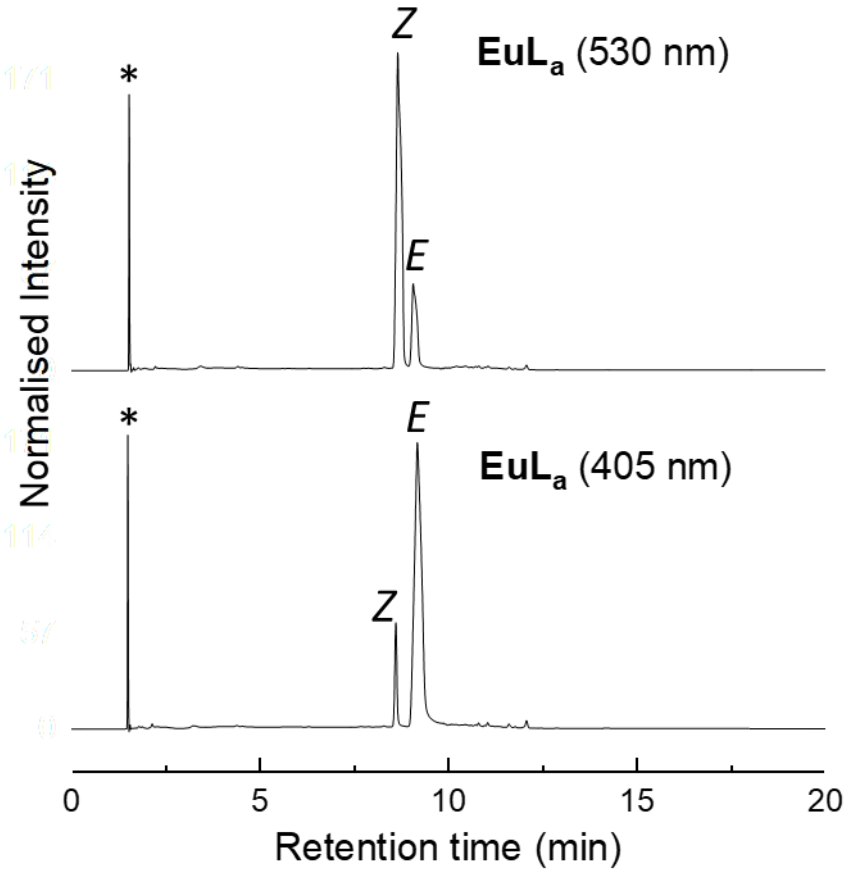

*Figure S35: HPLC trace of EuL_a upon irradiation with 530 nm and 405 nm for 10 minutes, respectively, recorded at 272 nm using method 1 where * represents the solvent front.*

Eu_2L_b

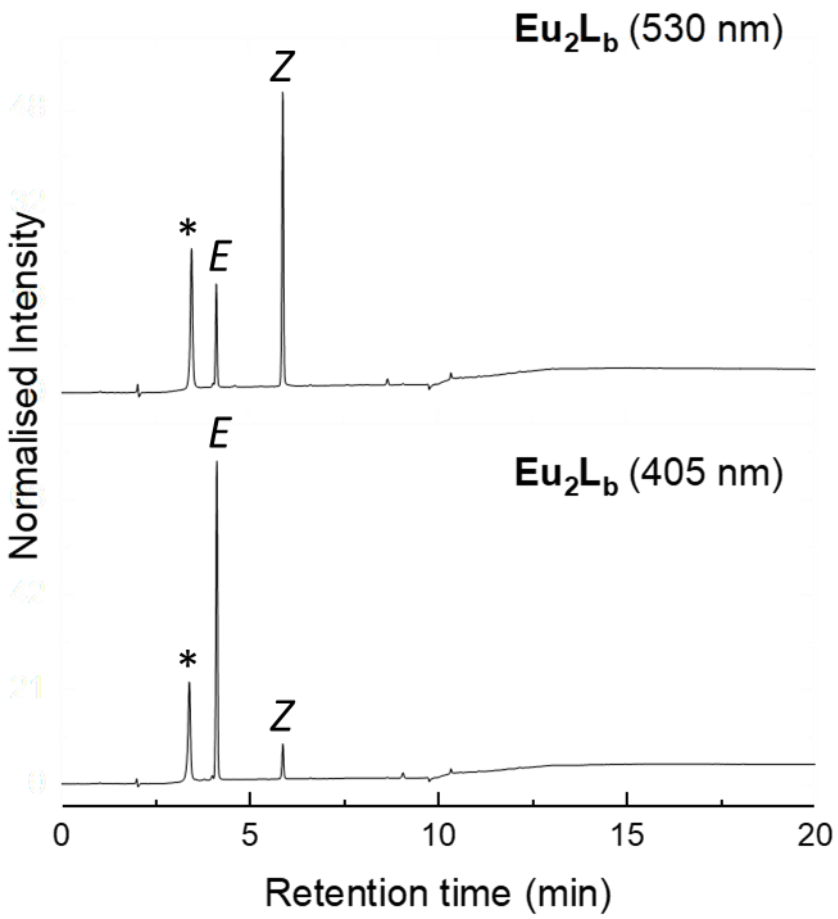

*Figure S36: HPLC trace of Eu_2L_b upon irradiation with 530 nm and 405 nm for 10 minutes, respectively, recorded at 272 nm using method 1 where * represents the solvent front.*

NdL_a

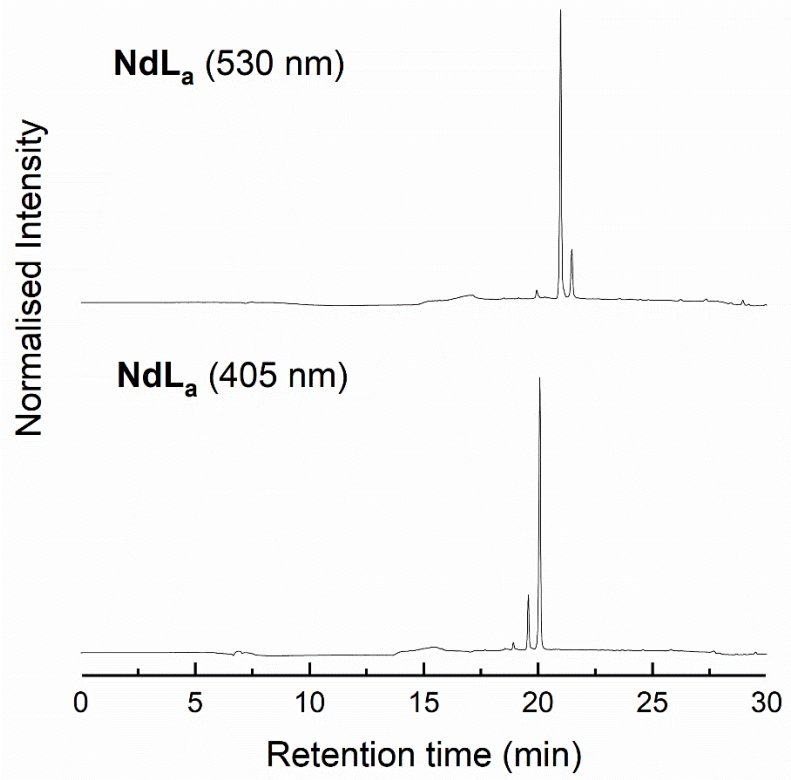

Figure S37: HPLC trace of NdL_a upon irradiation with 530 nm and 405 nm for 10 minutes, respectively, recorded at 272 nm using method 2.

Nd_2L_b

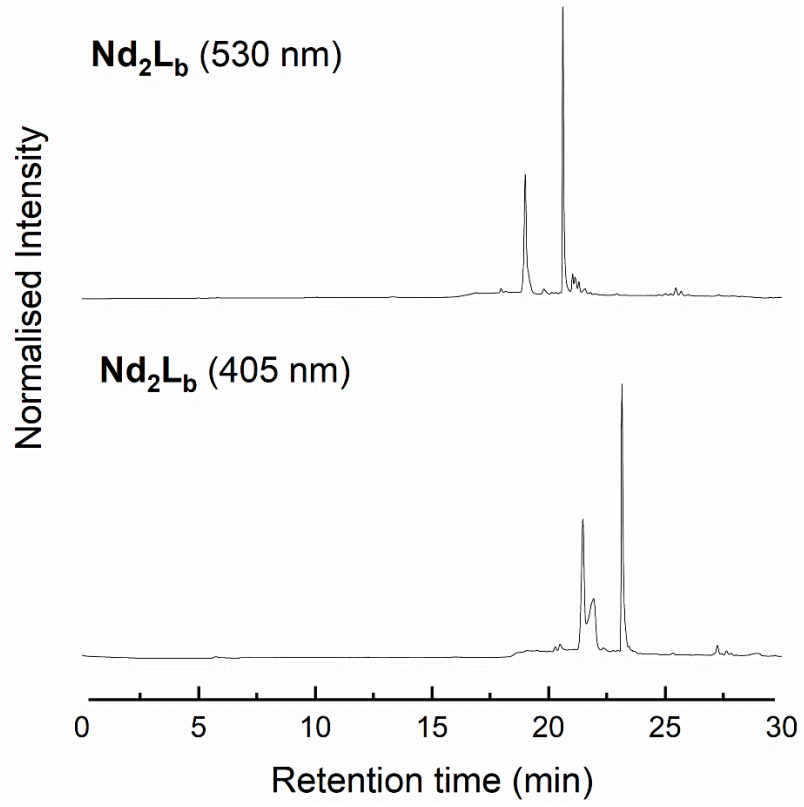

Figure S38: HPLC trace of Nd_2L_b upon irradiation with 530 nm and 405 nm for 10 minutes, respectively, recorded at 272 nm using method 2.

Photoswitching experiments

Photo-irradiation of liquid samples was carried out using Thorlabs high-power mounted LEDs; M530L4 (green, 530 nm) and M405L4 (purple, 405 nm) in-house custom built set-ups using optical components supplied by Thorlabs, as described in reference 3.[4] All UV-vis spectra were determined in DMSO solution. All measurements were performed at room temperature, unless otherwise stated, in a 10 mm quarts cuvette from Starna Scientific (23/Q /10) or Hellma Analytics (SUPRASIL). Electron absorption measurements were recorded on a Jasco V-770 UV-Visible/NIR spectrophotometer operated under Spectra ManagerTM suite. Points were recorded at 0.2 nm interval with UV/Vis bandwidth of 1 nm, UV/Vis response of 0.06 sec in continuous scan mode at the rate of 400 nm/min. For each compound, the *E* isomer sample at 40 μM was irradiated with the appropriate wavelength of light to generate the photo-stationary state, and another spectrum was run, this was repeated until the PSS had been reached. This was repeated for the *Z* isomer.

The photo-stationary states upon irradiation with 405 and 530 nm were determined by HPLC. Each sample was irradiated with either 405 or 530 nm light for 10 minutes. The isosbestic point for each complex was determined from absorbance measurements and found to be at 377 nm. Determined UV-vis absorption at 377 nm for each sample irradiated with light were analysed and the areas under the peaks integrated to give the relative ratios of each isomer at the PSS. Using the determined ratios after irradiation with both 405 and 530 nm light and the corresponding absorbance spectra, the absorbance of 100% *E*/*Z* was calculated.

$$PSS_E = a[E] + b[Z]$$

$$PSS_Z = c[E] + d[Z]$$

a = percentage of *E* at PSS_E , b = percentage of *Z* at PSS_E , c = percentage of *E* at PSS_z , d = percentage of *Z* at PSS_z.

To calculate the degree of isomerisation upon irradiation to excite the lanthanide the following equation was used:

$$ID = \frac{Abs_{Ex} - Abs_{PSS}}{Abs_{PSS}} \times 100$$

Where ID = Degree of isomerisation (%) Abs_{Ex} = Absorption after excitation of lanthanide, Abs_{PSS} = Abs at PSS (405 or 530 nm). This was calculated at the maximum absorbance wavelength of the n $\rightarrow\pi^*$ transition for both isomers. Once calculated this was compared with the original distribution of isomers in each PSS to give the new isomer distribution.

EuL_a

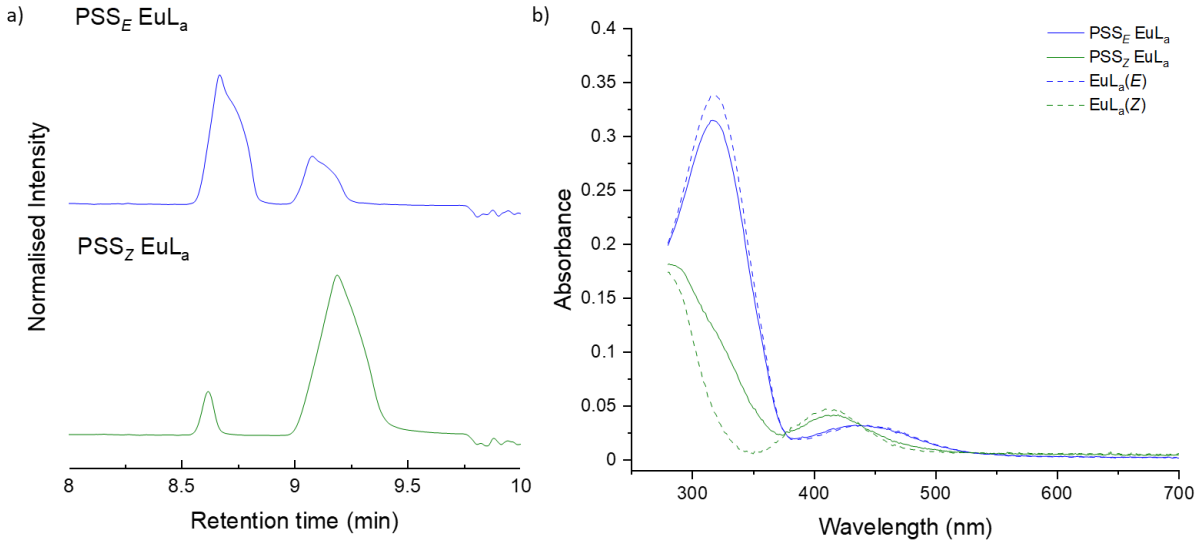

Figure S39: a) HPLC trace of EuL_a (PSS_E and PSS_Z) using method 1, blue line represents the trace after irradiation of EuL_a with 405 nm light for 10 minutes, the green line represents the trace after irradiation of EuL_a with 530 nm light for 10 minutes. b) Absorbance of EuL_a (PSS_E, PSS_Z, E and Z) solid blue line represents the trace after irradiation of EuL_a with 405 nm light for 10 minutes, the solid green line represents the trace after irradiation of EuL_a with 530 nm light for 10 minutes, the dashed blue and green line represent the calculated absorbance of pure E and Z isomers respectively.

Table S1: Percentage of each isomer (E and Z) present at PSS_E (405 nm) and PSS_Z (530 nm) as determined from the area under the curve of the 2 peaks in the HPLC trace for EuL_a.

	%*E*	**%Z**
405 nm	92	8
530 nm	26	74

Eu_2L_b

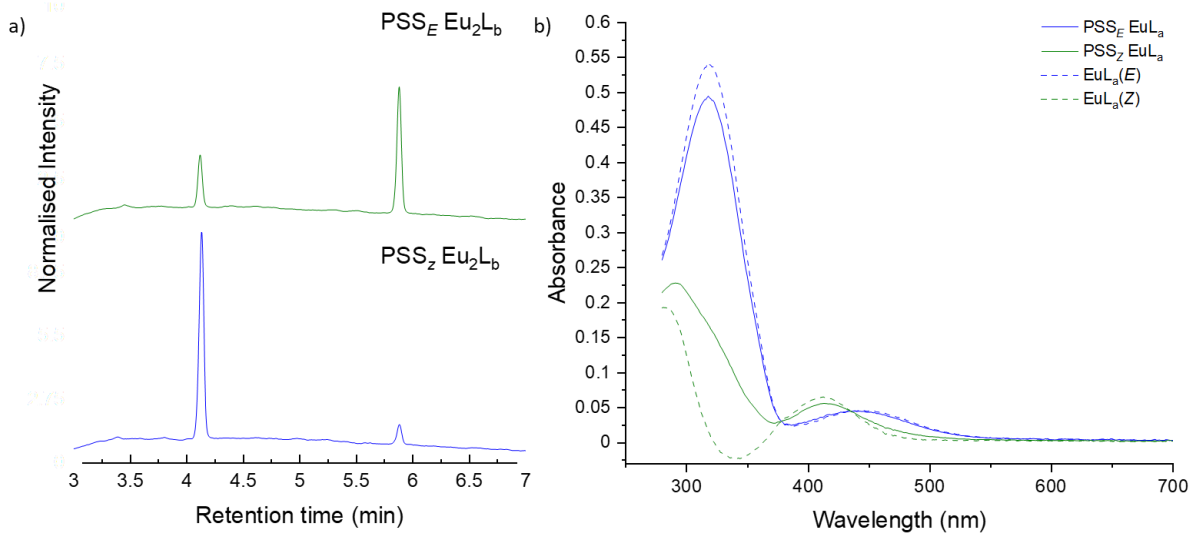

Figure S40: a) HPLC trace of Eu_2L_b (PSS_E and PSS_Z) using method 1, blue line represents the trace after irradiation of Eu_2L_b with 405 nm light for 10 minutes, the green line represents the trace after irradiation of Eu_2L_b with 530 nm light for 10 minutes. b) Absorbance of Eu_2L_b (PSS_E, PSS_Z, E and Z) solid blue line represents the trace after irradiation of Eu_2L_b with 405 nm light for 10 minutes, the solid green line represents the trace after irradiation of Eu_2L_b with 530 nm light for 10 minutes, the dashed blue and green line represent the calculated absorbance of pure E and Z isomers respectively.

Table S2: Percentage of each isomer (E and Z) present at PSS_E (405 nm) and PSS_Z (530 nm) as determined from the area under the curve of the 2 peaks in the HPLC trace for Eu_2L_b.

	%E	***%Z***
405 nm	91	9
530 nm	29	71

NdL_a

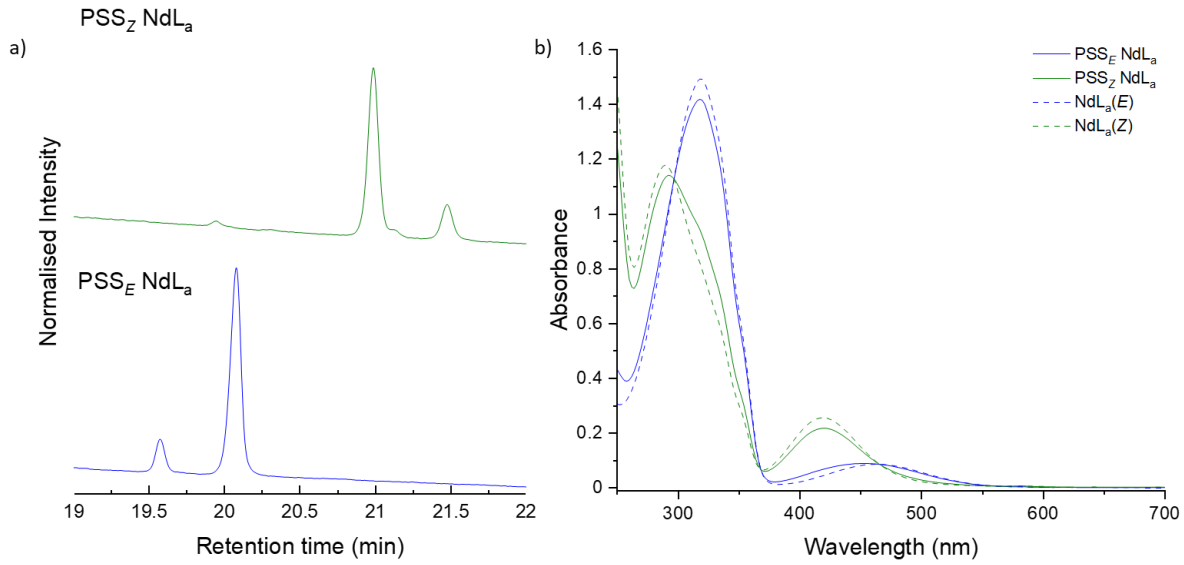

Figure S41: a) HPLC trace of NdL_a (PSS_E and PSS_Z) using method 2, blue line represents the trace after irradiation of NdL_a with 405 nm light for 10 minutes, the green line represents the trace after irradiation of NdL_a with 530 nm light for 10 minutes. b) Absorbance of NdL_a (PSS_E, PSS_Z, E and Z) solid blue line represents the trace after irradiation of NdL_a with 405 nm light for 10 minutes, the solid green line represents the trace after irradiation of NdL_a with 530 nm light for 10 minutes, the dashed blue and green line represent the calculated absorbance of pure E and Z isomers respectively.

Table S3: Percentage of each isomer (E and Z) present at PSS_E (405 nm) and PSS_Z (530 nm) as determined from the area under the curve of the 2 peaks in the HPLC trace for NdL_a.

	%*E*	**%Z**
405 nm	89	11
530 nm	18	82

Nd_2L_b

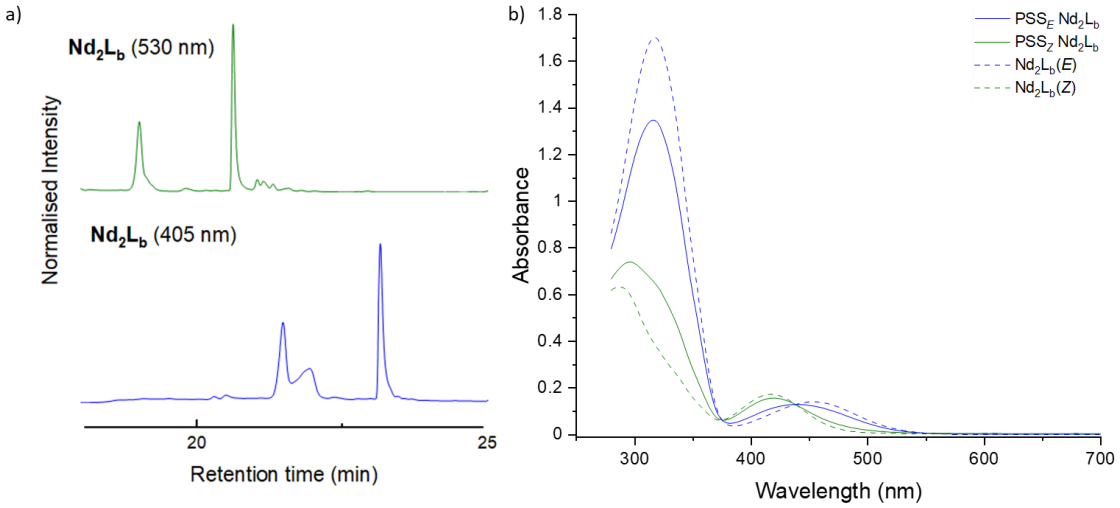

Figure S42: a) HPLC trace of Nd_2L_b (PSS_E and PSS_Z) using method 2, blue line represents the trace after irradiation of Nd_2L_b with 405 nm light for 10 minutes, the green line represents the trace after irradiation of Nd_2L_b with 530 nm light for 10 minutes. b) Absorbance of Nd_2L_b (PSS_E, PSS_Z, E and Z) solid blue line represents the trace after irradiation of Nd_2L_b with 405 nm light for 10 minutes, the solid green line represents the trace after irradiation of Nd_2L_b with 530 nm light for 10 minutes, the dashed blue and green line represent the calculated absorbance of pure E and Z isomers respectively.

Table S4: Percentage of each isomer (E and Z) present at PSS_E (405 nm) and PSS_Z (530 nm) as determined from the area under the curve of the 2 peaks in the HPLC trace for Nd_2L_b.

	%*E*	**%Z**
405 nm	73	27
530 nm	20	80

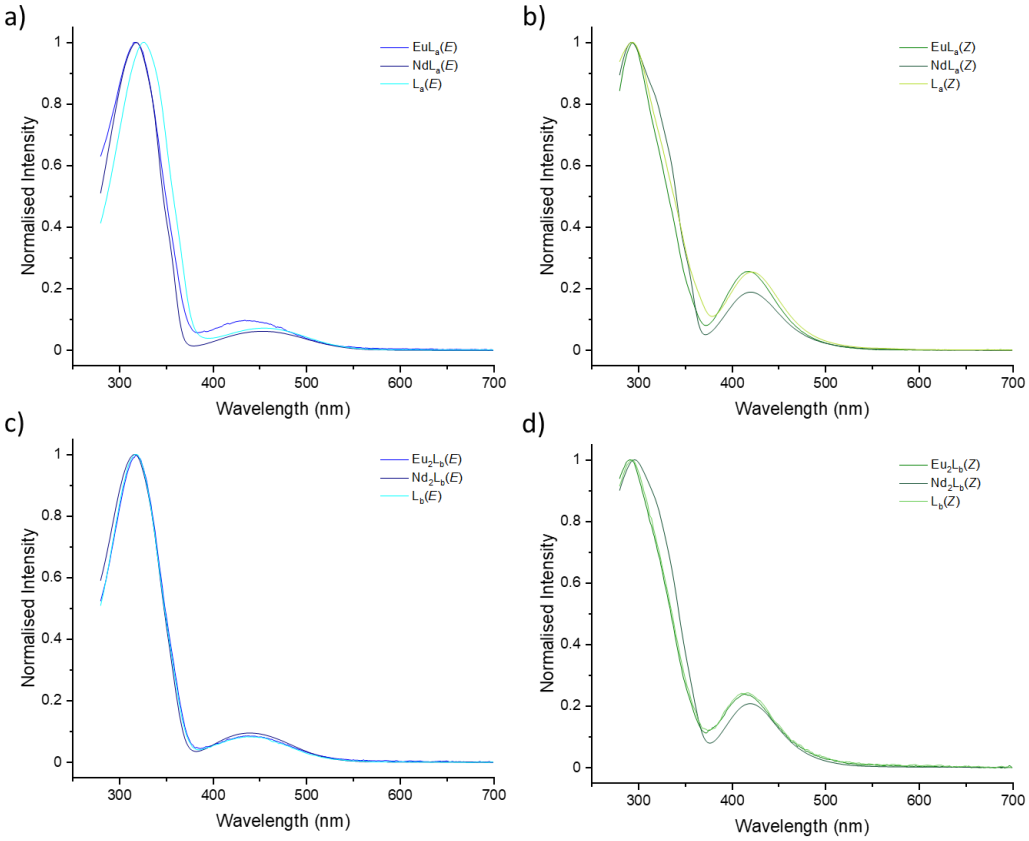

Figure S43: Normalised absorbance spectra a) Comparison of absorbance spectra of EuL_a, NdL_a and L_a after each sample was irradiated with 405 nm light for 10 minutes in DMSO b) Comparison of absorbance spectra of EuL_a, NdL_a and L_a after each sample was irradiated with 530 nm light for 10 minutes in DMSO c) Comparison of absorbance spectra of Eu_2L_b, Nd_2L_b and L_b after each sample was irradiated with 405 nm light for 10 minutes in DMSO b) Comparison of absorbance spectra of Eu_2L_b, Nd_2L_b and L_b after each sample was irradiated with 530 nm light for 10 minutes in DMSO.

Spectroscopy:

Steady state emission spectra

Steady State excitation and emission spectra of organic ligands were recorded on a Horiba Jobin Yvon Fluorolog® 3-12 Fluorometer equipped with a Hamamatsu R928 detector and a double-grating emission monochromator. S1 response was used throughout as luminescence output. Emission and excitation slits were fixed at 5 and 1 nm, respectively the step size was 1 nm and the integration time set to 0.1 s. Excitation were determined by the peaks in the absorbance spectra of each isomer and are detailed in the individual experiment.

Europium(III) excitation and emission spectra were carried out on a PTI QuantaMaster8075 instrument from Horiba Scientific using a xenon arc lamp for excitation. The excitation wavelength was fixed at 395 nm. The temperature was kept constant at 20 °C, with a Koolance EXT-440 liquid cooling system from Horiba Scientific. For samples recorded at 77 K, a constant nitrogen flow in the sample chamber was maintained to avoid condensation on the NMR tube Emission and excitation slits were fixed at 1 and 5 nm, respectively the step size was 0.5 nm and the integration time set to 0.2 s. The emission wavelength was set at 617 nm emission and excitation slits were set at 5 and 1 nm respectively, the step size was 0.5 nm and the integration time was 0.2 s.

Neodymium (III) emission spectra were measured on a custom built spectrometer.[5] The samples were excited by a supercontinuum laser (NKT SuperK Fianium FIU-15) that was coupled to a tuneable bandpass filter (NKT LLTF Contrast VIS/SWIR HP8). The laser power was set to 90% with the maximum repetition rate (78 MHz). A 750B grating was used for measurements below the 950 nm point, and a 1200B grating was used for measurements above 950 nm. The emission slit was set to 25 µm for all measurements. For neodymium(III), the excitation wavelength was set to 580 nm, a long-pass filter of 800 nm was used, and the centre wavelength of the detector set to 880 or 1050 nm for the two regions of interest. For samples recorded at 77K, a constant nitrogen flow in the sample chamber was maintained to avoid condensation on the cuvette.

Neodymium (III) excitation spectra were recorded by changing the wavelength of the excitation source through our own Python code that connects to the tuneable bandpass filter. At each excitation wavelength, an emission spectrum was recorded and integrated by summing all data points spanning the region of interest; the wavelength range chosen. Two different acquisitions were used: (1) the excitation source was scanned from 450 to 835 nm, the exposure time was 100 ms with 1 exposure per frame, and the data points were summed from 840 to 940 nm; (2) the excitation source was scanned from 773 to 920 nm, the exposure time was 1000 ms with 10 exposures per frame, and the data points were summed from 1040 to 1070 nm.[5, 6]

All spectra are corrected for lamp efficiency and solvent baselines.

Time resolved emission spectra

Time-resolved measurements were carried out on a PTI QuantaMaster8075 instrument from Horiba Scientific using a xenon flash lamp as the excitation source. All decay traces were fitted to a monoexponential decay using the Origin 2017 (OriginLab) software. Most lifetimes gave satisfactory fitting using a mono exponential decay function; fitting to a double exponential decay only improved the fit for **Eu_2L_b** at 77 K.

EuL_a

Steady State Measurements

E-Isomer

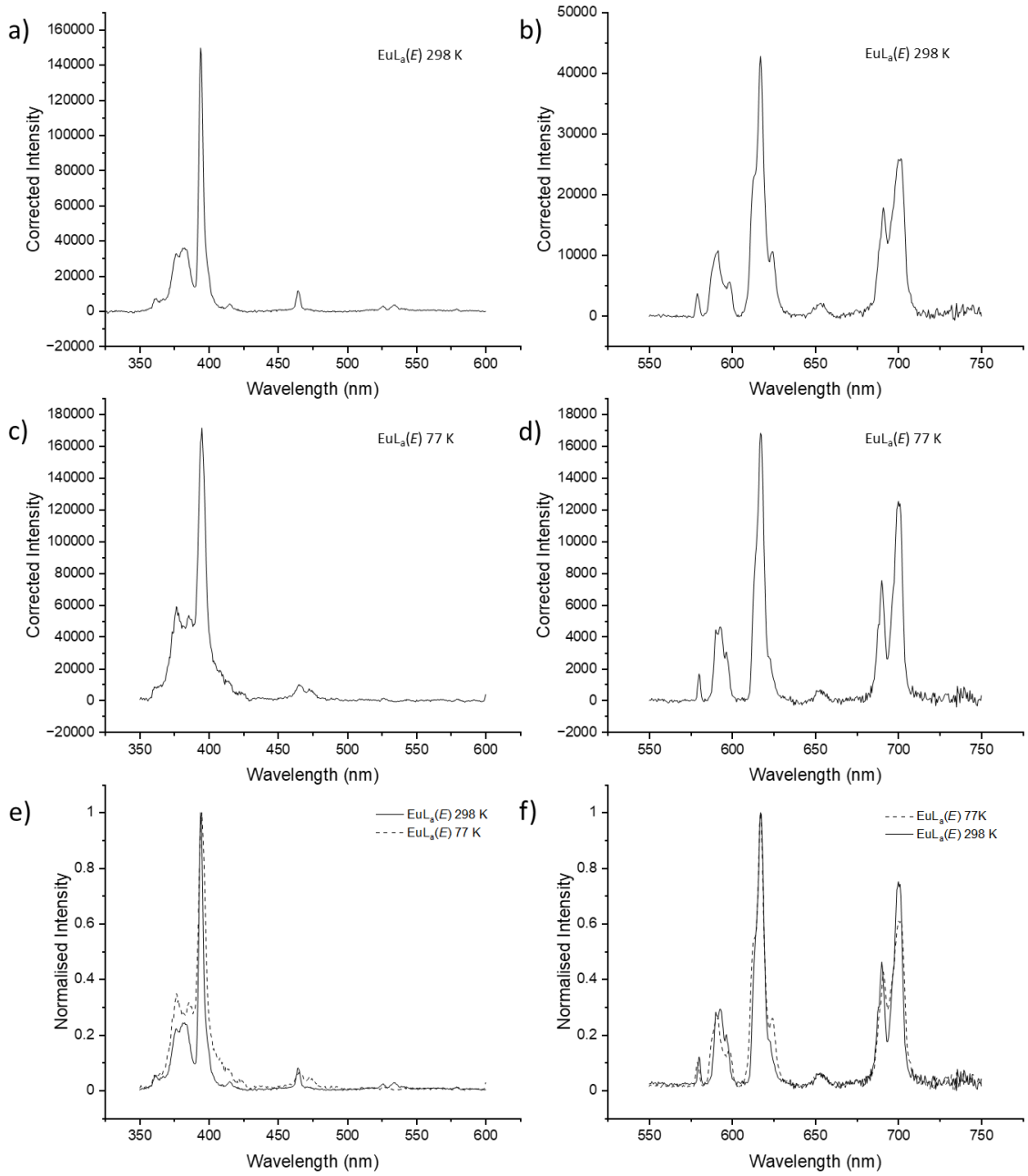

Figure S44: a) Excitation spectra of $EuL_a(E)$ at 298 K, λ_{em} = 616 nm, excitation slits 1 nm, emission slit 5 nm, integration time 0.2s b) Emission spectra of $EuL_a(E)$ at 298 K, λ_{ex} = 395 nm, emission slits 1 nm, excitation slit 5 nm, integration time 0.2s c) Excitation spectra of $EuL_a(E)$ at 77 K, λ_{em} = 616 nm, excitation slits 1 nm, emission slit 5 nm, integration time 0.2s d) Emission spectra of $EuL_a(E)$ at 77 K, λ_{ex} = 395 nm, emission slits 1 nm, excitation slit 5 nm, integration time 0. e) Comparison of a) and c) where intensities are normalised f) Comparison of b) and d) where intensities are normalised.

Z-Isomer

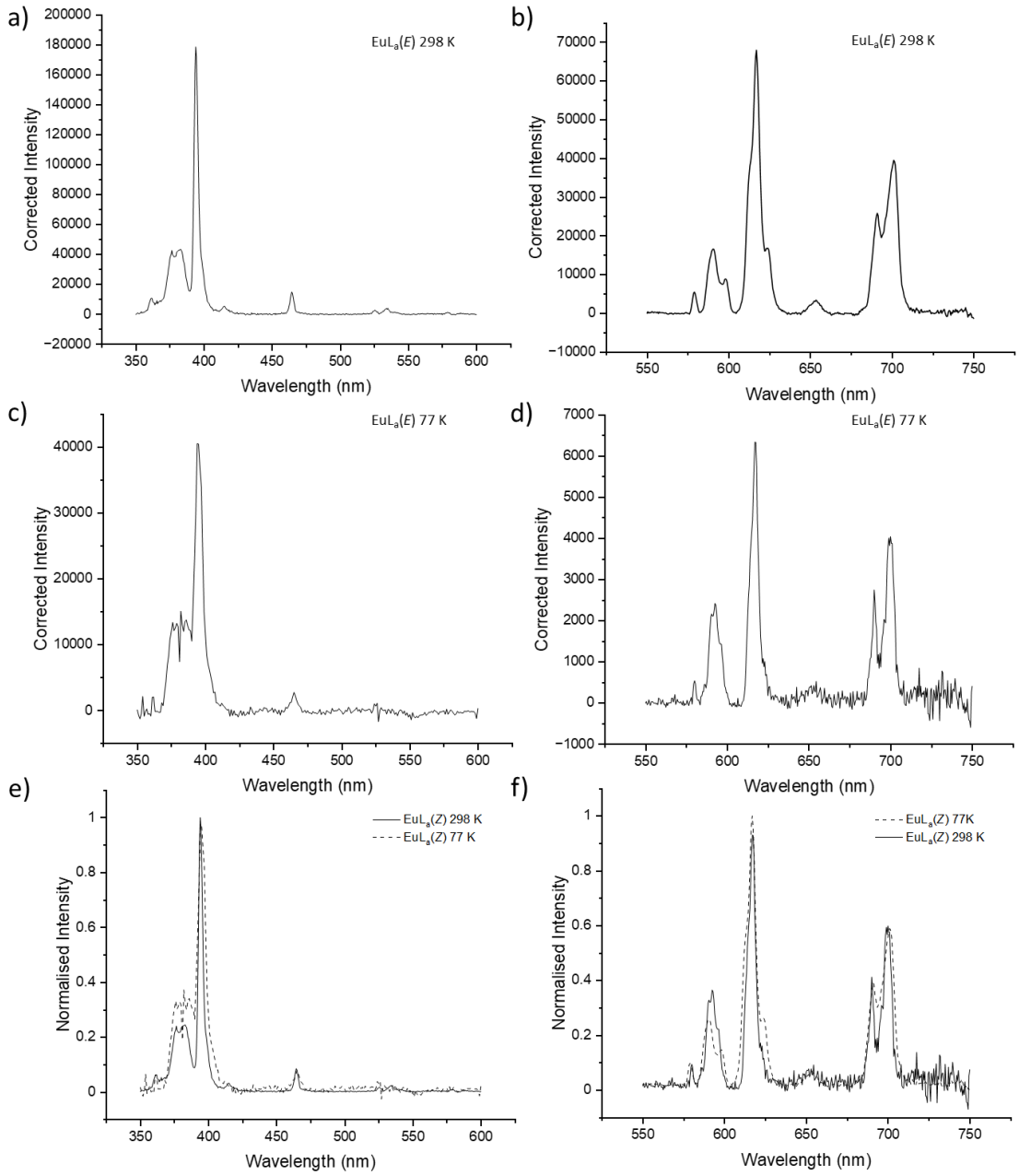

Figure S45: a) Excitation spectra of EuL$_a$(Z) at 298 K, λ_{em} = 616 nm, excitation slits 1 nm, emission slit 5 nm, integration time 0.2s b) Emission spectra of EuL$_a$(Z) at 298 K, λ_{ex} = 395 nm, emission slits 1 nm, excitation slit 5 nm, integration time 0.2s c) Excitation spectra of EuL$_a$(Z) at 77 K, λ_{em} = 616 nm, excitation slits 1 nm, emission slit 5 nm, integration time 0.2s d) Emission spectra of EuL$_a$(Z) at 77 K, λ_{ex} = 395 nm, emission slits 1 nm, excitation slit 5 nm, integration time 0.2s e) Comparison of a) and c) where intensities are normalised f) Comparison of b) and d) where intensities are normalised.

Comparison between Isomers

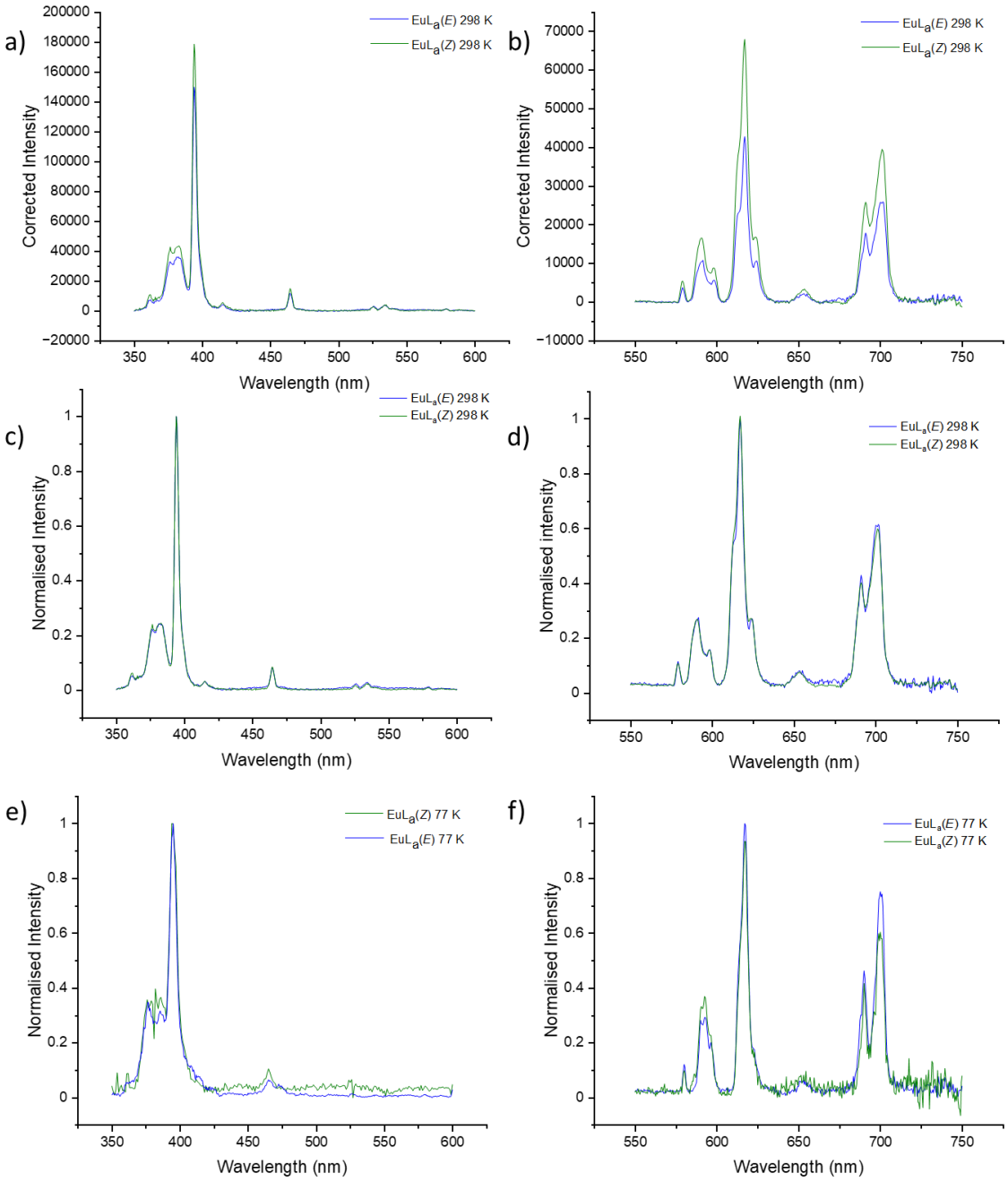

Figure S46: a) Excitation spectra of EuL$_a$(E) (blue line) and EuL$_a$(Z) (green line) at 298 K, λ_{em} = 616 nm, excitation slits 1 nm, emission slit 5 nm, integration time 0.2s b) Emission spectra of EuL$_a$(E) (blue line) and EuL$_a$(Z) (green line) at 298 K, λ_{ex} = 395 nm, emission slits 1 nm, excitation slit 5 nm, integration time 0.2s c) Excitation spectra of EuL$_a$(E) (blue line) and EuL$_a$(Z) (green line) at 298 K where intensities are normalised d) Emission spectra of EuL$_a$(E) (blue line) and EuL$_a$(Z) (green line) at 77 K, where intensities are normalised e) Excitation spectra of EuL$_a$(E) (blue line) and EuL$_a$(Z) (green line) at 77 K, λ_{em} = 616 nm, excitation slits 1 nm, emission slit 5 nm, integration time 0.2s where intensities are normalised f) Emission spectra of EuL$_a$(E) (blue line) and EuL$_a$(Z) (green line) at 77 K, λ_{ex} = 395 nm, emission slits 1 nm, excitation slit 5 nm, integration time 0.2s where intensities are normalised.

Time Resolved Measurements

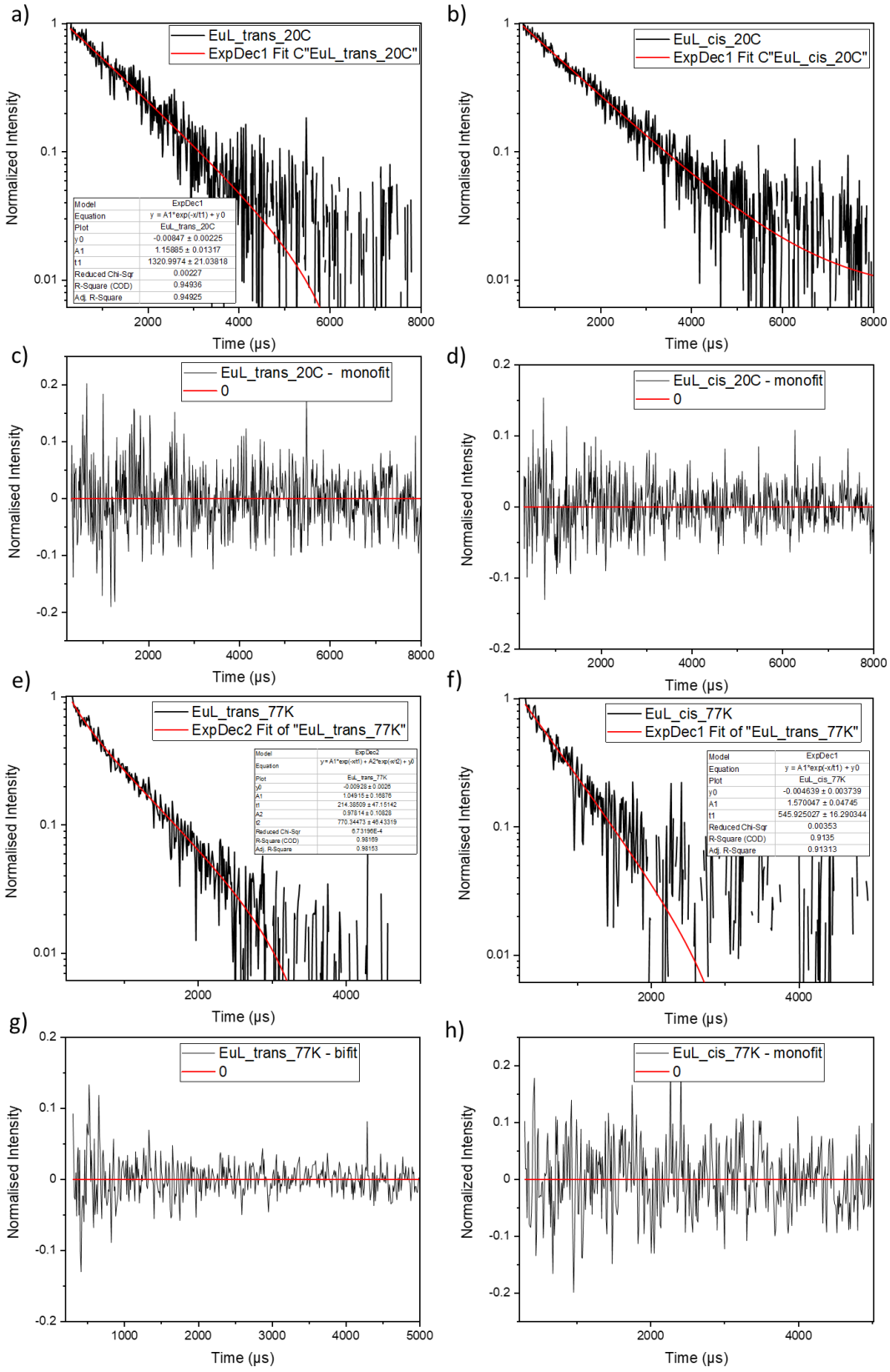

Figure S47: Time resolved luminescence decay a) $EuL_a(E)$ at 298 K λ_{ex} = 395 nm, λ_{em} = 616 nm, emission slit = 5 nm, excitation slit = 5 nm, delay time = 10 ms (black line), mono-exponential fit (red line) b) $EuL_a(Z)$ at 298 K λ_{ex} = 395 nm, λ_{em} = 616 nm, emission slit = 5 nm, excitation slit = 5 nm, delay time = 10 ms (black line), mono-exponential fit (red line) c)difference plot of mono exponential decay fits determined as the difference from the raw data for $EuL_a(E)$ at 298 K λ_{ex} =

395 nm, λ_{em} = 616 nm, emission slit = 5 nm, excitation slit = 5 nm, delay time = 10 ms d) difference plot of mono exponential decay fits determined as the difference from the raw data for EuL_a(Z) at 298 K λ_{ex} = 395 nm, λ_{em} = 616 nm, emission slit = 5 nm, excitation slit = 5 nm, delay time = 10 ms e) EuL_a(E) at 77 K λ_{ex} = 395 nm, λ_{em} = 616 nm, emission slit = 5 nm, excitation slit = 5 nm, delay time = 10 ms (black line), mono-exponential fit (red line) f) EuL_a(Z) at 77K λ_{ex} = 395 nm, λ_{em} = 616 nm, emission slit = 5 nm, excitation slit = 5 nm, delay time = 10 ms (black line), mono-exponential fit (red line) g)difference plot of mono exponential decay fits determined as the difference from the raw data for EuL_a(E) at 77 K λ_{ex} = 395 nm, λ_{em} = 616 nm, emission slit = 5 nm, excitation slit = 5 nm, delay time = 10 ms h) difference plot of biexponential decay fits determined as the difference from the raw data for EuL_a(Z) at 77 K λ_{ex} = 395 nm, λ_{em} = 616 nm, emission slit = 5 nm, excitation slit = 5 nm, delay time = 10 ms

Table S5: Lifetimes of EuL_a E and Z isomers at 298 K and 77K as determined by a mono-exponential fit at 298 K and biexponential fit at 77k of the luminescence decay in figure 40.

	τ (298 K) (ms)	**τ_1 (77 K) (ms)**	**τ_2 (77 K) (ms)**
E	1.15	0.21	0.77
Z	1.34	0.55	-

Eu_2L_b

Steady State Measurements

E-Isomer

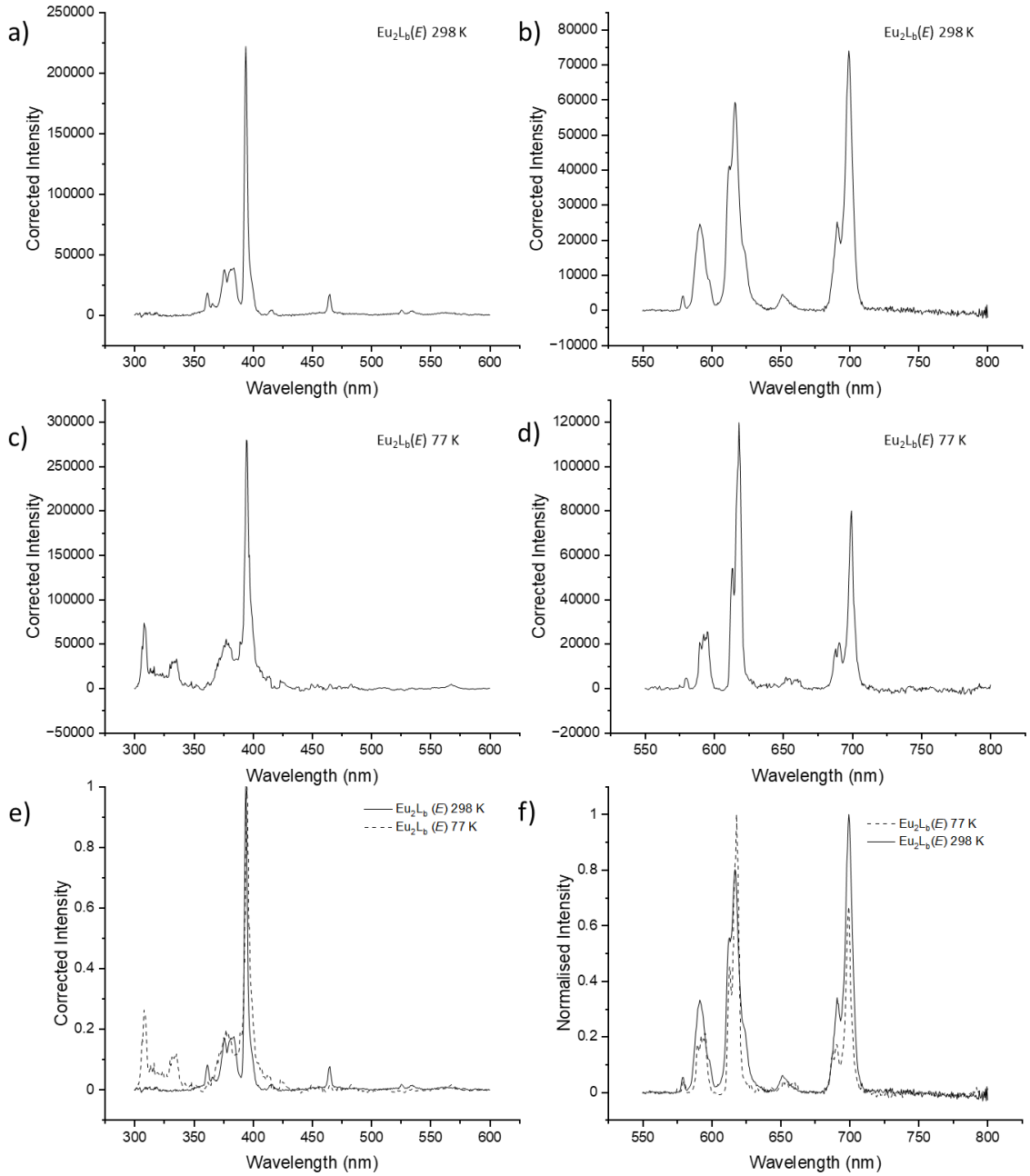

Figure S48: a) Excitation spectra of Eu_2L_b(E) at 298 K, λ_{em} = 616 nm, excitation slits 1 nm, emission slit 5 nm, integration time 0.2s b) Emission spectra of Eu_2L_b (E) at 298 K, λ_{ex} = 395 nm, emission slits 1 nm, excitation slit 5 nm, integration time 0.2s c) Excitation spectra of Eu_2L_b (E) at 77 K, λ_{em} = 616 nm, excitation slits 1 nm, emission slit 5 nm, integration time 0.2s d) Emission spectra of Eu_2L_b (E) at 77 K, λ_{ex} = 395 nm, emission slits 1 nm, excitation slit 5 nm, integration time 0. e) Comparison of a) and c) where intensities are normalised f) Comparison of b) and d) where intensities are normalised.

Z-Isomer

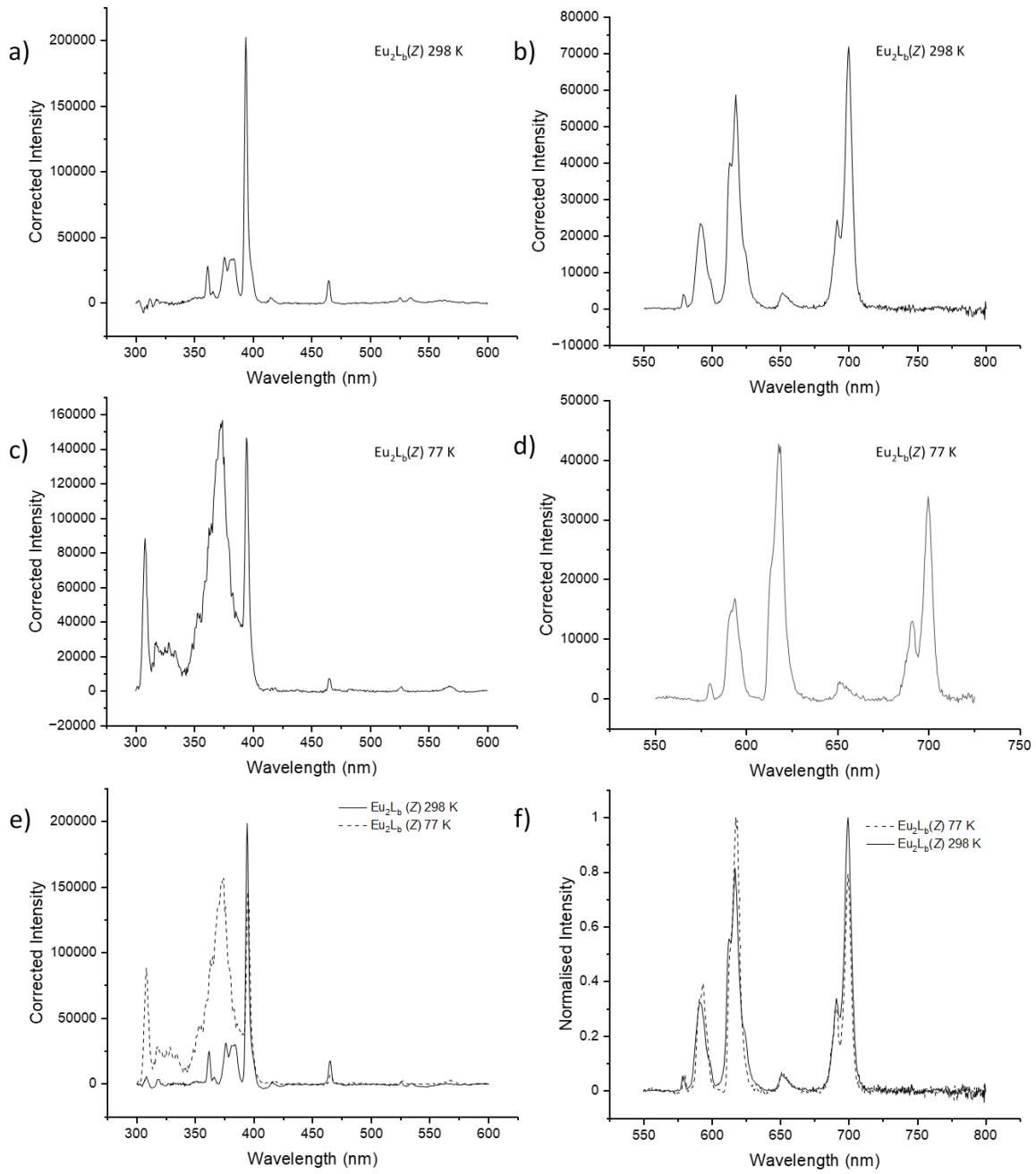

Figure S49: a) Excitation spectra of Eu_2L_b(Z) at 298 K, λ_{em} = 616 nm, excitation slits 1 nm, emission slit 5 nm, integration time 0.2s b) Emission spectra of Eu_2L_b (Z) at 298 K, λ_{ex} = 395 nm, emission slits 1 nm, excitation slit 5 nm, integration time 0.2s c) Excitation spectra of Eu_2L_b (Z) at 77 K, λ_{em} = 616 nm, excitation slits 1 nm, emission slit 5 nm, integration time 0.2s d) Emission spectra of Eu_2L_b (Z) at 77 K, λ_{ex} = 395 nm, emission slits 1 nm, excitation slit 5 nm, integration time 0.2s e) Comparison of a) and c) where intensities are normalised f) Comparison of b) and d) where intensities are normalised.

Comparison between Isomers

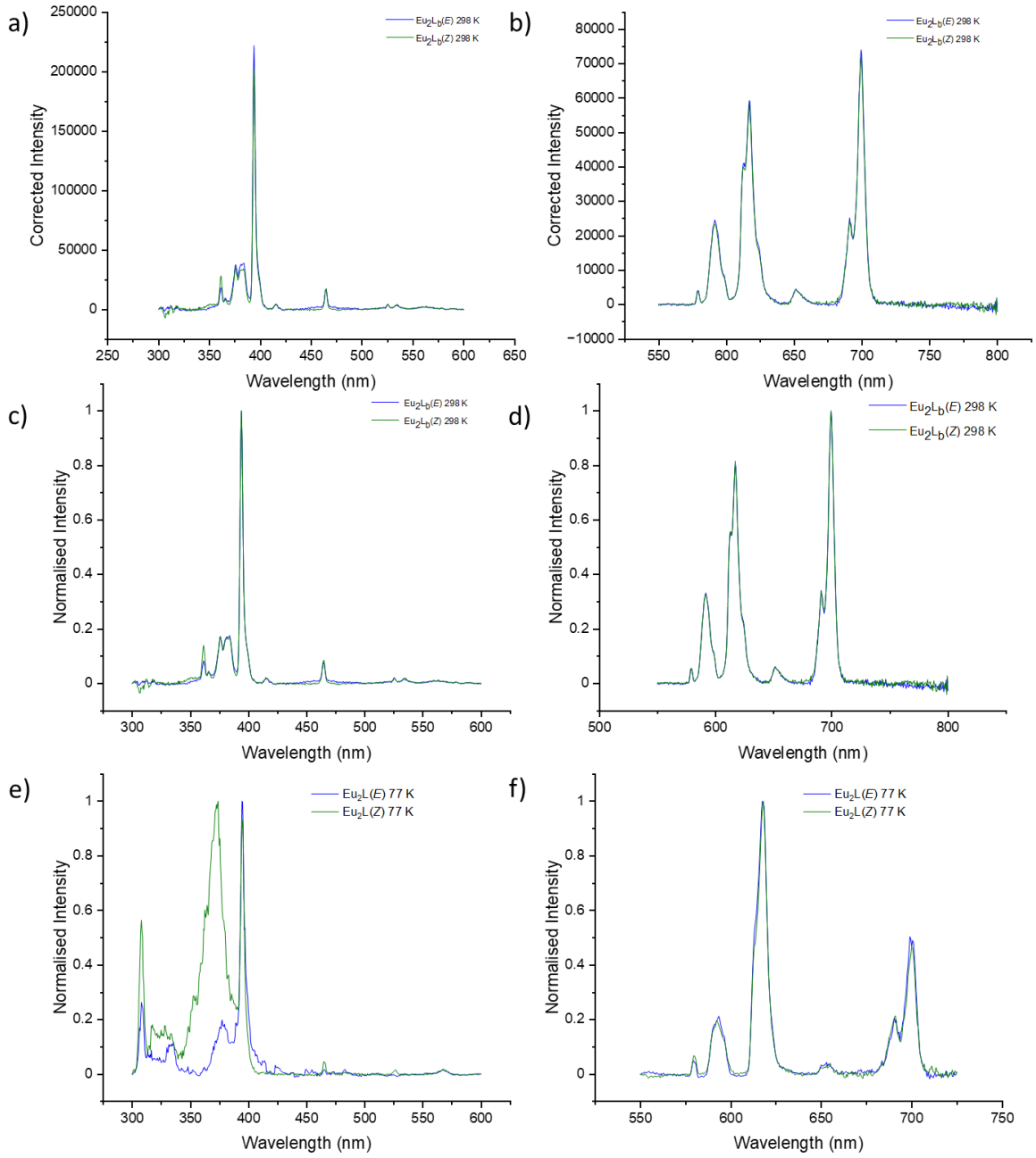

Figure S50: a) Excitation spectra of Eu_2L_b(E) (blue line) and Eu_2L_b (Z) (green line) at 298 K, λ_{em} = 616 nm, excitation slits 1 nm, emission slit 5 nm, integration time 0.2s b) Emission spectra of Eu_2L_b (E) (blue line) and Eu_2L_b (Z) (green line) at 298 K, λ_{ex} = 395 nm, emission slits 1 nm, excitation slit 5 nm, integration time 0.2s c) Excitation spectra of Eu_2L_b (E) (blue line) and Eu_2L_b (Z) (green line) at 298 K where intensities are normalised d) Emission spectra of Eu_2L_b (E) (blue line) and Eu_2L_b (Z) (green line) at 77 K, where intensities are normalised e) Excitation spectra of Eu_2L_b (E) (blue line) and Eu_2L_b (Z) (green line) at 77 K, λ_{em} = 616 nm, excitation slits 1 nm, emission slit 5 nm, integration time 0.2s where intensities are normalised f) Emission spectra of Eu_2L_b (E) (blue line) and Eu_2L_b (Z) (green line) at 77 K, λ_{ex} = 395 nm, emission slits 1 nm, excitation slit 5 nm, integration time 0.2s where intensities are normalised.

Time Resolved Measurements

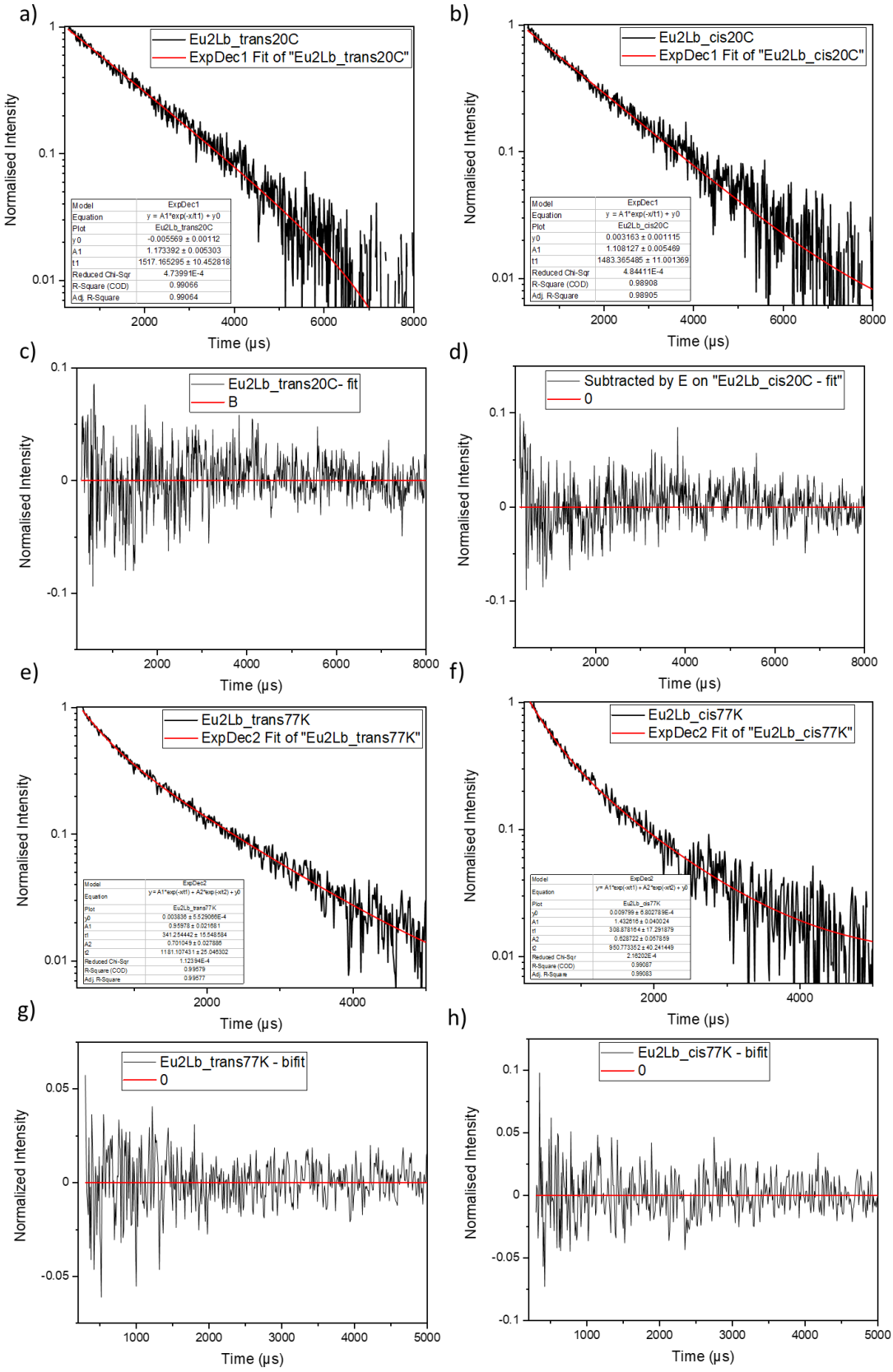

Figure S51: Time resolved luminescence decay a) $Eu_2L_b(E)$ at 298 K λ_{ex} = 395 nm, λ_{em} = 616 nm, emission slit = 5 nm, excitation slit = 5 nm, delay time = 10 ms (black line), mono-exponential fit (red line) b) Eu_2L_b (Z) at 298 K λ_{ex} = 395 nm, λ_{em} =

616 nm, emission slit = 5 nm, excitation slit = 5 nm, delay time = 10 ms (black line), mono-exponential fit (red line) c) difference plot of mono exponential decay fits determined as the difference from the raw data for Eu_2L_b(E) at 298 K λ_{ex} = 395 nm, λ_{em} = 616 nm, emission slit = 5 nm, excitation slit = 5 nm, delay time = 10 ms d) difference plot of mono exponential decay fits determined as the difference from the raw data for Eu_2L_b (Z) at 298 K λ_{ex} = 395 nm, λ_{em} = 616 nm, emission slit = 5 nm, excitation slit = 5 nm, delay time = 10 ms e) Eu_2L_b(E) at 77 K λ_{ex} = 395 nm, λ_{em} = 616 nm, emission slit = 5 nm, excitation slit = 5 nm, delay time = 10 ms (black line), mono-exponential fit (red line) f) Eu_2L_b(Z) at 77K λ_{ex} = 395 nm, λ_{em} = 616 nm, emission slit = 5 nm, excitation slit = 5 nm, delay time = 10 ms (black line), biexponential fit (red line) g)difference plot of mono exponential decay fits determined as the difference from the raw data for Eu_2L_b (E) at 77 K λ_{ex} = 395 nm, λ_{em} = 616 nm, emission slit = 5 nm, excitation slit = 5 nm, delay time = 10 ms h) difference plot of biexponential decay fits determined as the difference from the raw data for Eu_2L_b (Z) at 77 K λ_{ex} = 395 nm, λ_{em} = 616 nm, emission slit = 5 nm, excitation slit = 5 nm, delay time = 10 ms

Table S6: Lifetimes of Eu_2L_b E and Z isomers at 298 K and 77K as determined by a mono-exponential fit at 298 K and a biexponential fit at 77 k of the luminescence decay in figure 44.

	τ (298 K) (ms)	**τ_1(77 K) (ms)**	**τ_2(77 K) (ms)**
E	1.52	0.34	1.18
Z	1.48	0.31	0.95

Comparison between Mono and Bimetallic Complexes

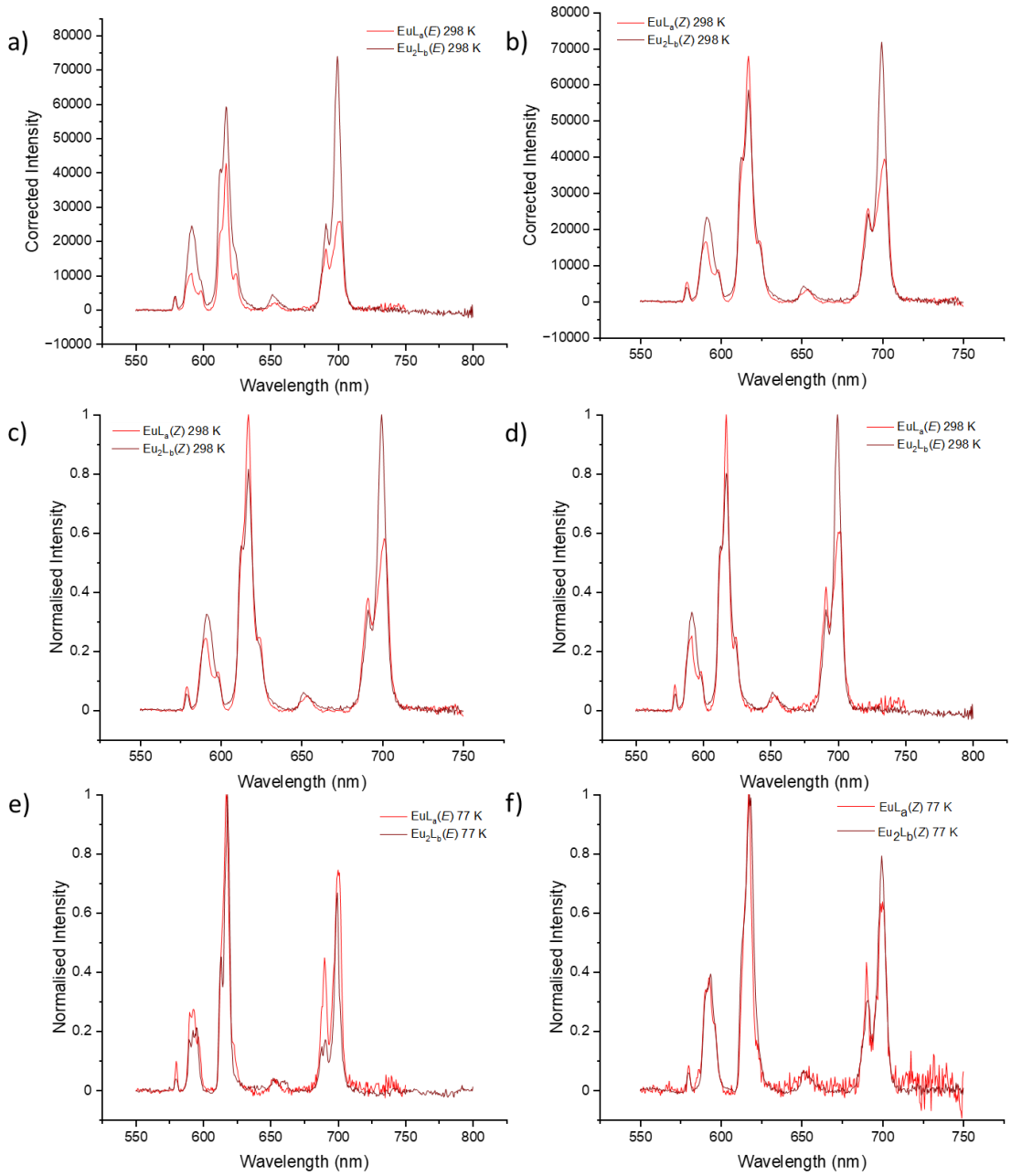

Figure S52: Emission spectra a) EuL_a(E) (red line) and Eu_2L_b (E) (dark red line) at 298 K λ_{ex} = 395 nm, emission slits 1 nm, excitation slit 5 nm, integration time 0.2s b) EuL_a (Z) (red line) and Eu_2L_b (Z) (dark red line) at 298 K, λ_{ex} = 395 nm, emission slits 1 nm, excitation slit 5 nm, integration time 0.2s c) EuL_a(Z) (red line) and Eu_2L_b (Z) (dark red line) at 298 K λ_{ex} = 395 nm, emission slits 1 nm, excitation slit 5 nm, integration time 0.2s where intensities are normalised d) EuL_a(E) (red line) and Eu_2L_b (E) (dark red line) at 298 K λ_{ex} = 395 nm, emission slits 1 nm, excitation slit 5 nm, integration time 0.2s where intensities are normalised e) EuL_a(E) (red line) and Eu_2L_b (E) (dark red line) at 77 K λ_{ex} = 395 nm, emission slits 1 nm, excitation slit 5 nm, integration time 0.2s where intensities are normalised f) EuL_a(Z) (red line) and Eu_2L_b (Z) (dark red line) at 77 K λ_{ex} = 395 nm, emission slits 1 nm, excitation slit 5 nm, integration time 0.2s where intensities are normalised.

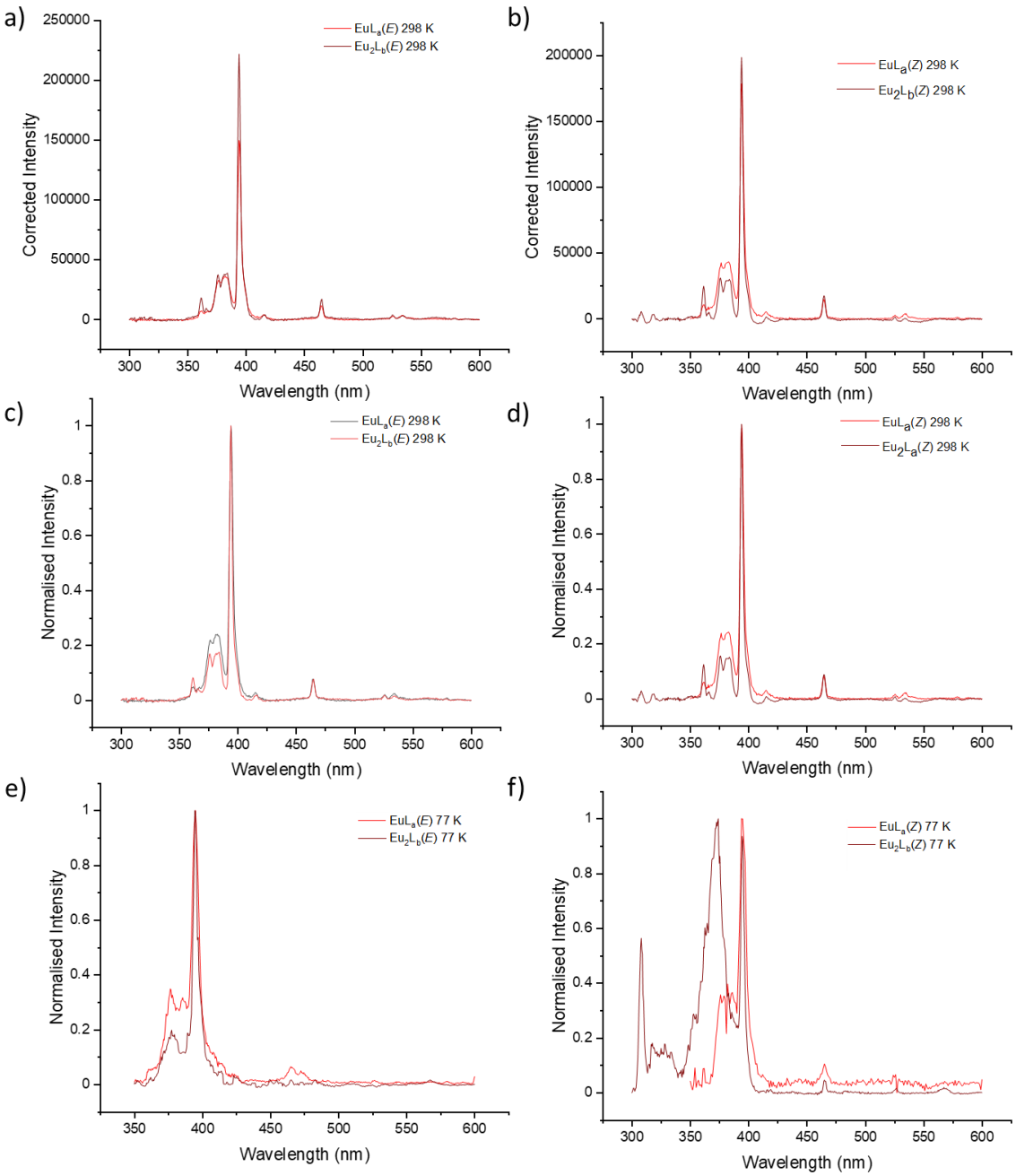

Figure S53: Excitation spectra a) EuL_a(E) (red line) and Eu_2L_b (E) (dark red line) at 298 K λ_{em} = 616 nm, emission slits 5 nm, excitation slit 1 nm, integration time 0.2s b) EuL_a (Z) (red line) and Eu_2L_b (Z) (dark red line) at 298 K, λ_{em} = 616 nm, emission slits 5 nm, excitation slit 1 nm, integration time 0.2s c) EuL_a(E) (red line) and Eu_2L_b (E) (dark red line) at 298 K λ_{em} = 616 nm, emission slits 5 nm, excitation slit 1 nm, integration time 0.2s where intensities are normalised d) EuL_a(Z) (red line) and Eu_2L_b (Z) (dark red line) at 298 K λ_{em} = 616 nm, emission slits 5 nm, excitation slit 1 nm, integration time 0.2s where intensities are normalised e) EuL_a(E) (red line) and Eu_2L_b (E) (dark red line) at 77 K λ_{em} = 616 nm, emission slits 5 nm, excitation slit 1 nm, integration time 0.2s where intensities are normalised f) EuL_a(Z) (red line) and Eu_2L_b (Z) (dark red line) at 77 K λ_{em} = 616 nm, emission slits 5 nm, excitation slit 1 nm, integration time 0.2s where intensities are normalised.

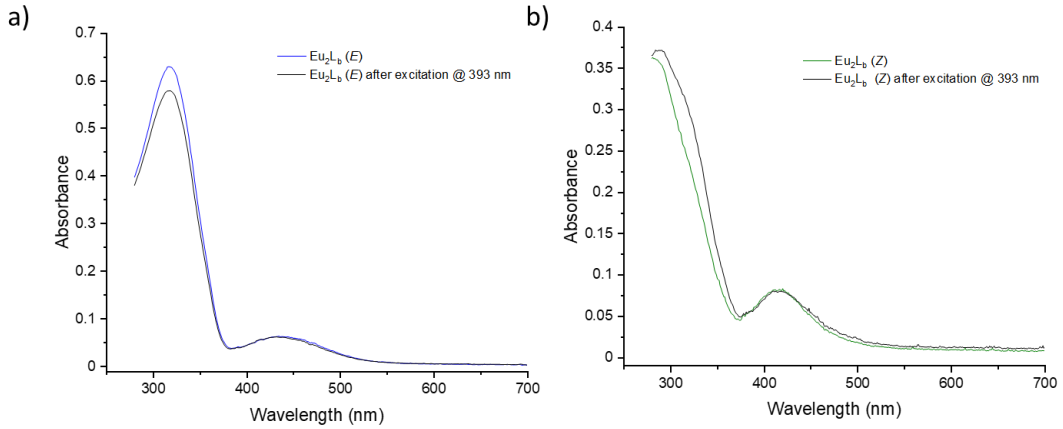

Figure S54: a) stacked absorbance spectra of Eu_2L_b at $PSS_{405\,nm}$ (blue line) and absorbance of the same sample after irradiation with 393 nm light during the course of running an emission scan (black line) b) stacked absorbance spectra of Eu_2L_b at $PSS_{530\,nm}$ (green line) and absorbance of the same sample after irradiation with 393nm light during the course of running an emission scan (black line).

NdL_a

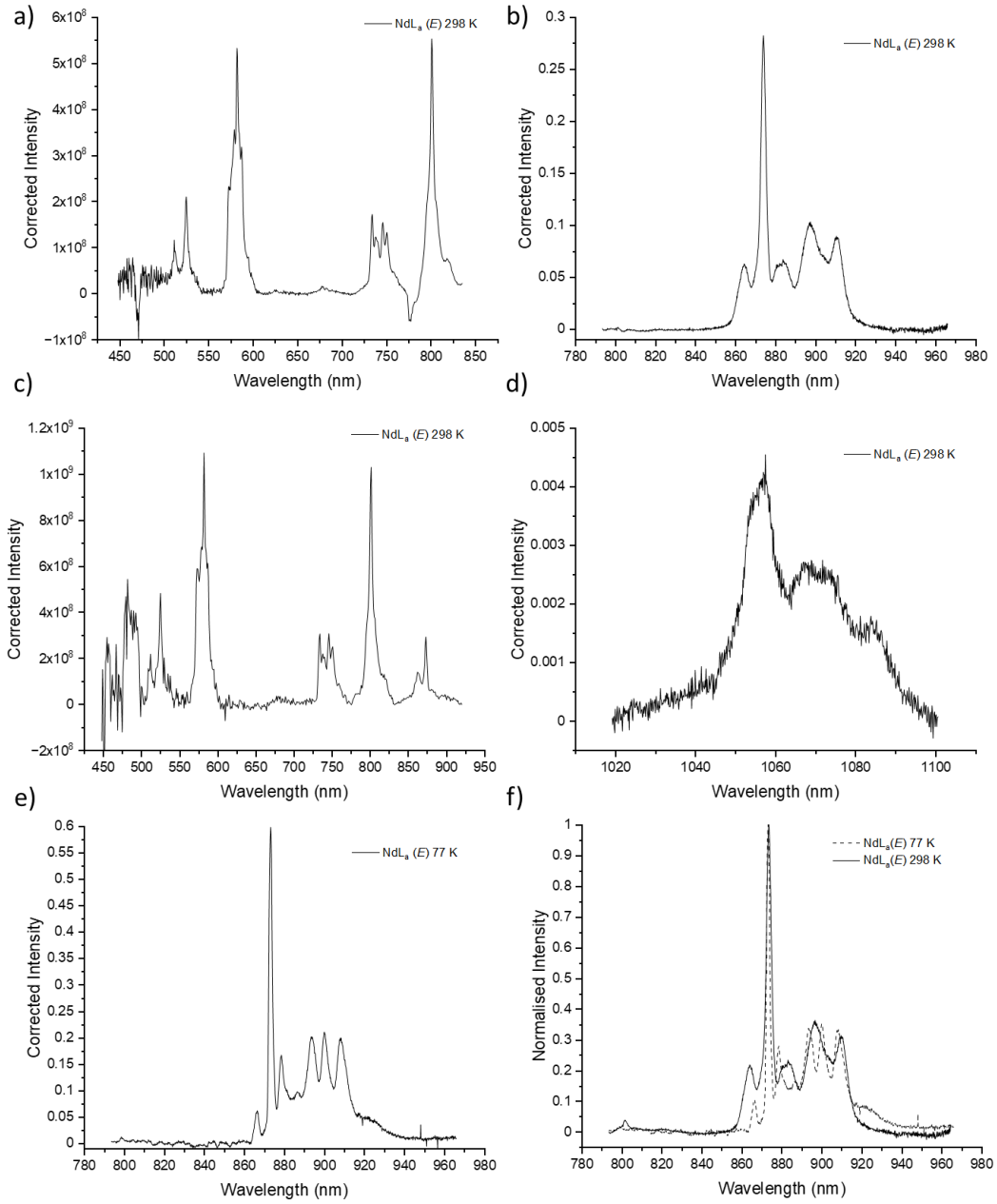

Figure S55: a) Excitation spectra of NdL_a (E) 298 K ($\rightarrow {}^4I_{9/2}$) λ_{em} = 880 nm, exposure time 100 ms, 1 exposure per frame b) Emission spectra of NdL_a (E) 298 K (${}^4F_{3/2} \rightarrow {}^4I_{9/2}$) λ_{ex} = 580 nm, emission slit at 25 µm c) Excitation spectra of NdL_a (E) 298 K ($\rightarrow {}^4I_{11/2}$) λ_{em} = 1060 nm, exposure time 100 ms, 1 exposure per frame d) Emission spectra of NdL_a (E) 298 K (${}^4F_{3/2} \rightarrow {}^4I_{11/2}$) λ_{ex} = 580 nm, emission slit at 25 µm e) Emission spectra of NdL_a (E) 77 K (${}^4F_{3/2} \rightarrow {}^4I_{9/2}$) λ_{ex} = 580 nm, emission slit at 25 µm f) Comparison of b) (black line) and e) (dashed line) where intensities are normalised

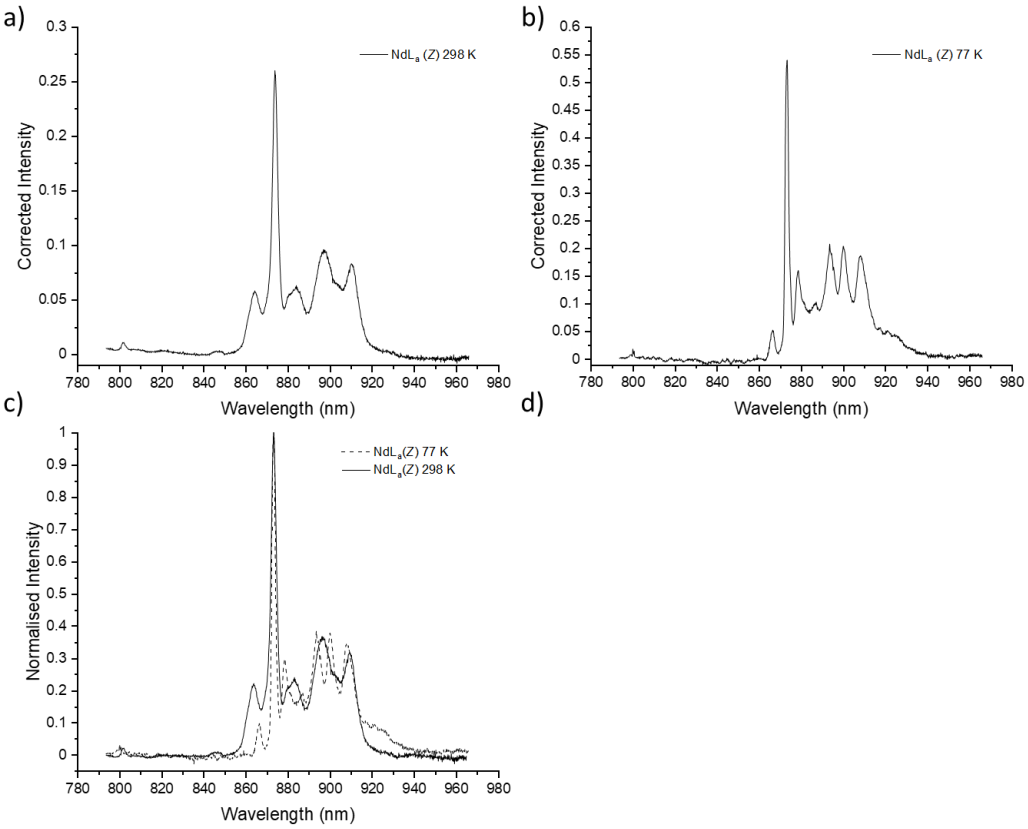

Figure S56: a) Emission spectra of NdL$_a$ (Z) 298 K ($^4F_{3/2} \rightarrow {}^4I_{9/2}$) λ_{ex} = 580 nm, emission slit at 25 µm B) Emission spectra of NdL$_a$ (Z) 77 K ($^4F_{3/2} \rightarrow {}^4I_{9/2}$) λ_{ex} = 580 nm, emission slit at 25 µm c) Comparison of a) (black line) and b) (dashed line) where intensities are normalised.

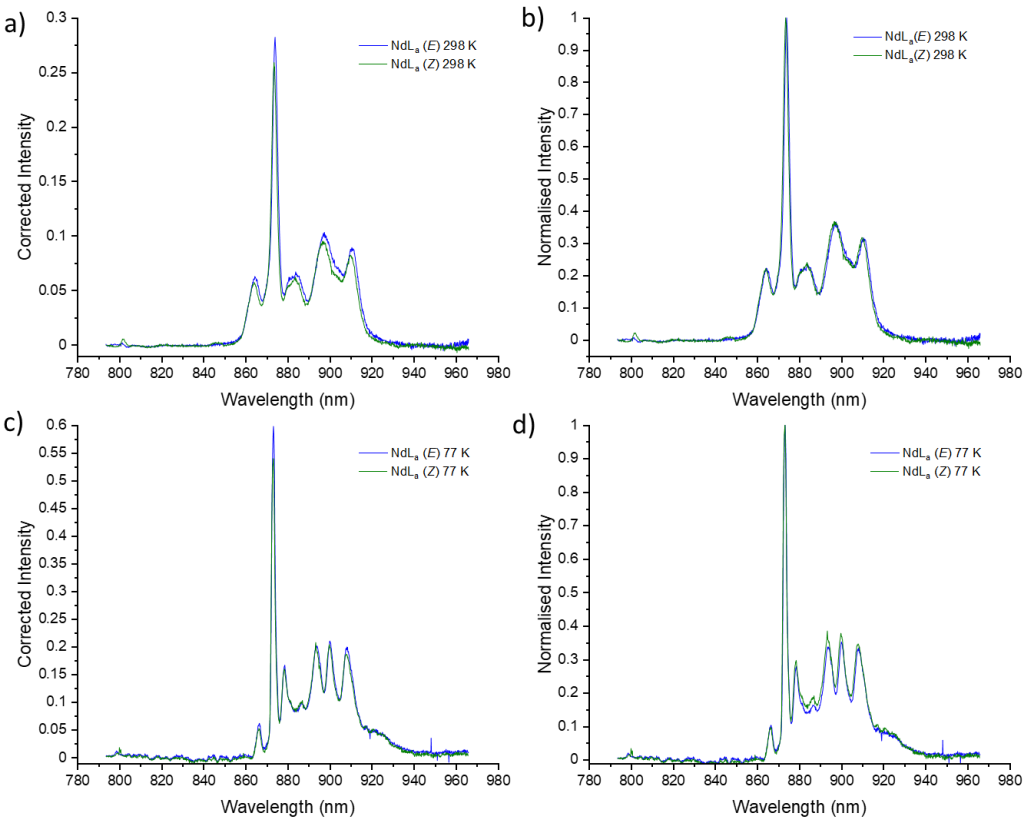

Figure S57: a) Emission spectra of NdL$_a$ (E) (blue line) and NdL$_a$ (Z) (green line) at 298 K ($^4F_{3/2} \rightarrow {}^4I_{9/2}$) , λ_{ex} = 580 nm, emission slit at 25 µm b) Emission spectra of NdL$_a$ (E) (blue line) and NdL$_a$ (Z) (green line) at 298 K ($^4F_{3/2} \rightarrow {}^4I_{9/2}$) , λ_{ex} = 580 nm, emission slit at 25 µm where intensities are normalised c) Emission spectra of NdL$_a$ (E) (blue line) and NdL$_a$ (Z) (green line) at 77 K ($^4F_{3/2} \rightarrow {}^4I_{9/2}$) , λ_{ex} = 580 nm, emission slit at 25 µm d) Emission spectra of NdL$_a$ (E) (blue line) and NdL$_a$ (Z) (green line) at 77K ($^4F_{3/2} \rightarrow {}^4I_{9/2}$) , λ_{ex} = 580 nm, emission slit at 25 µm where intensities are normalised.

Nd_2L_b

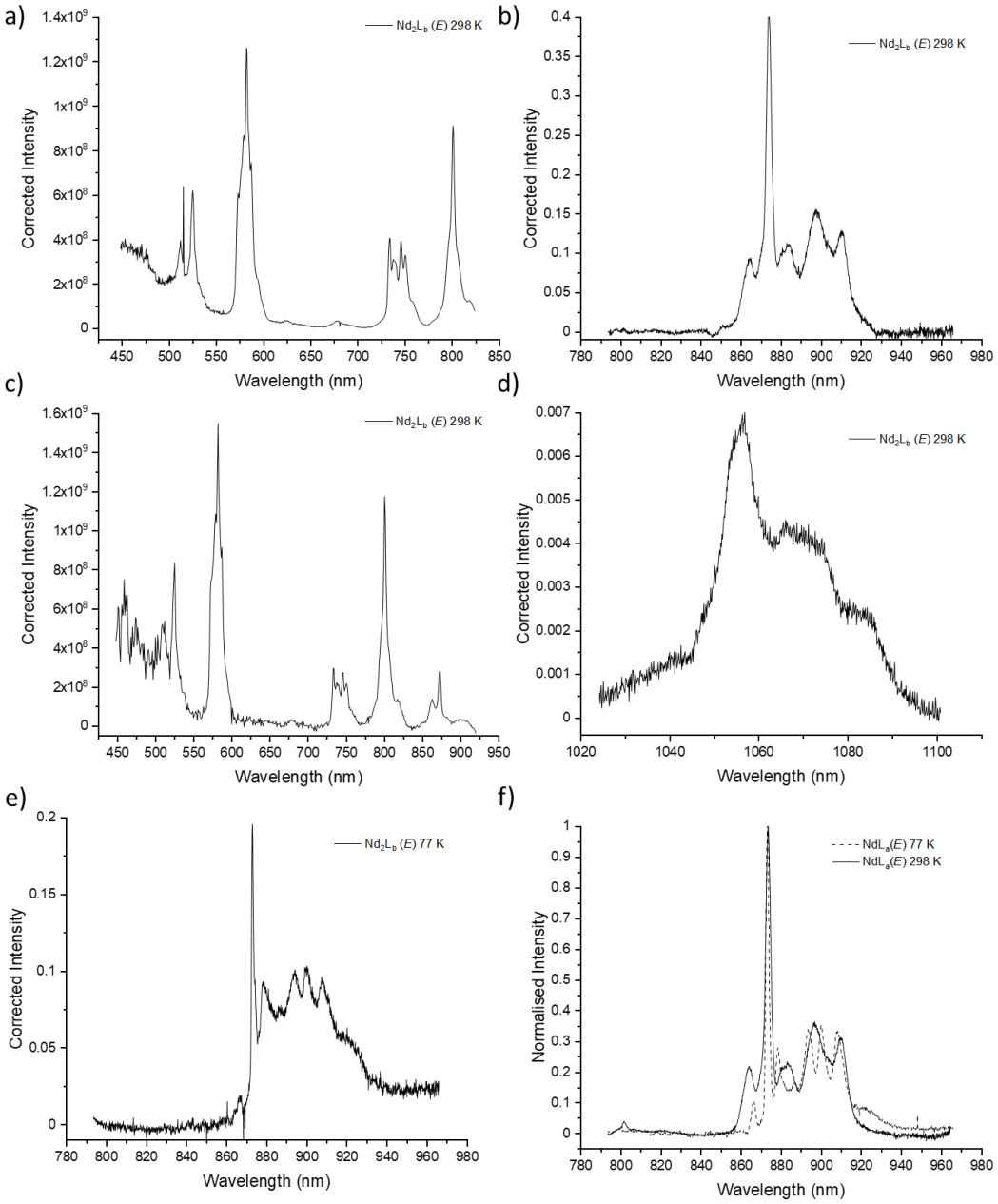

Figure S58: a) Excitation spectra of Nd_2L_b (E) 298 K ($\rightarrow {}^4I_{9/2}$) λ_{em} = 880 nm, exposure time 100 ms, 1 exposure per frame b) Emission spectra of Nd_2L_b (E) 298 K (${}^4F_{3/2} \rightarrow {}^4I_{9/2}$) λ_{ex} = 580 nm, emission slit at 25 µm c) Excitation spectra of Nd_2L_b (E) 298 K ($\rightarrow {}^4I_{11/2}$) λ_{em} = 1060 nm, exposure time 100 ms, 1 exposure per frame d) Emission spectra of Nd_2L_b (E) 298 K (${}^4F_{3/2} \rightarrow {}^4I_{11/2}$) λ_{ex} = 580 nm, emission slit at 25 µm e) Emission spectra of Nd_2L_b (E) 77 K (${}^4F_{3/2} \rightarrow {}^4I_{9/2}$) λ_{ex} = 580 nm, emission slit at 25 µm f) Comparison of b) (black line).

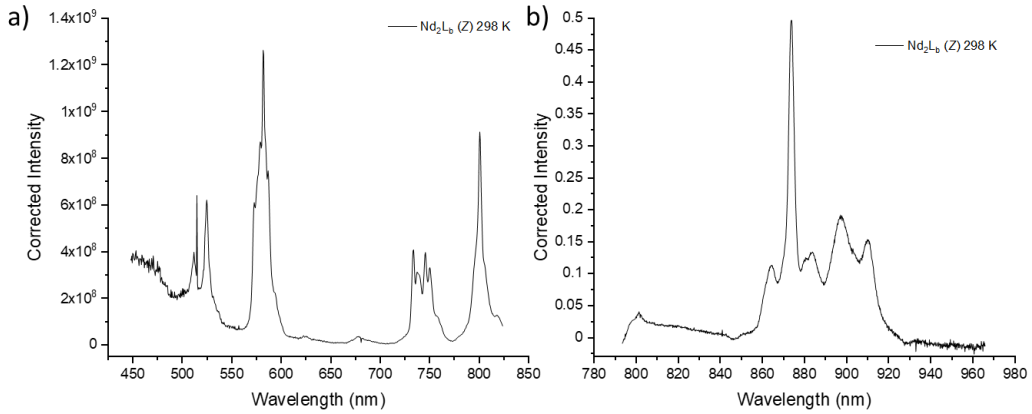

Figure S59: a) Excitation spectra of Nd_2L_b (Z) 298 K ($\rightarrow {}^4I_{9/2}$) λ_{em} = 880 nm, exposure time 100 ms, 1 exposure per frame b) Emission spectra of Nd_2L_b (Z) 298 K ($^4F_{3/2} \rightarrow {}^4I_{9/2}$) λ_{ex} = 580 nm, emission slit at 25 µm c) Emission spectra of Nd_2L_b (Z) 298 K ($^4F_{3/2} \rightarrow {}^4I_{11/2}$) λ_{ex} = 580 nm, emission slit at 25 µm.

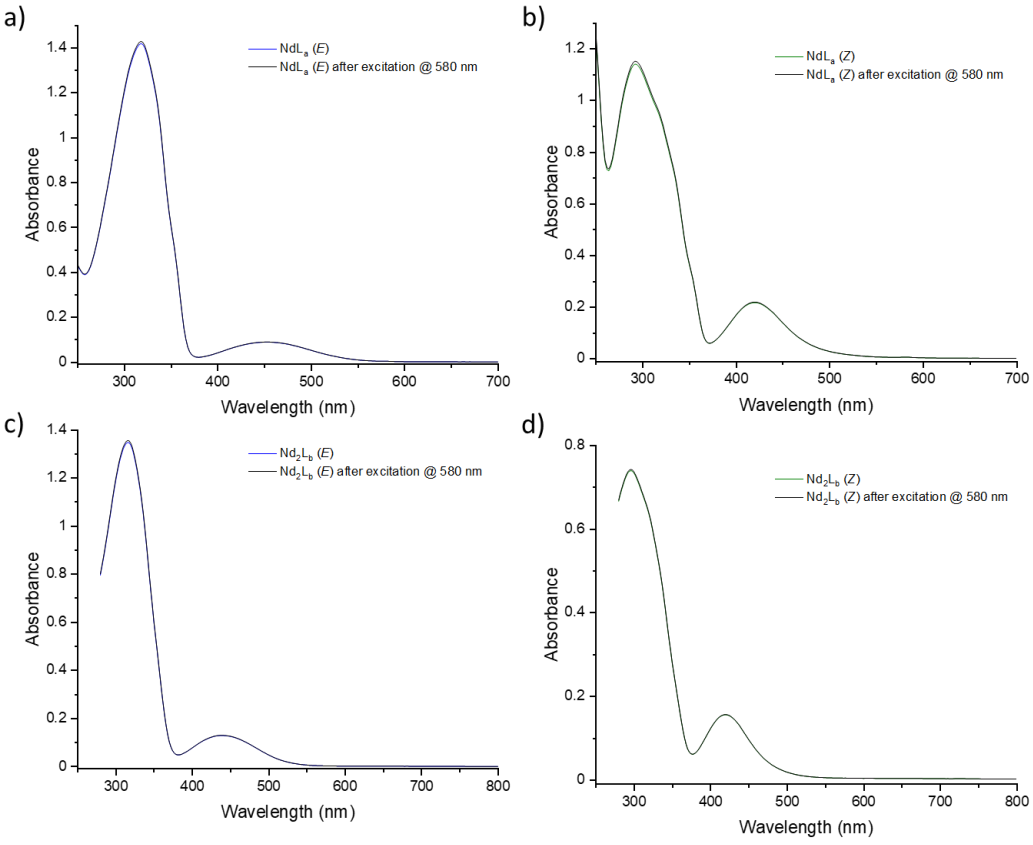

Figure S60: a) stacked absorbance spectra of NdL_a at $PSS_{405\ nm}$ (blue line) and absorbance of the same sample after irradiation with 580nm light during the course of running an emission scan (black line) b) stacked absorbance spectra of NdL_a at $PSS_{530\ nm}$ (green line) and absorbance of the same sample after irradiation with 580nm light during the course of running an emission scan (black line) c) stacked absorbance spectra of Nd_2L_b at $PSS_{405\ nm}$ (blue line) and absorbance of the same sample after irradiation with 580nm light during the course of running an emission scan (black line) d) stacked absorbance spectra of Nd_2L_b at $PSS_{530\ nm}$ (green line) and absorbance of the same sample after irradiation with 580nm light during the course of running an emission scan (black line).

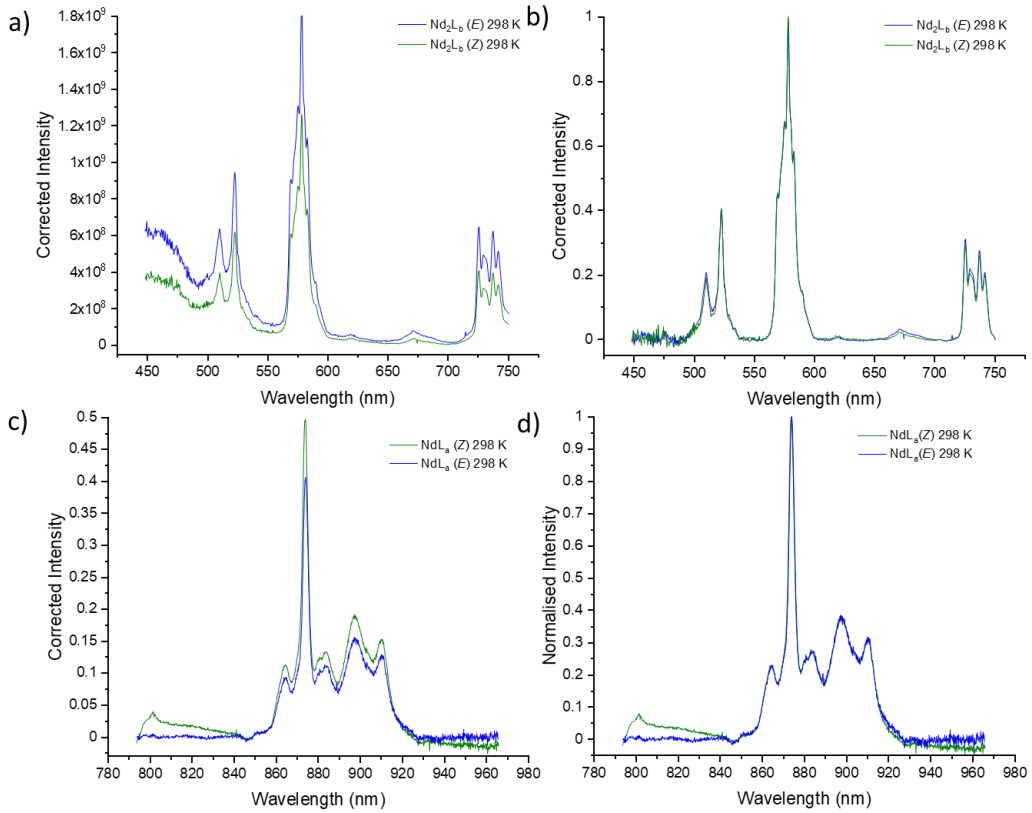

Figure S61: a) Excitation spectra of Nd_2L_b (E) (blue line) and Nd_2L_b (Z) (green line) at 298 K ($\rightarrow {}^4I_{9/2}$) , λ_{em} = 880 nm, emission slit at 25 µm b) Excitation spectra of Nd_2L_b (E) (blue line) and Nd_2L_b (Z) (green line) at 298 K ($\rightarrow {}^4I_{9/2}$) , λ_{em} = 880 nm, emission slit at 25 µm where intensities are normalised c) Emission spectra of Nd_2L_b (E) (blue line) and Nd_2L_b (Z) (green line) at 298 K ($^4F_{3/2} \rightarrow {}^4I_{9/2}$) , λ_{ex} = 580 nm, emission slit at 25 µm d) Emission spectra of Nd_2L_b (E) (blue line) and Nd_2L_b (Z) (green line) at 298 K ($^4F_{3/2} \rightarrow {}^4I_{9/2}$) , λ_{ex} = 580 nm, emission slit at 25 µm where intensities are normalised.

Comparison between Mono and Bimetallic Complexes

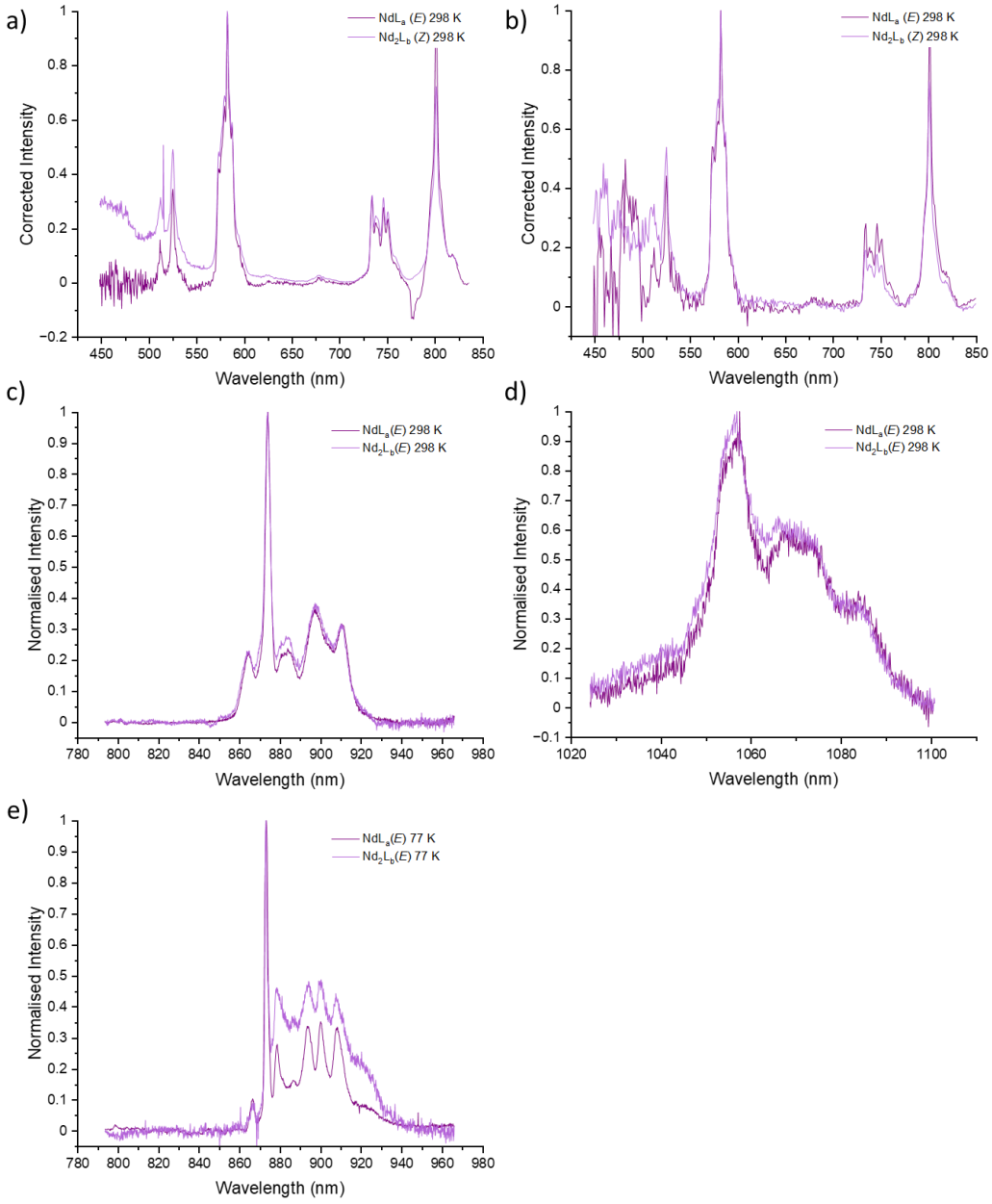

Figure S62: a) Excitation spectra of NdL_a (E) (dark purple line) and Nd_2L_b (E) (light purple line) at 298 K ($\rightarrow {}^4I_{9/2}$) , λ_{em} = 880 nm, emission slit at 25 µm where intensities have been normalised b) Excitation spectra of NdL_a (E) (dark purple line) and Nd_2L_b (E) (light purple line) at 298 K ($\rightarrow {}^4I_{11/2}$) , λ_{em} = 1060 nm, emission slit at 25 µm where intensities have been normalised c) Emission spectra of NdL_a (E) (dark purple line) and Nd_2L_b (E) (light purple line) at 298 K ($^4F_{3/2} \rightarrow {}^4I_{9/2}$) λ_{ex} = 580 nm, emission slit at 25 µm d) Emission spectra of NdL_a (E) (dark purple line) and Nd_2L_b (E) (light purple line) at 298 K ($^4F_{3/2} \rightarrow {}^4I_{11/2}$) λ_{ex} = 580 nm, emission slit at 25 µm e) Emission spectra of NdL_a (E) (dark purple line) and Nd_2L_b (E) (light purple line) at 298 K ($^4F_{3/2} \rightarrow {}^4I_{9/2}$) λ_{ex} = 580 nm, emission slit at 25 µm.

L_a

Steady State Measurements

E- isomer

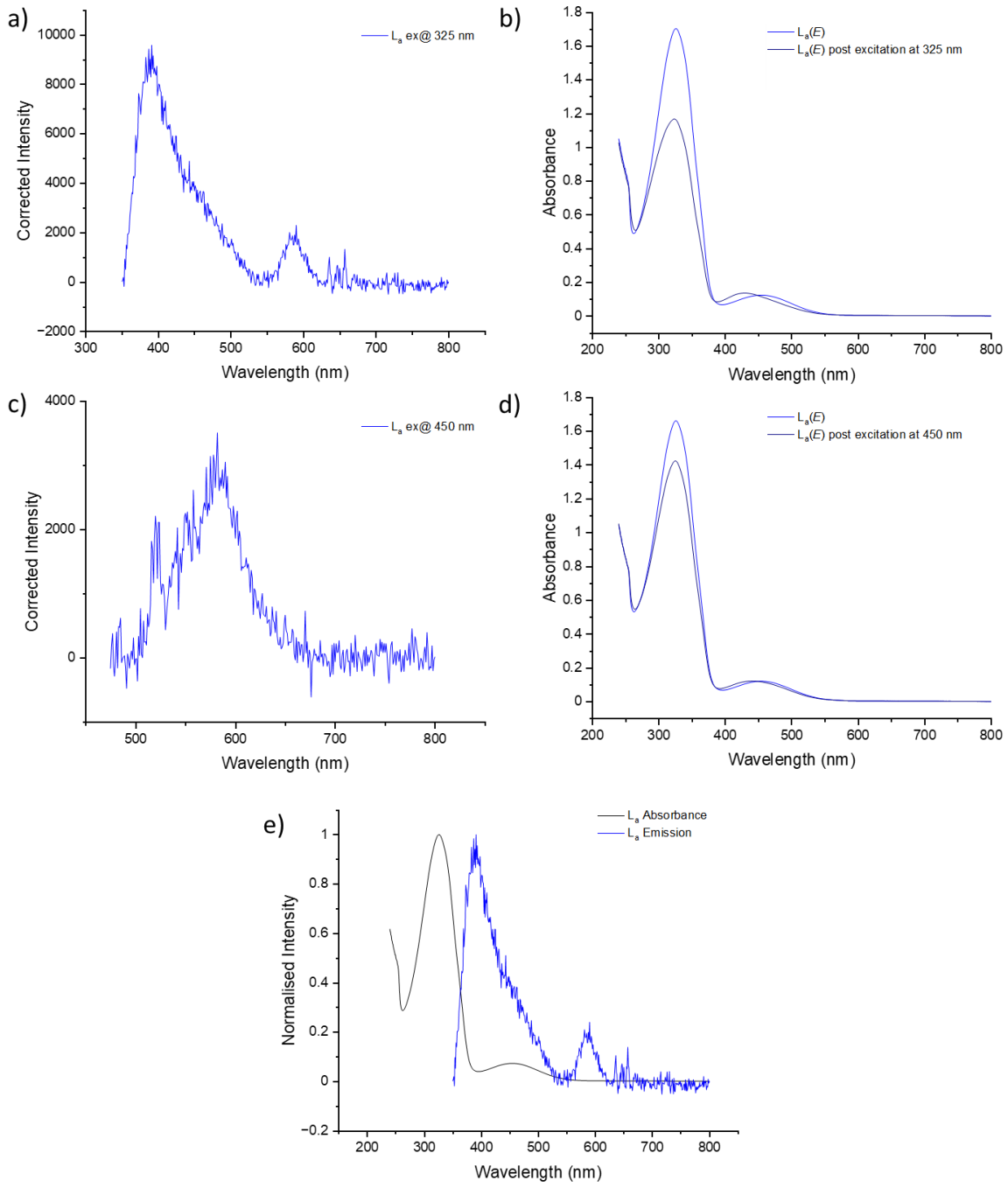

Figure S63: a) L_a emission when excited into the n→π transition at 325 nm, excitation slit at 5 nm, emission slit at 1 nm, integration time 0.1 s b) Absorbance of L_a upon irradiation with 405 nm light for 10 minutes (blue line) and after the same sample was excited into the n→π *transition at 325 nm (navy line) c) L_a emission when excited into the π→π* at 450 nm, excitation slit at 5 nm, emission slit at 1 nm, integration time 0.1 s d) Absorbance of L_a upon irradiation with 405 nm light for 10 minutes (blue line) and after the same sample was excited into the π→π *transition at 450 nm (navy line) e) Normalised Intensities of both absorbance of L_a(E) (black line)* and emission when excited into the *n→π* transition at 325 nm, excitation slit at 5 nm, emission slit at 1 nm, integration time 0.1s (blue line), showing the stokes shift.*

Z- isomer

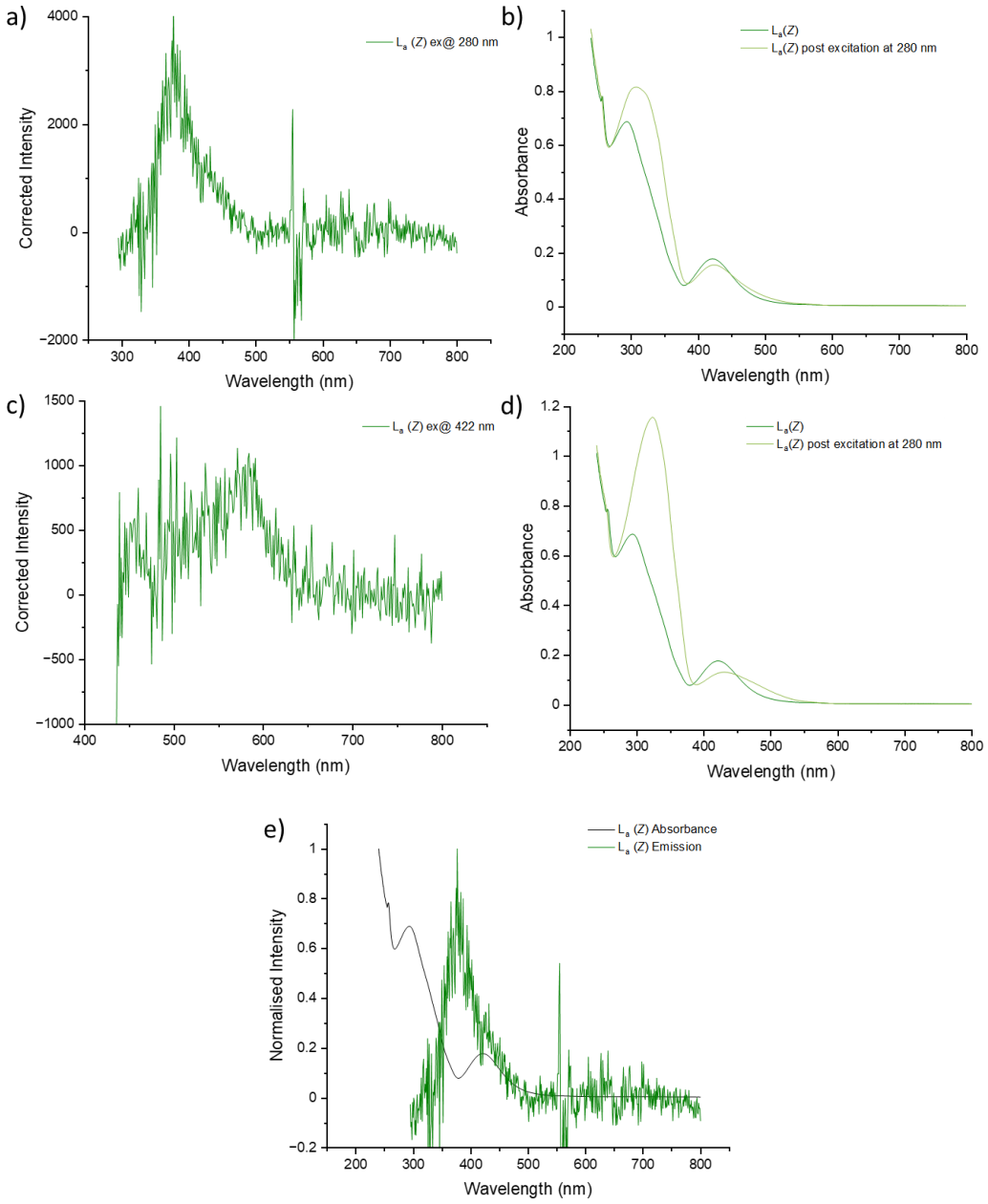

Figure S64: a) L_a (Z) emission when excited into the n→π transition at 280 nm, excitation slit at 5 nm, emission slit at 1 nm, integration time 0.1 s b) Absorbance of L_a upon irradiation with 530 nm light for 10 minutes (dark green line) and after the same sample was excited into the n→π *transition at 280 nm (light green line) c) L_a (Z) emission when excited into the π→π* at 422 nm, excitation slit at 5 nm, emission slit at 1 nm, integration time 0.1 s d) Absorbance of L_a upon irradiation with 530 nm light for 10 minutes (dark green line) and after the same sample was excited into the π→π *transition at 422 nm (light green line) e) Normalised Intensities of both absorbance of L_a(Z) (black line)* and emission when excited into the *n→π* transition at 280 nm, excitation slit at 5 nm, emission slit at 1 nm, integration time 0.1s (dark green line), showing the stokes shift.*

Steady State Measurements

E- isomer

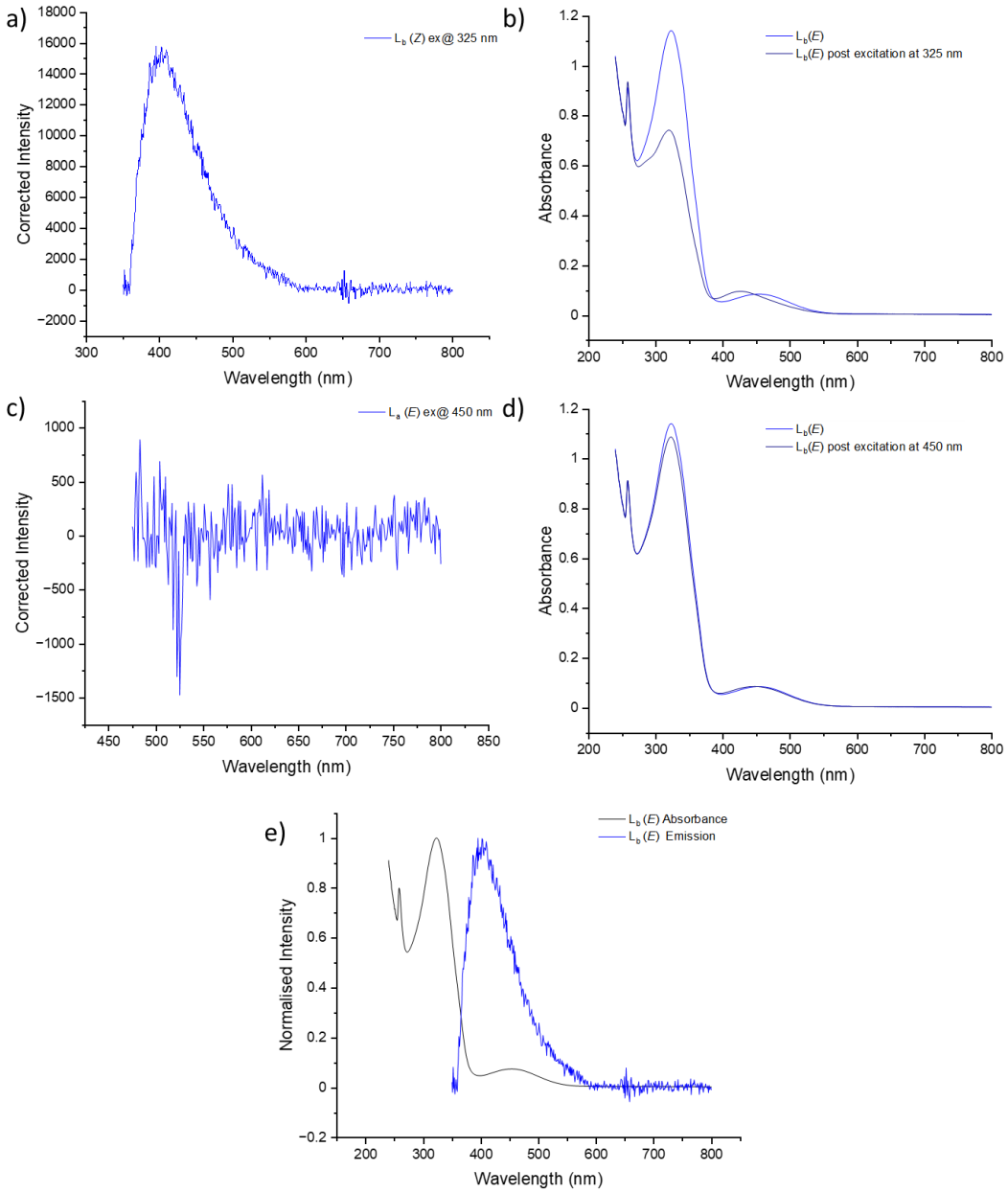

Figure S65: L_b emission when excited into the n→π transition at 325 nm, excitation slit at 5 nm, emission slit at 1 nm, integration time 0.1 s b) Absorbance of L_b upon irradiation with 405 nm light for 10 minutes (blue line) and after the same sample was excited into the n→π *transition at 325 nm (navy line) c) L_b emission when excited into the π→π* at 450 nm, excitation slit at 5 nm, emission slit at 1 nm, integration time 0.1 s d) Absorbance of L_b upon irradiation with 405 nm light for 10 minutes (blue line) and after the same sample was excited into the π→π *transition at 450 nm (navy line) e) Normalised Intensities of both absorbance of L_b(E) (black line)* and emission when excited into the *n→π* transition at 325 nm, excitation slit at 5 nm, emission slit at 1 nm, integration time 0.1s (blue line), showing the stokes shift.*

Z- isomer

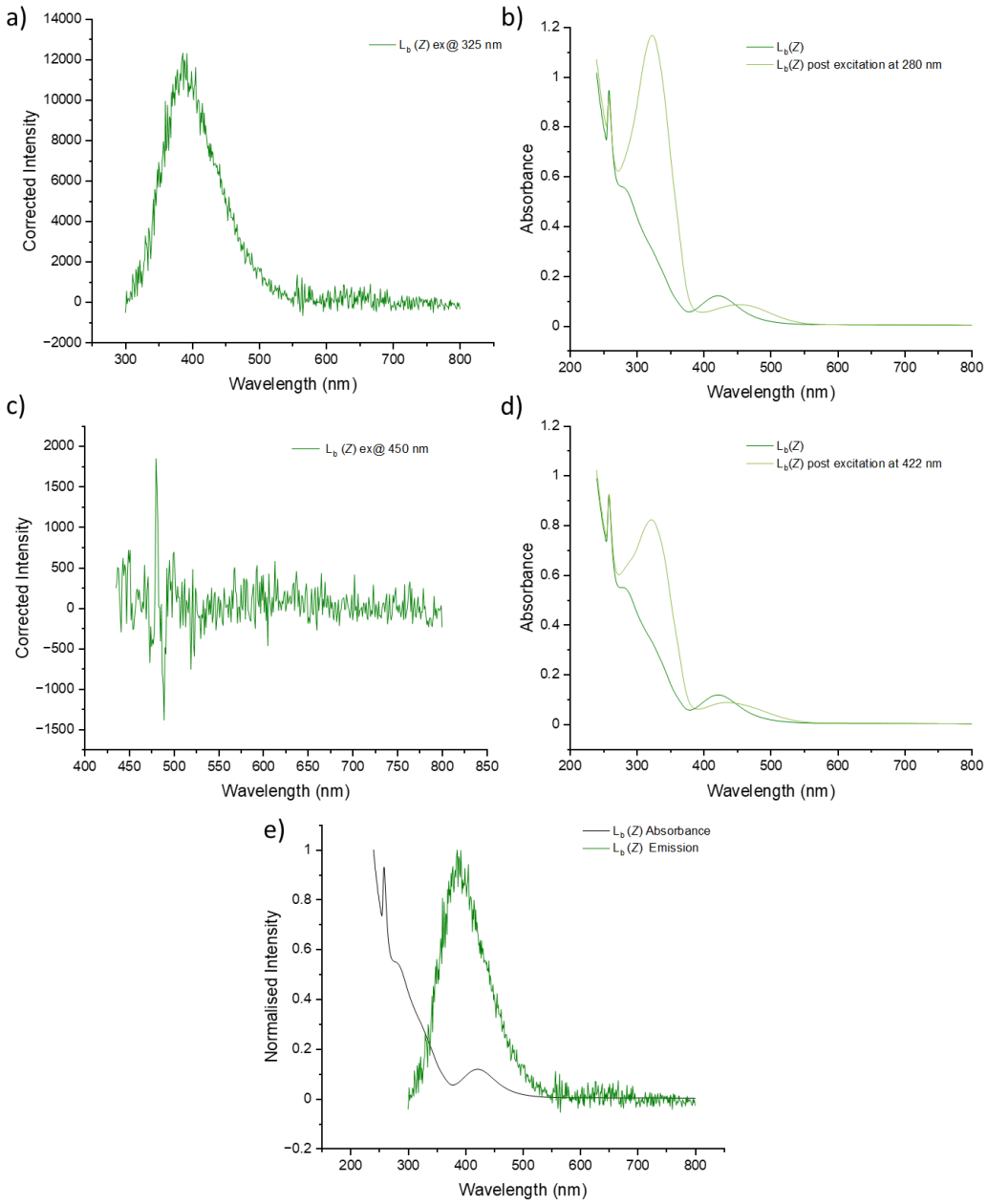

Figure S66: a) L_b (Z) emission when excited into the n→π transition at 280 nm, excitation slit at 5 nm, emission slit at 1 nm, integration time 0.1 s b) Absorbance of L_b upon irradiation with 530 nm light for 10 minutes (dark green line) and after the same sample was excited into the n→π *transition at 280 nm (light green line) c) L_b (Z) emission when excited into the π→π* at 422 nm, excitation slit at 5 nm, emission slit at 1 nm, integration time 0.1 s d) Absorbance of L_b upon irradiation with 530 nm light for 10 minutes (dark green line) and after the same sample was excited into the π→π *transition at 422 nm (light green line) e) Normalised Intensities of both absorbance of L_b (Z) (black line)* and emission when excited into the *n→π* transition at 280 nm, excitation slit at 5 nm, emission slit at 1 nm, integration time 0.1s (dark green line), showing the stokes shift.*

References

1. A. Kerckhoffs, Z. Bo, S. E. Penty, F. Duarte and M. J. Langton, *Org Biomol Chem*, 2021, **19**, 9058-9067.
2. A. L. Leistner, S. Kirchner, J. Karcher, T. Bantle, M. L. Schulte, P. Gödtel, C. Fengler and Z. L. Pianowski, *Chem-Eur J*, 2021, **27**, 8094-8099.
3. C. Alexander, J. A. Thom, A. M. Kenwright, K. E. Christensen, T. J. Sørensen and S. Faulkner, *Chem Sci*, 2023, **14**, 1194-1204.
4. A. Kerckhoffs, K. E. Christensen and M. J. Langton, *Chem Sci*, 2022, **13**, 11551-11559.
5. P. R. Nawrocki, V. R. M. Nielsen and T. J. Sørensen, *Methods Appl Fluores*, 2022, **10**, 045007.
6. V. R. M. Nielsen, P. R. Nawrocki and T. J. Sorensen, *J Phys Chem A*, 2023, **127**, 3577-3590.